NORTHWESTERN UNIVERSITY

Microphysiologic Models of Human Ectocervical Tissue to Study Steroid Hormone Action During Homeostasis, Infection, and Oncogenic Transformation

A DISSERTATION

SUBMITTED TO THE GRADUATE SCHOOL

IN PARTIAL FULLFILLMENT OF THE REQUIREMENTS

for the degree

DOCTOR OF PHILOSOPHY

Field of Life Sciences

By

Kelly Elizabeth McKinnon

Evanston, ILLINOIS

June 2018

Abstract

There is a shortage of research models that adequately represent the unique mucosal environment of human ectocervical tissue, which has limited the development of new therapies for treating infection or cancer. I hypothesized that engineering the microenvironment of ectocervical tissue with *in vivo*-like endocrine and paracrine support, would enable squamous differentiation and hormone response. An interdisciplinary approach was taken to generate and characterize three distinct microphysiologic tissue culture models to study hormone-action in the human cervix. These microphysiologic models mimicked many aspects of *in vivo* physiology, including squamous maturation, hormone response, and mucin production, which are important components of barrier defense. Additionally, mRNA transcripts for several mucins not previously reported in the ectocervix and the differentiation-dependent localization of known ectocervical mucins were identified in both native and engineered tissue. To investigate genomic pathways that may influence physiology and infectivity during the menstrual cycle, RNA sequence analysis was performed on patient-matched engineered tissue after follicular and luteal phase hormone treatments. Follicular phase hormones were associated with proliferation, transcription, and cell adhesion, while luteal phase samples expressed genes involved in immune cell recruitment, inflammation, and protein modifications. In summary, I developed three microphysiologic human ectocervical tissue models that differentiate, produce mucins, and respond to hormones, and defined ovarian hormone-action in the

human ectocervix during the menstrual cycle, highlighting potential mechanisms that may influence infectivity. This will be useful for a variety of research applications, such as drug development and toxicology studies, development of preventative and therapeutic treatments, and basic research on hormone action in a critical reproductive tissue for women's health that has been historically understudied.

Acknowledgements

First, I'd like to thank my mentor Dr. Teresa Woodruff. Teresa, it has been a great honor to work with and learn from you over the past 4 years. Joining your lab was the best decision I made in graduate school. Thank you so much for taking me in, building me up, and pushing me past what I perceived to be my limits. Your unique and interdisciplinary approach to mentoring and unwavering support were exactly what I needed to succeed, and I cannot even imagine what grad school would have been like if you were not my mentor. I will always be proud to "be the brand, wear the brand," and I hope wherever I end up in my career will make you proud to say I'm one of yours. Thank you for everything.

I would also like to thank Dr. Spiro Getsios. I was fortunate enough to have two amazing mentors for the first two years of my dissertation work. Spiro, thank you so much for joining my mentoring team and opening my eyes to the world of epithelial cell biology. Your passion, authenticity and brilliant mind never ceased to inspire me to be a better scientist. My best writing has always come after thinking, "What would Spiro say?" and remembering your witty comments and questions that always made me think more critically and write more clearly. I am so grateful, and I know your influence will continue to have an impact on my science.

I'd like to acknowledge Dr. Danielle Maatouk. Danielle became an unofficial mentor to me early on and was a role model for an entire generation of new scientists in our department. She showed us that it is possible to have it all – you could be a woman in science, have a family and a career, and excel at both – something we are frequently told is not possible. Danielle's legacy will live on through her students, and all of us whom she took under her wing and inspired.

To my committee, both past and present, Dr. Laimonis Laimins, Dr. Julie Kim, Dr. Monica Laronda, and Dr. Tom Hope – thank you. I have learned so much from all of you, and it was clear that you all really cared about my development and training. I could not have asked for a better committee. Thank you so much for everything you taught me over the years!

To Team Cervix: Sasha– your optimism and enthusiasm made it such a pleasure to work with you. Thank you for helping me with my early research! Rhit – it was awesome having you as a mentee and friend, and I'm so excited for your future. Thank you for your endless IHC and cervix appreciation, your hard work, and for your sense of humor that made getting through the hard times a lot easier. Chloe – thank you so much for volunteering your time to work with us. You became such a valuable asset to Team Cervix and a PCR expert! I really enjoyed having you on the team, and I know you're going to be an awesome MD! Jovanka – you have overcome so much and it's so inspiring. I was immediately impressed with how quickly you learned biology without any former training. I'm so proud of you and I look forward to following your career! To the others that I claim as Team Cervix – Saurabh and Megan, thank you for getting up super early to consent and collect tissue. This project would not have been possible without your dedication. Chanel, Keisha, Nina – Thank you for your histological expertise, and your beautiful cervix sectioning! Paul, Silvia and Aya – Thank you for your technical expertise! Dr. Kruti Maniar – thank you for pathology expertise and commitment to our research!

Thank you to all of the patients who donated tissue through Northwestern University Prentice Women's Hospital and the Gynecological Tissue Library. Thank you to our UH3 collaborators – Draper Lab, Kim Lab, Burdette Lab, and Getsios Lab - it was such an honor to work with so many talented researchers on such an awesome project!

To my Woodruff family past and present – thank you so much for being my Chicago family! To "my boys" as TK used to say: Max, my lab husband – getting through grad school would have been a lot harder without you. I'm going to miss our late nights in the lab and our daily trips to Starbucks. Thank you for always being there to lift me up and empathize. Peter – I'm so glad our time in the Woodruff lab overlapped. I'll always remember Wednesday Wine (or Thirsty Thursday) and I know we'll remain lifelong friends! Hunter – thank you for your friendship, your love of people named Leah, your endless music and movie knowledge, and your dedication to the microfluidics projects! Monica – I have learned so much from you and really enjoyed working with you in all of our different PPE over the years. I cannot wait to join your lab and be able to work with you and Kelly again! To all of the lab managers – Kelly, Chris, Sarah – you

guys are amazing and deserve so much credit for keeping the Woodruff lab functional. Soyoun, your smile and kind heart, brightened my day so many days – thank you for being you. To all other Woodruff lab members who I've been fortunate enough to work with, and all of the enterprise – you have all left your mark on me – thank you for everything.

Thank you to Dr. Patrick Coppock for believing in me and going out of your way to help me find research opportunities. I don't think you will ever know how much of an impact you had. I certainly would have never ended up at Emory without your strategic help, which is what catapulted my success since then. You went about things differently, and genuinely cared about where I ended up. You taught me to love organic chemistry, and how to be a good mentor and pay it forward. Sincerely, thank you. Thank you to Dr. George Beck, my first real research experience was in your lab, and this is where I fell in love with bench work, and with cancer biology, and knew a career in science was right for me. I learned so much in your lab that helped me during graduate school. Thank you so much for all of your support and everything you taught me. You really made a difference.

To my friends who helped keep me sane through this crazy process – thank you. Alex, I'm so glad we were roomies on interview weekend and both ended up at NU. You have been such an important part of my life here and I can't imagine what graduate school would have been like without you. It is so weird to think we won't be in the same place for much longer, but I know wherever we end up, you and Mike will remain lifelong friends. Thank you both for your friendship and support. To all of my other DGPeople – Tania, Stephie, Kevin, Jeremy, Bella and everyone else - getting to know you all has been awesome and I'm so thankful our cohort became so close. Michelle, Ry, Mel, Heather, Tyler and all my TrisLoves – thank you for always giving me perspective, for always believing in me. Special thanks to Michelle – my platonic soulmate – for just…getting it. Your passion, creativity, and unending determination have always inspired me. Thank you for our DDNs and for always reading my writing and giving general audience feedback - you really helped craft my science communication skills.

To my family – you have all been such a huge support throughout this process. It has been hard being so far away from everyone but knowing the "family channel" was always there made the distance not seem so far. Dad, there were times I wasn't sure you'd be around to see me finish, but I am so grateful you are part of that 3% statistic and get to be a witness to this. Thank you for your strength and courage and all the wisdom you've imparted on me, as well as the stubbornness and resilience that I inherited from you. Mom, thank you for all of your sacrifices. Your determination to go back to school with three small children and go on to get your masters showed me that anything is possible and it's never too late to try again. I learned how to be a strong, independent woman and not let anything stop me from reaching my goals from watching you do the same. Kris, thank you for your perspective and encouragement. You've been a constant support and have always treated me as your own daughter and I appreciate you so much. Heather and Daniel, thank you for always believing in me, supporting me, and encouraging me through the highs and lows of PhD student life. I love you all!

And finally, huge thanks to my loving and supportive wife. Leah, my solid rock, my best friend, my love, there are no words to properly express my gratitude for everything you've sacrificed to help me reach my goals. Since we met first year, you have always put me first. You were happy to pick up the household slack when I was overwhelmed or had important deadlines coming up. I know without a doubt my success was made possible by your sacrifices. This has always been a team effort – and we finally made it! With all of my heart, thank you.

List of Abbreviations

ALI	air-liquid interface
BM	basement membrane
BP	biological process
C-7	control (no hormone treatment) on day 7
C-14	control (no hormone treatment) on day 14
CC	cellular component
cDNA	complimentary DNA
Ct	cycle threshold
DCES	decellularized ectocervical scaffold
DNA	deoxyribonucleic acid
E2	estradiol
ECM	extra-cellular matrix
ECT	engineered cervical tissue
EGF	epidermal growth factor
EM	ectocervix media
ERα	estrogen receptor alpha
ERβ	estrogen receptor beta
FC	fold change
FM	fibroblast media
FP	follicular phase
FPKM	fragments per kilobase per million
FRT	female reproductive tract
FSH	follicle stimulating hormone
GM	growth media
GO	gene ontology
H&E	hematoxylin & eosin
hCG	human chorionic gonadotropin
HIV	human immunodeficiency virus
HPV	human papillomavirus
HSV	herpes simplex virus
IF	immunofluorescence
LH	luteinizing hormone
LMP	last menstrual period
LP	luteal phase
MF	molecular function
MM	maturation media
NCI	National Cancer Institute
OCT	organotypic cervical tissue
P4	progesterone
PR	progesterone receptor

PT	patient tissue
qRT-PCR	quantitative real time polymerase chain reaction
RCT	recellularized cervical tissue
RNA	ribonucleic acid
RNAseq	RNA sequence
ST	StringTie

.

Table of Contents

List of Figures and Tables

Chapter I.

The Human Ectocervix: Biology, Endocrinology, and Pathology

Introduction

The female reproductive tract (FRT) undergoes dynamic changes during reproductive years in order to facilitate fertilization, pregnancy, and birth, with each of the organs of the FRT responding to steroid hormones estradiol (E2) and progesterone (P4) secreted by ovarian granulosa cells prior to and following ovulation. The downstream tissues - the fallopian tube, uterus, and cervix – have tissue-specific responses to these hormones based on biological function. In the case of the cervix, epithelial cells respond to E2 and P4 to create the optimal environment for sperm cell survival and motility during the fertile period, protecting sperm cells from natural defense mechanisms of the vaginal vault, which function to prevent pathogenic infection but can also inhibit sperm motility. Ectocervical epithelium is a primary site for infection and is also susceptible to viral transformation and cancer; however, the role of E2 and P4-regulation in these processes is not well understood. A better understanding of cervical physiology and the role of endocrine signaling during homeostasis will provide insight into how these mechanisms could be targeted for preventative and therapeutic treatment of infection and cancer. This chapter discusses the distinct characteristics of ectocervical biology, endocrinology, and pathology as currently understood, and the gaps in knowledge that have prevented progress in this area.

Biology

Cervical tissue architecture

The cervix is the narrow tube-like structure that extends from the inferior portion of the uterus into the vaginal vault and consists of two anatomically and functionally distinct portions. The endocervix is the inner canal that is directly connected to the uterus, while the ectocervix is the outer portion located within the vaginal vault. The endocervix is lined with simple columnar epithelium, which forms crypts and secretes mucins that contribute to cervical mucus (*1*). In contrast, ectocervical tissue is made up of many layers of squamous epithelial cells in different states of differentiation, attached to a dense stroma containing fibroblasts and immune cells, such as macrophages, leukocytes and natural killer cells (*2, 3*). The stratified squamous epithelium is constantly regenerated in order to maintain an effective barrier, and thus a precise balance must be achieved between proliferating and differentiating epithelial cells. Similar to keratinocytes in epidermis, ectocervical epithelial cells can be grouped into four layers with distinct characteristics. However, differentiated epithelial cells do not resemble the granular and cornified phenotypes characteristic of suprabasal keratinocytes. Instead, ectocervical epithelial cells can be grouped into four subsets: basal, parabasal, intermediate and superficial cells (Figure 1.1).

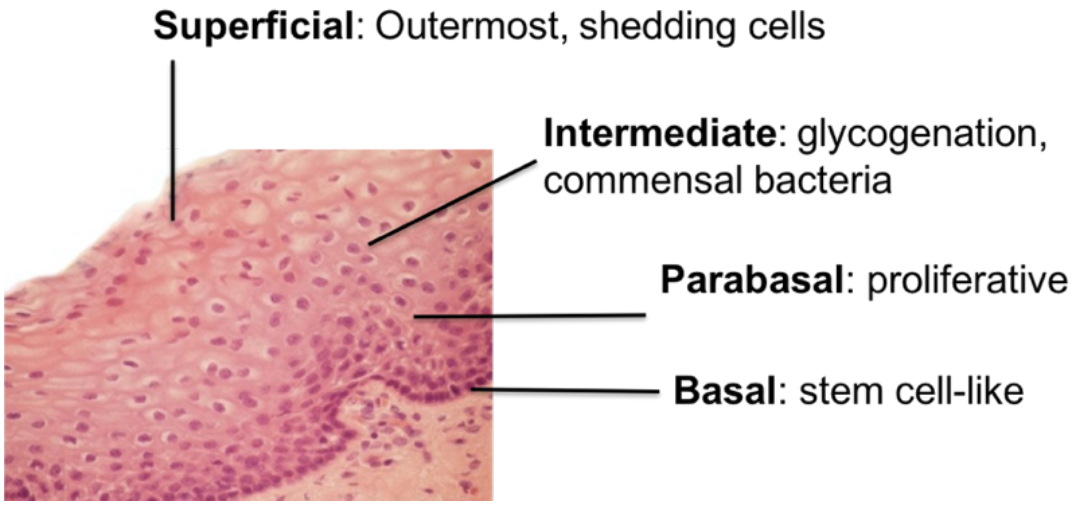

Figure 1.1 Stratified squamous architecture of human ectocervical epithelium. Basal cells attach to the basement membrane and give rise to the next few layers of cells, the proliferative, parabasal cells. The intermediate layers of cells are heavily glycogenated to support the commensal bacteria populations in the cervix. The most apical cells are known as the superficial layer, and these cells are constantly being shed as tissue is regenerated.

As in skin and other stratified tissues, the stem cell-like basal cells give rise to the other layers of cells; however, it is the parabasal cells in the next few layers of cells that are the primary proliferative subset in ectocervical epithelium (*4*). The basal and parabasal cells are tightly adhered to each other as indicated by the high expression of adherens and tight junction proteins, such E-cadherin (ECAD) and Claudin1 (CLDN1) in these cells, which decreases as cells become more differentiated in the intermediate layers (*4*). These junctions play a role in adhesion, cellular communication and maintaining a selectively permeable epithelial seal that must be penetrable to immune cells and factors but not to microorganisms or other potential foreign substances (*5-7*). Accordingly, this selective permeability can be influenced by a number of factors including cytokine signaling (*5*), endocrine signaling (*8-10*), inflammation and infection (*11, 12*).

The more differentiated intermediate cells have exited the cell cycle for terminal differentiation and are characterized by a large cytoplasmic to nuclear ratio, and abundant glycogenation, which supports the commensal population of bacteria that naturally inhabit the lower female reproductive tract (*13, 14*). The most apical layers of cells, known as the superficial cells, are characterized by small nuclei and have a long, flattened phenotype. Junctional proteins that are highly expressed in the more basal cells are no longer present or are highly permeable in these cells (*4*), which are continuously shed as the epithelium renews itself.

Function of ectocervical mucosa

The dynamic biology of the cervix enables various functions throughout life, such as facilitating sperm entry into the upper FRT for fertilization, maintaining a robust barrier against infection, and maintaining pregnancy to term. The human cervix evolved to coordinate all of these functions in response to endocrine signals from the ovary. As ovulation approaches, and E2 levels increase, the microenvironment of the cervix changes dramatically. It has been demonstrated that in response to high E2, endocervical mucus changes in composition, enabling sperm motility through the acidic environment of the vaginal vault and into the upper FRT. For example, Gipson et al previously found that in cervical mucus collected from women during different phases of their menstrual cycles, mRNA transcripts of the major gel-forming mucin of endocervical epithelial cells, MUC5B, is highest just before ovulation (*15*). Additionally, Wira et al have demonstrated that the secretion of many anti-microbial peptides in reproductive epithelial cells is dependent on menstrual cycle phase (*3, 16*). In the case of the cervix, this includes human beta-defensin 2 (HBD2) and secretory leukocyte protease inhibitor (SLPI), which can inhibit bacterial, fungal and viral infections, but may also inhibit sperm motility (*16-19*). Because of this down-regulation of secreted immune factors, there is increasing concern that there may be a "window of vulnerability" in which pathological infection is more likely. Studies in non-human primates implicate ovarian hormones in increased susceptibility to infection; however, receptor-mediated mechanisms for this phenomenon remain unclear. Indeed, hormones can also cause decreases in epithelial thickness (*20*), increased cytokine signaling and immune cell recruitment (*21*), changes in expression of

tight junction proteins (*7, 8*), and other changes in properties that may affect barrier permeability and defense, such as the production of mucins.

Mucins are large glycosylated proteins that provide lubrication and hydration and are an important component of mucosal barrier function. Indeed, the importance of mucins for barrier function in the female reproductive tract, eyes, digestive tract, lungs, and intestinal mucosa is well-documented, and disruption of normal mucin expression is associated with infection and disease in each of these tissues (*15, 22-25*). Endocervical epithelium expresses gel-forming, secreted mucins that make up cervical mucus and the composition of this mucus is dependent on menstrual cycle phase in order to facilitate sperm entry (*1, 25-27*). In contrast, the ectocervix expresses membrane-associated mucins that do not contribute to the secreted cervical mucus (*27, 28*). Mucins expressed in the ectocervix remain on the surface of the epithelium, which protects ectocervical tissue in numerous ways. For instance, mucins provide lubrication and hydration that help prevent friction-induced tears that would allow microbial infiltration. Additionally, transmembrane mucins were shown to trap microorganisms, including fungi, bacteria, and viruses, preventing them from reaching their target cells and establishing infection (*1, 15, 23, 29, 30*). Mucosal barrier function is also enhanced by the ability of mucins to bind antibodies, suggesting mucosal epithelium could potentially act as a reservoir for therapeutic treatments (*24, 31, 32*). Accordingly, studies are underway to target mucins for vaccine adjuvant-development and other therapeutic interventions associated with infection and disease (*33, 34*)

In addition to junctions, mucins, and secreted immune factors, additional mechanisms also play a role in mucosal barrier defense during homeostasis. For example, the glycogenated intermediate cells of ectocervical epithelial cells support a commensal bacterial population of lactobacilli that are not inhibited by secreted anti-microbial peptides characteristic of the FRT (*16*). This bacterial population metabolizes glycogen and produces lactic acid, which is responsible for the high pH of the lower female reproductive tract – an additional component of barrier defense (*14*). Additionally, healthy populations of lactobacilli in the lower FRT can prevent other microbial populations from establishing infection in these cells (*14, 35*), making them a vital part of barrier protection in ectocervical tissue.

In summary, the unique tissue architecture and physiology of the human ectocervix support the dynamic functions of the cervix throughout life. Balancing proliferation and differentiation, mucin production, immune factor secretion, pH and commensal bacteria, in order to achieve these functions, requires precisely regulated hormone-action in the cervix. However, hormone receptor-mediated mechanisms for these events remain largely unknown. A better understanding of estradiol and progesterone signaling during homeostasis will provide insight into how these pathways are overcome in infection and cancer, and potentially reveal new therapeutic targets.

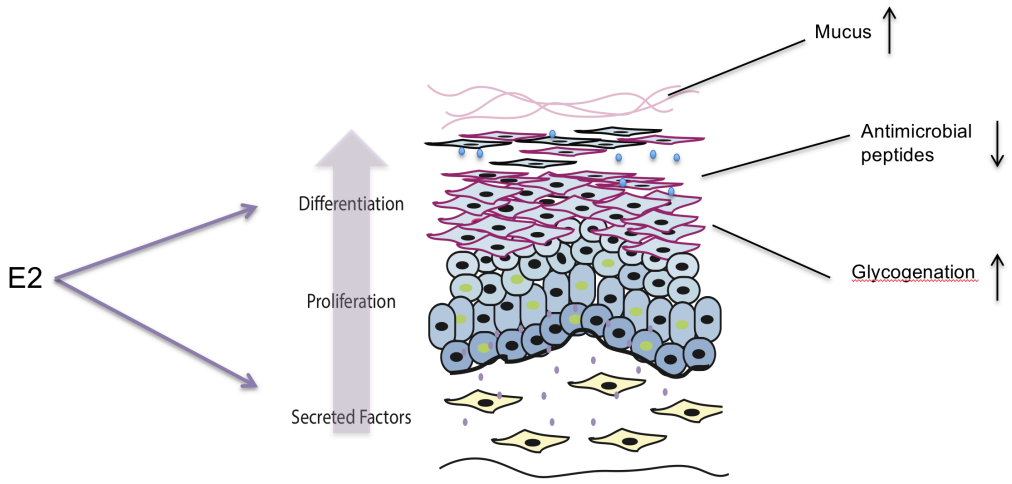

Figure 1.2 Estradiol regulation of ectocervical tissue
Estradiol, produced by the ovary in response to pituitary hormones, regulates epithelium through both direct and indirect, paracrine mechanisms. Estradiol targets estrogen receptors in stromal cells and epithelial cells, and both are necessary to maintain homeostasis. E2 has also been shown to increase mucus production, decrease antimicrobial peptides, and increase glycogenation, but clinical significance in humans remains unclear.

Endocrinology

Estradiol signaling

In response to follicle-stimulating hormone (FSH) produced by the pituitary gland, ovarian follicles develop and mature, and the somatic granulosa cells secrete increasing amounts of E2 leading up to ovulation of an oocyte, which is triggered by pituitary luteinizing hormone (LH). After ovulation, E2 secretion decreases, and the corpus luteum secretes high levels of P4. The downstream female reproductive tract tissues respond to E2 and P4 to maintain their tissue-specific roles in homeostasis. Both estrogen receptor alpha and beta (ERα/β) are expressed in the ectocervix; however, ERα is commonly thought to be the dominant estrogen receptor in the female reproductive tract (*36-40*), and less is known about the role of ERβ in these tissues. ERα is expressed in both epithelial and stromal cells of the FRT, and studies in mice have shown that ERα is necessary for differentiation. For example, in ERα-knockout mice, ectocervical epithelium is thinner and fails to differentiate, suggesting a role for ERα signaling in differentiation (*40*). However, ERα has been widely reported to increase proliferation in many different cell types including reproductive tissues (*41, 42*), and thus we cannot rule out that loss of differentiation in ERα-knockout mice may be due to loss of ERα-induced proliferation, preventing proper differentiation, rather than due to a direct role for ERα in differentiation.

Progesterone signaling

Progesterone receptor (PR) expression is under the control of ERα in the uterus, vagina and cervix (*38*), as well as many other tissues, and thus expression of ERα is necessary for PR expression. This suggests E2 produced in the follicular phase primes cervical epithelium for the progesterone-dominant luteal phase. However, the role of P4 in ectocervical tissue during the luteal phase remains unclear. Several studies in vaginal tissue, which is thought to be morphologically and genetically similar to ectocervical tissue, have shown changes occurring in response to progesterone, such as thinning of the epithelium and decreased glycogenation (*20, 28*), but the clinical significance of these findings remains unclear. In the uterus, progesterone has a much more dominant, and well-established role. For example, P4 regulates the thickening of endometrium each month in preparation for implantation by a fertilized egg. However, much less is known about the role of P4 signaling in the cervix. Previously, Arslan et al characterized gene expression in human endocervical tissue during follicular phase and luteal phases by microarray and found distinctly different genomic profiles based on menstrual cycle phase (*41*). In this study, luteal phase genes were associated with oxidative stress, chromatin remodeling, inflammation and immune cell regulation. However, ectocervical tissue was not evaluated in this study.

Models that more closely represent the complex signaling mechanisms occurring between reproductive tissues will be necessary to understand and develop treatments for many of women's reproductive health problems.

Hormone-mediated paracrine signaling

The stromal cells of the female reproductive tract play an important role in development, differentiation and hormonal regulation. During development, the simple columnar basal epithelia of the Mullerian duct differentiate into epithelia of the fallopian tubes, uterus, cervix and upper vagina, which differ genetically and morphologically (*43-45*). This was shown to be dependent on tissue-specific stroma and is reversible when combined with stroma from a different region (*38, 40, 46*). For example, when neonatal mouse uterine epithelium was recombined with vaginal mesenchyme, the simple columnar uterine cells differentiated into stratified squamous cells with a vaginal epithelial phenotype, and vice versa (*45*) highlighting the importance of the microphysiologic environment for proper tissue differentiation during development. Additionally, Ye et al showed that uterine mesenchyme was sufficient to differentiate human embryonic stem cells into hormone-responsive uterine-like epithelial cells, that responded to estrogen by secreting uterine-specific glycodelin, further supporting that differentiation in the FRT is dependent on paracrine signals from the mesenchyme during development (*47*). Studies in mice have shown that even as adults, stromal cells continue regulating FRT epithelium, such as the inhibitory effect of progesterone on uterine epithelium, and the proliferative effect of estradiol on vaginal/cervical epithelium, which require stromal hormone receptor expression (*39, 40, 48*). This supports the hypothesis that both epithelial and stromal hormone receptors are necessary for proper endocrine signaling in ectocervical mucosal cultures and highlights the increasing need for more physiological models, which will be described in chapters 3 and 4.

Pathology

Sexually transmitted infections can have devastating effects on women's health, such as infertility, cancer, or even death (*49-51*). As one of the first tissues to come into contact with potential pathogens during sexual intercourse, ectocervical tissue is highly prone to infection. While treatments exist for common bacterial infections, viral infections such as human immunodeficiency virus (HIV), herpes simplex virus (HSV), and human papillomavirus (HPV) still have no cures and remain an intense focus of investigation for new treatments.

Human papillomavirus is the causative agent of cervical cancer, and despite the introduction of the HPV vaccine in 2006, remains the most common sexually transmitted infection (STI) with approximately 80% of women contracting the infection during their lifetimes (*52*). The currently available HPV vaccines have not eradicated HPV infection, which is partly due low participation among the targeted age-group (*53-56*), and thus we are far from reaching the percentage of immunized population needed for herd immunity. Additionally, the HPV vaccine targets the highest risk strains, HPV16 and HPV18, which account for about 70% of cervical cancer cases; however, the other 30% of cervical cancers have been associated with 8 other high-risk strains, for which there are no available vaccines (*57*). Up to one million women a year in the US undergo treatment for HPV-induced neoplasia or early-stage cancer, which has not changed in decades and involves the surgical removal of the portion of cervix affected, or total hysterectomy. While these treatments effectively remove the cancer, many women suffer from infertility or impaired fertility as a result (*49, 58-60*).

In the case of other common viral infections HSV and HIV, each of which can have devastating physical and social effects, there are still no FDA-approved vaccines or cures. Better therapeutic interventions are needed to prevent and treat viral infections in reproductive tissues, but the lack of *in vivo* or *in vitro* models that adequately represent human physiology has prevented progress. For example, two-dimensional (2D) in vitro epithelial cultures are unable to undergo squamous maturation, and only a subset of cells remains viable. Model species such as mice and non-human primates (NHPs) are commonly used to study reproductive diseases, but these common models are not naturally hosts to the viral infections that target humans, and thus studies of initial infection and natural course of disease may have limited applicability to humans. Additionally, these species differ biologically from humans in many ways that may influence infectivity, such as increased epithelial thickness in NHPs or the presence of cornified epithelium in mice (*61, 62*). It is clear that more human-like models that take into account female-specific biology and endocrinology are needed in order to develop better treatments for gynecological issues that affect women.

In the next chapter I highlight advances in the bioengineering of female reproductive tissues for research and clinical use that have occurred simultaneously to this work and are changing the way we think about modeling organ function. In chapter 3, I outline the development of three microphysiologic models using different bioengineering techniques and discuss the benefits and limitations of each. In chapter 4, I further characterize the most *in vivo*-like of the microphysiologic models – the engineered cervical tissue - through RNA seq analysis, which revealed distinct transcriptional profiles

dependent on menstrual cycle phase that may influence susceptibility to pathogenic infection. Finally, in chapter 5, I discuss conclusions and the future directions for microphysiologic modeling of hormone action in the human ectocervix.

Chapter II.

Engineering the Female Reproductive Tract

Reproductive organs communicate through hormones to support fertilization, implantation, embryo development, and eventually birth. Reproductive hormones are also important for development and homeostasis in many tissues outside of the reproductive system, such as the brain, bones and heart. Today, reproductive organ models are being developed to support physiologic function of reproductive tissues in order to advance both clinical and research discoveries. These engineered tissues are more physiologically relevant than past models for studying reproductive development, homeostasis, and other natural states, such as pregnancy and aging, as well as diseased states, such as cervical cancer or endometriosis. Engineered tissues are an important aspect of precision medicine, as we will soon be able to develop patient-specific tissue models to understand individual reproductive physiology and develop personalized treatments. Herein I briefly describe current trends in engineering women's reproductive tract tissues, with a focus on technology and advancements that have been achieved over the past few years.

Engineering the Fallopian Tube

During ovulation, an oocyte is released from the ovary into the lumen of the fallopian tube, where it will encounter a single layer of ciliated and secretory epithelial cells. These cells create the specific niche for fertilization by providing a reservoir for

sperm (*63*). In response to ovarian hormones, beating cilia and factors secreted into the oviduct fluid, such as OVGP1, enhance capacitation and motility of sperm, increasing the likelihood of fertilization (*63*).

To better understand the microenvironment of the fallopian tube during fertilization and embryo development, many recent studies have used 3D co-culture methods, which helps maintain epithelial cell polarity and differentiation. Lamy et al cultured bovine oviductal fibroblasts and epithelial cells on opposite sides of a trans-well, enabling epithelial-stromal interactions at the air-liquid interface (*64*). Similarly, Zhu et al cultured human fallopian tube epithelium on a trans-well at the air-liquid interface. In this study, hormonal cues were provided by murine ovarian follicles engineered to mimic the human reproductive cycle (*65*). In both cases, the authors detected beating cilia, and OVGP1 and other secreted factors were detectable in the culture medium, mimicking *in vivo* oviduct fluid (*64, 65*). Fallopian tube epithelium that was co-cultured with hormone-secreting ovarian follicles, showed cyclic differences in secreted factors and a thicker epithelium. Interestingly, the addition of fallopian tube epithelial cells to ovarian follicle cultures seemed to enhance ovarian function, as evidenced by the increased levels of progesterone secreted by the corpus luteum after ovulation (*65*), suggesting cross-talk between reproductive organs may play an important role in reproductive processes.

To examine possible interactions between the embryo and oviductal epithelium after fertilization, Garcia et al co-cultured bovine oviductal epithelium with bovine embryos, and showed that cross-talk may involve BMP signaling (*66*). Ferraz et al further elucidated the oviduct environment using microfluidics to generate an oviduct-on-a-chip

system capable of supporting fertilization (*67, 68*). When sperm and oocytes were introduced to this system, oocyte penetration was supported, while polyspermy and parthenogenic activation, common occurrences in current IVF systems, were prevented (*67*). These recent advances in bioengineering increase our understanding of the microenvironment of the fallopian tube during fertilization and early embryo development and will allow us to create more physiologically accurate conditions for IVF and embryo culture.

Engineering the Uterus

With advances in reproductive technologies and IVF, many women who struggle with infertility are able to achieve pregnancy. However, in the case of absolute uterine factor infertility (AUFI), gestational surrogacy has historically been the only option. Recent studies explored the use of tissue engineered uterine constructs for research and treatment of AUFI and other reproductive syndromes that affect uterine function.

Decellularized uterine tissue has been used for endometrial epithelial regeneration in mice (*69*), rats (*70*) pigs (*71*), and humans (*72, 73*). These models have shed light on molecular mechanisms of epithelial regeneration and repair during the menstrual cycle and reproduction. For example, Hiraoka et al used decellularized murine uterus to determine that STAT3 is activated during endometrial regeneration, identifying a potential therapeutic target for AUFI (*69*).

Engineered tissue also holds promise for clinical treatments of uterine infertility and other reproductive conditions. In a rat model, Hellstrom et al used *in vitro*

bioengineered uterine tissue to repair native uterine tissue *in vivo* and support a healthy pregnancy (*70*). In 2016, Campo et al decellularized an entire porcine uterus (*71*). The decellularized porcine uterus was then recellularized with primary human endometrial cells, providing proof-of-concept that porcine scaffolds can support human endometrial regeneration. Olalekan et al used human decellularized endometrium as a scaffold for re-population with primary epithelial and stromal cells to establish long-term cultures that respond to a 28-day menstrual cycle (*72, 73*).

Many of these technologies mimic natural physiology with the end goal of being transplanted back into the body for therapeutic intervention. However, Partridge et al developed a "biobag" that is able to carry out uterine and placental functions ex vivo (*74*). Acting as an artificial uterus, this biobag consists of a pumpless arteriovenous circuit within a closed fluid environment with continuous fluid exchange. In this system, blood flow is driven by the fetal heart and accessed through umbilical vasculature—the first time this has been achieved. The authors found that these biobags were able to support fetal lambs for at least 4 weeks with normal heart and growth rates, and no organ failure. While the factors causing premature birth, including AUFI and cervical incompetency, are not completely understood, the potential of biobags to extend fetal development by 4 weeks could be the difference between life and death.

Engineering the Cervix

The cervix is regulated by ovarian hormones and must act as both a passageway for sperm, and a barrier against pathogenic infection. There is growing interest in

bioengineering cervical tissue using primary cervical cells to study fertility, contraception and mechanisms of disease (*28, 75-77*). To date, several 3D physiologic models have been developed to model sexually transmitted infections (STIs). However, many of the disease models use keratinocytes derived from neonatal foreskin instead of primary cervical epithelial cells, due to limitations in obtaining this rare tissue. These keratinocyte models provide an effective way for studying pathogens that can affect women, but do not adequately represent female cervical biology. For example, keratinocytes develop into cornified epithelium, and do not produce mucins. Cervical mucins play an important role in fertility and maintaining lubrication and hydration of the cervix, as well as providing barrier and immune defense against pathogens (*1, 26*), and should be a vital part of any physiological cervical model.

Over the past few years, several physiological models of human cervical epithelium have been developed. De Gregorio et al developed a cell-instructive stroma using primary fibroblasts to generate a scaffold-free ECM able to support partial epithelial differentiation (*75*). Using immortalized cell line cultures on decellularized neonatal foreskin, Zuk et al generated both cancerous and normal cervical models (*76*). While both of these models exhibited properties of epithelial differentiation, the overall epithelial thickness appeared reduced, and the morphology of the tissue resembled a neoplastic state, limiting our ability to study differentiation and homeostasis. We saw similar results in our reconstructed tissue models using ECM as a scaffold in chapter 3. This indicates there is still something missing from each of these systems that is necessary for squamous maturation and long-term viability.

In the next chapter, I combine several bioengineering techniques to develop novel 3D models that more accurately phenocopy normal *in vivo* cervical physiology. These models build on previous 3D models by incorporating both primary cervical fibroblasts as well as 3T3 feeder cells into a collagen hydrogel to create a stromal equivalent. Primary epithelial cells seeded on the stromal equivalent differentiate, produce mucins, and respond to menstrual cycle-like endocrine loops. While we are not yet close to using engineered cervical tissue therapeutically, these engineered tissues will be a valuable research tool and move the field forward by taking into account the critical role of endocrine and paracrine signaling in the FRT.

Chapter III.

Development of Ectocervical Tissue Models with Physiologic Endocrine Signaling

There is growing interest in developing a three-dimensional (3D) human ectocervical tissue model that accurately recapitulates *in vivo* human physiology for studies of infection, disease, and cancer. To date, several 3D models have been developed from neonatal foreskin to study viral infection and oncogenic transformation (*77-80*). These keratinocyte models provide an effective way to study many of the pathogens that can infect reproductive tissues, but they more closely resemble cutaneous skin than the mucosal epithelium present in the ectocervix, which is anatomically and physiologically distinct. Since infection and HPV-induced cancers are exponentially higher in mucosal tissues than epidermis, a model that accurately reflects the distinct physiology of cervical tissue is necessary to improve treatments for women. Recently, Zuk et al generated normal and cancerous cervical tissue models by seeding normal or cancerous immortalized cervical cells onto dermis obtained from neonatal foreskin (*76*). Histological analysis showed many layers of epithelial cells grew on the dermis in each case, but the normal cervix model did not recapitulate the distinct histology of mature differentiated cervical epithelium, and instead resembled a more neoplastic phenotype. A model developed by DeGregorio et al used primary cervical stromal cells to generate ECM, which was then seeded with primary epithelial cells (*75*). This model more closely mimics non-neoplastic tissue, though the epithelium still appeared much thinner than normal pre-menopausal cervical tissue, and

IHC analysis showed low expression of E-cadherin and basement membrane component laminin, indicating cells may not be well adhered to each other, and perhaps not properly attached to the regenerated stroma due to decreased basement membrane integrity. While each of these models are useful, they were not able to fully replicate the distinct histology of differentiated, non-neoplastic epithelium.

While hormone responsiveness of reproductive tissues is well-documented in the literature, many *in vitro* ectocervical studies did not include physiologic concentrations of hormones. Several included static concentrations of E2 or P4, while others included supraphysiologic concentrations or no hormone supplementation. Additionally, the role of stromal cells in epithelial differentiation and endocrine signaling in reproductive tissues has been well-documented in mice (*38, 40, 46*). Indeed, tissue-specific stromal cells express hormone receptors, and hormone-induced paracrine signaling between the stroma and epithelium are vital for maintaining homeostasis. We hypothesized that engineering the microphysiologic environment of ectocervical tissue, including endocrine and paracrine signaling, would support epithelial growth, differentiation and long-term culture of human ectocervical tissue, enabling studies of infection, barrier defense mechanisms, and hormone response in a critically understudied tissue.

We sought to evaluate three methods of microphysiologic modeling that have been successfully utilized to model other stratified tissues, such as epidermis, cornea and esophagus (*80-82*), with the addition of physiologic concentrations of ovarian hormones and tissue-specific stroma. Here we present methodology, validation and characterization

of recellularized ectocervical tissue, organotypic cervical tissue, and engineered cervical tissue with physiologic endocrine support.

Materials and Methods

Study participants and tissue acquisition

Subjects evaluated in this study were recruited between January 2015 and July 2017. Ectocervical tissue samples were collected with written consent from women undergoing hysterectomies at Northwestern University Prentice Women's Hospital (Chicago, IL), according to an Institutional Review Board-approved protocol. Participants included women aged 32-49. To increase replicability, stringent guidelines were developed to identify a comparable set of samples for analysis. Inclusion criteria were: women who had not been on reproductive hormone treatments or contraceptives the 6 months prior to surgery, and whose date of reported last menstrual period (LMP) was consistent with uterine cycle staging as determined by pathologist. Women who reported abnormal cycles or women in which significant cervical pathology was indicated (such as koilocytosis, neoplasia, infection, or cervicitis) were excluded from this study. By establishing these criteria, we aimed to minimalize extraneous variables enabling a rigorous analysis of hormone action in human ectocervical tissue. After surgical removal, hysterectomy tissue was held in saline until pathological examination, and remaining ectocervical tissue was placed in Hank's buffered saline solution at 4°C until processing. Samples for RNA analysis of patient tissue (PT) were received the day of surgery and flash frozen in LN2,

then stored at -80°C. Patient samples used for engineered cervical tissue and histological analysis of native patient tissue were received within 24 hours of surgery and processed depending on downstream application.

Murine tissue collection

All mice were and provided food and water housed in polypropylene cages and exposed to 12-hour light/dark cycles at 23±1°C with 30-50% relative humidity. Animals were fed Teklad Global irradiated 2919 or 2916 chow (Teklad Global), which has minimal phytoestrogens. All methods were approved by the Northwestern University Institutional Animal Care and Use Committee (IACUC). All experiments, procedures, and methods were carried out in accordance with the IRB-approved guidelines and regulations. Ovaries were isolated from 12-day-old CD-1 female mice as previously described (27). For organotypic co-culture, ovaries were cut into four even pieces and two quarters of ovarian pieces were placed on a 0.4 μm cell culture insert (EMD Millipore Co), with 700μl growth media (Table 3.1).

Ectocervical cell isolation, expansion, and culture

Epithelial cells were isolated using techniques previously established for human keratinocyte cultures (17). Briefly, tissue was trimmed of excess stroma, cut into 4-6mm pieces, and placed in dispase (1 U/mL) in DMEM/F-12 (Stemcell Technologies) overnight. Epithelial cells were removed from stroma with forceps after 24 hours. Cells were dissociated using 0.25% trypsin and spun down at 1000G for 5 minutes. Epithelial cells

were plated on 25% confluent feeder layers of J2-3T3 treated with mitomycinC (Calbiochem) for 2-2.5 hours to induce cell cycle arrest and prevent fibroblasts from taking over the culture before establishment of epithelial cells. Feeder cells were cultured in Fibroblast Media (FM) until co-culture. Epithelial co-cultures with feeder cells were cultured in Ectocervical Media (EM) with additional 5% FBS and 10 ng/ml EGF. Feeder layers were changed every 2-3 days.

Stromal fibroblasts were isolated through explant outgrowth, as described previously (28). Briefly, after removing epithelium, remaining tissue was placed in 0.25% trypsin for 2-3 hours at 37°C. Tissue was rinsed with PBS, and explants cultured at 37°C in FM. Media was changed every 2-3 days. Once fibroblasts migrated out, tissue was removed, and fibroblasts continued to proliferate and expand. All primary cells were passage 3 or earlier and never cryopreserved. See Table 3.1 for culture media formulations.

Decellularization and recellularization of ectocervical tissue

Human ectocervical tissue was trimmed of excess stroma until the tissue was approximately 1mm thick, and contained the most apical stromal compartment, and epithelium. Tissue pieces were then incubated with 0.1% SDS for 48h, as has previously been demonstrated in ovarian and endometrial tissues (29, 30) to remove all cellular material. The ECM left behind was rinsed in PBS and cut into 3mm by 3mm pieces to generate decellularized ectocervical scaffolds (DCES).

Table 3.1 Culture media formulations

Media name	Components
Growth media	50% αMEM Glutamax
	50% F-12 Glutamax
	Supplemented with:
	3 mg/ml bovine serum albumin (BSA, MP Biomedicals)
	0.5 mg/ml bovine fetuin (Sigma-Aldrich)
	5 μg/ml insulin
	5 μg/ml transferrin
	5 μg/ml selenium (Sigma-Aldrich)
Maturation media	50% αMEM Glutamax
	50% F-12 Glutamax
	Supplemented with:
	10% fetal bovine serum (FBS, Fisher)
	1.5 IU/ml human chorionic gonadotropin (hCG, Sigma-Aldrich)
	10 ng/ml epidermal growth factor (EGF, BD Biosciences)
	10 mIU/ml FSH
Ectocervical media	50% DMEM HG with glutamine (Sigma)
	50% DMEM:F-12 (Sigma)
	Supplemented with:
	10ug/ml gentamicin (Sigma)
	0.25ug/ml Amphotericin B (Cellgro)
	0.4ug/ml hydrocortisone (Sigma)
	10ng/ml cholera toxin (Sigma)
	5% FBS (Fisher)
	1% ectocervical supplement cocktail mix:
	180 uM adenine (Sigma)
	5ug/ml human recombinant insulin (Sigma)
	5ug/ml human apo-transferrin (Sigma)
	5 ug/ml triiothyronine, T3 (Sigma)
Fibroblast media	DMEM HG (Sigma)
	Supplemented with:
	10% neonatal calf serum (Fisher)
	10 ug/ml gentamicin (Sigma)
	0.25 ug/ml Amphotericin B (Cellgro)

Similar to methods used by Ridky et al to produce differentiated epithelium on devitalized dermis (14), the stromal compartments of the scaffolds were placed basement membrane-side down on a 12mm cell culture insert and seeded with 10^6 primary fibroblasts in a small amount of FM (approximately 100µl) to encourage attachment to the scaffold rather than the insert. After 8-24 hours, 700µl of FM was added to submerge tissue. After 2-3 days of culture, scaffolds were placed basement membrane-side up and cultured for two weeks to allow stromal cell integration. At this time, 10^6 epithelial cells were seeded in a small amount of EM on the apical side of scaffolds. The recellularized cervical tissue (RCT) was cultured for two weeks at the air-liquid interface in EM supplemented with 0.1nM E2 to promote differentiation.

Preparation of explant tissue models for culture

Ectocervical tissue was washed twice with PBS containing 1% penicillin/streptomycin and processed for culture within 24 hours of surgery. Tissue was trimmed of excess stroma until pieces were approximately 1mm thick and contained both stromal and epithelial compartments. Three-millimeter biopsy punches of trimmed tissue were then transferred to cell culture inserts for culture at an air-liquid interface. Tissue explants were cultured without hormones for 2-5 days before exogenous hormone treatments or co-culture with murine ovarian tissue.

Generation of engineered ectocervical tissue

To generate a cervical stromal equivalent, methods used to generate engineered dermis from neonatal foreskin were adapted with changes (17). We seeded $3x10^5$ primary fibroblasts and $3x10^5$ J2-3T3 feeder cells in a collagen hydrogel consisting of: 4mg/ml rat tail collagen, 10% reconstitution buffer, 10% 10x DMEM (Sigma), 15µl/ml 0.5 N NaOH, and ddH2O to final volume of 2ml collagen per well. Hydrogels were formed on 30mm cell culture inserts (EMD Millipore Co) in deep-well plates at 37°C for 30 minutes, and then submerged in FM. After 24 hours, 10^6 epithelial cells were seeded on each hydrogel and submerged with EM+5% EGF above (2ml) and below the cell-culture insert (14ml). Once a monolayer of epithelial cells developed (5-7 days), engineered cervical tissue (ECT) was cultured at an air-liquid interface with 9ml EM for 5-7 days before beginning hormone treatments.

Ovarian hormone cycle and exogenous hormone treatments

To recapitulate human menstrual cycle hormone secretion, murine ovaries were cultured over 28 days, with the inclusion of both follicular phase (FP) and luteal phase (LP) pituitary hormones. During FP (days 0-14), tissues were co-cultured at 37°C in 5% CO2 for 14 days with GM containing 10 mIU/ml recombinant follicle-stimulating hormone (FSH). On day 14, cultured ovarian tissue was stimulated with Maturation Media (Table 3.1), containing human chorionic gonadotropin (hCG, Sigma-Aldrich) for 16 hours at 37°C in 5% CO2 to trigger ovulation. During the luteal phase (day 14 to day 28), culture media did not contain FSH. For exogenous hormone treatments, estradiol (E2) and progesterone

(P4) solutions were made in 100% EtOH and stored at -20°C between uses. Four combinations of E2 and P4 were cycled through media over 14-28 days, to model ovarian hormone signaling during follicular and luteal phases, as we have previously shown (31). Engineered and explantc tissues were exposed to increasing levels of E2 (0.1nM-1.0nM) for FP treatments (days 0-7 or 0-14), and rising levels of P4 (10nM-50nM) combined with decreasing E2 (1nM-0.01nM) in the LP treatments (days 8-14 or 14-28), with media replenished every 24-48 hours.

Histological, immunofluorescence and PAS analysis

Ovarian, and reconstructed or native ectocervical tissue were fixed in 10% formalin overnight. Tissues were dehydrated in ascending concentrations of ethanol (50%-100%) before being embedded in paraffin using an automated tissue processor. Sections were cut for hematoxylin and eosin (H&E), immunofluorescence, and PAS staining. For immunofluorescence, antigen retrieval was performed using sodium citrate buffer (pH 6) in a pressure cooker for 35 mins. Sections were blocked with 10% goat serum for 1h, before incubation with primary antibodies overnight at 4°C (Table 3.2). Sections were then stained with fluorescent secondary antibodies for 1 hour and imaged using NikonE600 fluorescent microscope. ImageJ software was used to measure epithelium in H&E-stained sections, from basement membrane to apical surface of epithelium every 100μm along entire length of the ECT, as has been shown previously (32). Measurements were made by two researchers per sample and averaged to determine thickness (μm). Statistical significance was determined by 2-tailed, paired, student T-test in GraphPad Prism 7.

Table 3.2 Antibodies used in study

Target	Name of Antibody	Catalog #	Species	Dilution
ESR1	Anti-Estrogen Receptor Alpha [SP1]	Abcam, ab16660	Rabbit monoclonal	1:100
PGR	Anti-Progesterone Receptor A/B	Cell Signaling, 8757	Rabbit monoclonal	1: 50
MUC1	Anti-Mucin 1 [EPR1023]	Abcam, ab109185	Rabbit monoclonal	1:100
MUCL1	Anti-Small Breast Epithelial Mucin	Biorbyt, orb186052	Rabbit polyclonal	1: 50
MUC4	Anti-Mucin 4 [8G-7]	Abcam, ab52263	Mouse monoclonal	1:100
E-CAD	Anti-E-Cadherin	Abcam, ab76055	Mouse monoclonal	1:100
Ki67	Anti-Ki67	Abcam, ab833	Rabbit polyclonal	1:50
CK13	Anti-Cytokeratin 13 [DE-K13]	Abcam, ab9383	Mouse monoclonal	1:200
CK14	Anti-Cytokeratin 14	Abcam, ab9220	Mouse monoclonal	1:50
COLVII	Anti-Collagen VII	Abcam, Ab93350	Rabbit polyclonal	1:100
COL I	Anti-Collagen I	RD1-9001106	Rabbit polyclonal	1:100
COL IV	Anti-Collagen IV	Abcam, Ab6586	Rabbit polyclonal	1:100
Laminin	Anti-Laminin	Sigma, L993	Rabbit polyclonal	1:100
Rabbit IgG	Goat Anti-Rabbit IgG (H+L) Secondary Antibody, Alexa Fluor 568	Invitrogen, A11011	Goat polyclonal	1:500
Mouse IgG	Goat Anti-Mouse IgG (H+L) Secondary Antibody, Alexa Fluor 488	Invitrogen, A11001	Goat polyclonal	1:500

Total RNA isolation

Flash-frozen NCT weighing up to 100mg was pulverized using a Biopulverizer (Biospec) and placed in 700µl of Qiazol (Qiagen). Tissue solution was needle-sheared and then further broken down in Qiashredder columns (Qiagen). A RNEasy mini-kit (Qiagen) was used for total RNA isolation, according to manufacturer's instructions. Engineered tissue was washed with PBS (Ca++, Mg+) before removing tissue from insert with a razor blade. Forceps were used to separate epithelium from collagen hydrogel for RNA analysis. Epithelium was placed in 700µl of Qiazol, needle-sheared, and RNA was isolated by RNAEasy mini-kit as described above. Concentrations of RNA were determined using a nano-drop spectrophotometer and RNA was stored in RNAse free water at -80°C until analysis.

Quantitative real time polymerase chain reaction (qRT-PCR)

One µg of isolated RNA per sample was combined with 4µl of SuperScript VILO Mastermix (Invitrogen) and RNAse-free ddH2O to equal 20µl reactions for cDNA synthesis. Samples were incubated at 25°C for 10 minutes, 42°C for 60 minutes, before terminating reactions at 85°C for 10 minutes, per VILO instructions. qRT-PCR reactions were performed in triplicate using a StepOnePlus real-time PCR system (Thermo Fisher) and IDT gene expression assays (Integrated DNA Technologies, IL) to determine relative expression of each gene. All reactions were run 40 cycles (95°C for 15 sec, 60°C for 1 min) after initial 3 min incubation at 95°C. Cycle thresholds (Ct) were calculated and normalized with ribosomal 18S (18s rRNA) gene expression as a control. Ct was placed at

approximate level where increases in amplification were parallel between samples. Gene expression in PT was calculated using the -log2(ΔCt) method and displayed as fold change between sample groups. Gene expression in ECT was calculated using the –log2(ΔΔCt) method, relative to patient-specific control for each treatment, and represented as FC over the corresponding control. Two-tailed, paired, student T-test was used to determine significance in engineered tissue and two-tailed Mann Whitney test was used to determine significance in patient tissue.

Results

Development of recellularized ectocervical tissue model

A 3D model of human ectocervical tissue was developed using primary ectocervical epithelial cells seeded on decellularized ectocervical tissue scaffolds (DCES). To generate the DCES, we adapted methods used successfully in human ovary and endometrium, with changes (29, 30). Tissue (n=6) was incubated in 0.1% SDS for 48 hours, which removed cells while leaving intact ECM. Decellularization efficiency was confirmed by evaluating H&E and DAPI staining in histological sections, which revealed that contrary to patient tissue (PT), the decellularized scaffold showed no nuclear staining (Figure 3.1 A-B, D-E), indicating cellular material was effectively removed from the ECM. To ensure basement membrane integrity, which is necessary for epithelial cell adhesion, we performed immunofluorescence (IF) analysis of basement membrane (BM) component collagen 7 (COL7) and observed similar localization and staining intensity in PT and DCES.

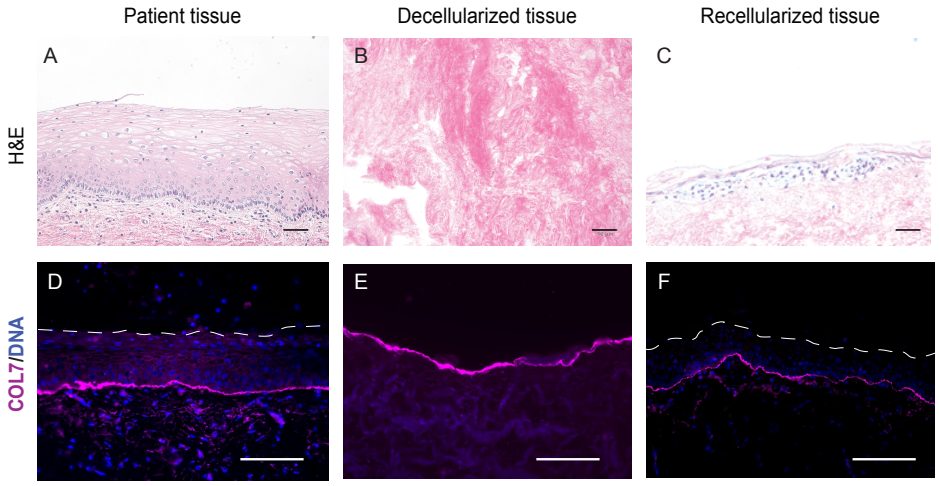

Figure 3.1 Development of a recellularized human ectocervical tissue model.
A recellularized ectocervical tissue model from human ectocervical tissue was developed and histology compared with native patient tissue. While patient tissue (PT) showed abundant nuclei in H&E and DAPI stained sections (A, D), the decellularized tissue lacked nuclear staining (B, E), demonstrating cellular material was effectively removed from the ECM skeleton. Basement membrane integrity was examined by COL7 expression, which revealed intact basement membrane in the decellularized tissue (E), closely resembling that of PT (D). Decellularized ectocervical tissue was used as a scaffold for culture of primary ectocervical cells, with stromal cells seeded in the stromal compartment of the ECM, and epithelial cells seeded on the basement membrane. H&E and IF analysis of recellularized tissue revealed several layers of epithelial cells on top of an intact basement membrane, and stromal cells throughout the ECM (C, F). Scale bars=50 μm.

This indicated the basement membrane remained relatively intact through the decellularization process (Figure 3.1D, E).

To recellularize the DCES, we adapted methods used by Ridky et al to recellularize devitalized dermis scaffolds, with changes (14). Scaffolds generated from 4 patients were seeded with primary ectocervical fibroblasts on the basal side of the DCES, opposite from the basement membrane and cultured for two weeks. Primary epithelial cells from two patients were seeded on the apical, basement membrane side of two scaffolds per patient. Recellularized cervical tissue (RCT) was cultured at an air-liquid interface (ALI) for two weeks (n=4). To evaluate cell localization and tissue architecture, we performed H&E and IF staining, and observed cells throughout the stromal region of the recellularized cervical tissue (RCT), and layers of epithelial cells on top of the DCES (Figure 3.1C,F). Epithelial cells underwent partial differentiation but never reached the full squamous maturation characteristic of native patient tissue. In summary, decellularized ectocervical scaffolds maintain basement membrane integrity and can support long-term culture of primary ectocervical stromal and epithelial cells; however, epithelial cell differentiation was impaired under the conditions tested in our studies.

Development and characterization of organotypic explant ectocervical tissue models

Organotypic culture models have been developed for many human tissues and are a valuable research tool for studying physiology at the tissue level. Previously, we have developed an *ex vivo* female reproductive tract that consisted of organotypic or reconstructed models of murine ovary, and human fallopian tube, uterus, cervix, and liver

in a microfluidic culture system, which supported communication between tissues (*73*). Murine ovarian tissue was engineered to secrete hormones in a pattern that mimics the human hormone cycle by supplementing culture medium with pituitary hormones FSH and LH. Cycling steroid hormones E2 and P4, along with other secreted factors, were circulated between each of the tissues, providing endocrine support over 28 days. While this system is useful for studying tissue-tissue interactions, a less complex method is needed to accelerate studies of ectocervical tissue at the cellular and molecular level.

We aimed to develop a static culture system that would support physiologic responses in ectocervical tissue. To achieve this, we took 3mm biopsy punches of patient cervical tissue that had been trimmed of extra tissue from the stromal side until tissue was approximately 1mm thick and contained both stromal and epithelial regions (Figure 3.2A). Explants were cultured at the air-liquid interface on cell culture inserts for 14-28 days and provided endocrine support through the addition of varying concentrations of exogenous hormones E2 and P4 to mimic hormone signaling during the follicular and luteal phases (FP and LP) of the human menstrual cycle (Figure 3.2B, C), or through co-culture with murine ovarian tissue that was stimulated to secrete human levels of hormones, as we have previously shown (*73*). Interestingly, in the first two weeks of culture, the entire epithelium appeared to detach from the underlying stroma; however, H&E analysis of remaining stromal tissue showed that a basal layer of epithelial cells remained, and these cells then regenerated the differentiated epithelium (Figure 3.3).

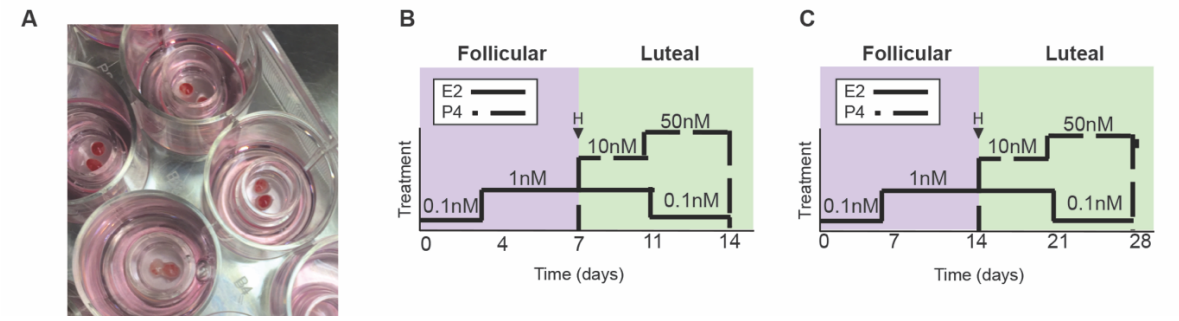

Figure 3.2 Development of an organotypic ectocervical tissue model.
Small biopsy punches were taken from patient tissue that contained both stromal and epithelial regions and cultured at the air-liquid interface (A). Endocrine support was provided with murine ovarian tissue stimulated to secrete human menstrual cycle-like hormones over 28 days, or with step-wise exogenous hormone treatments that mimic normal concentrations of hormones throughout the menstrual cycle in either a 28-day culture, or a reduced 14-day culture, harvesting tissue for analysis mid-cycle after follicular phase (FP) hormones or at the end of the cycle after luteal phase (LP) hormones (B,C).

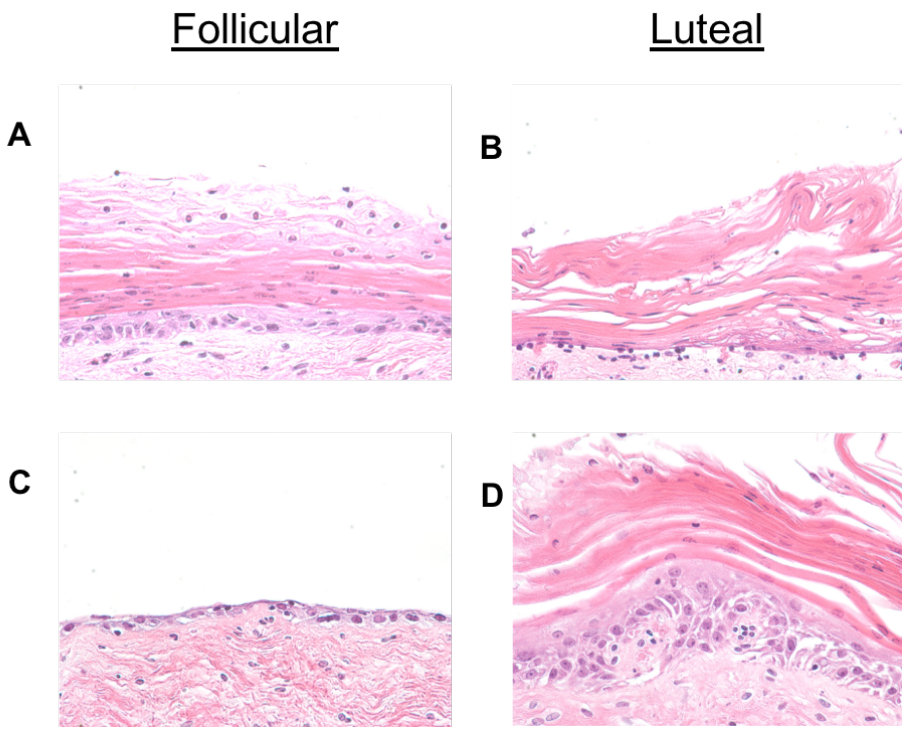

Figure 3.3 Organotypic tissue culture regenerates epithelium after initial shedding. Organotypic cervical tissue models were cultured 14-28 days with murine ovarian or exogenous hormone treatments. While all samples shed their epithelium within a week of culture, a layer of basal cells was left behind (C), which was then able to regenerate layers of cells and remain viable for the entire culture (A, B, D); however, the timing of epithelial regeneration was inconsistent.

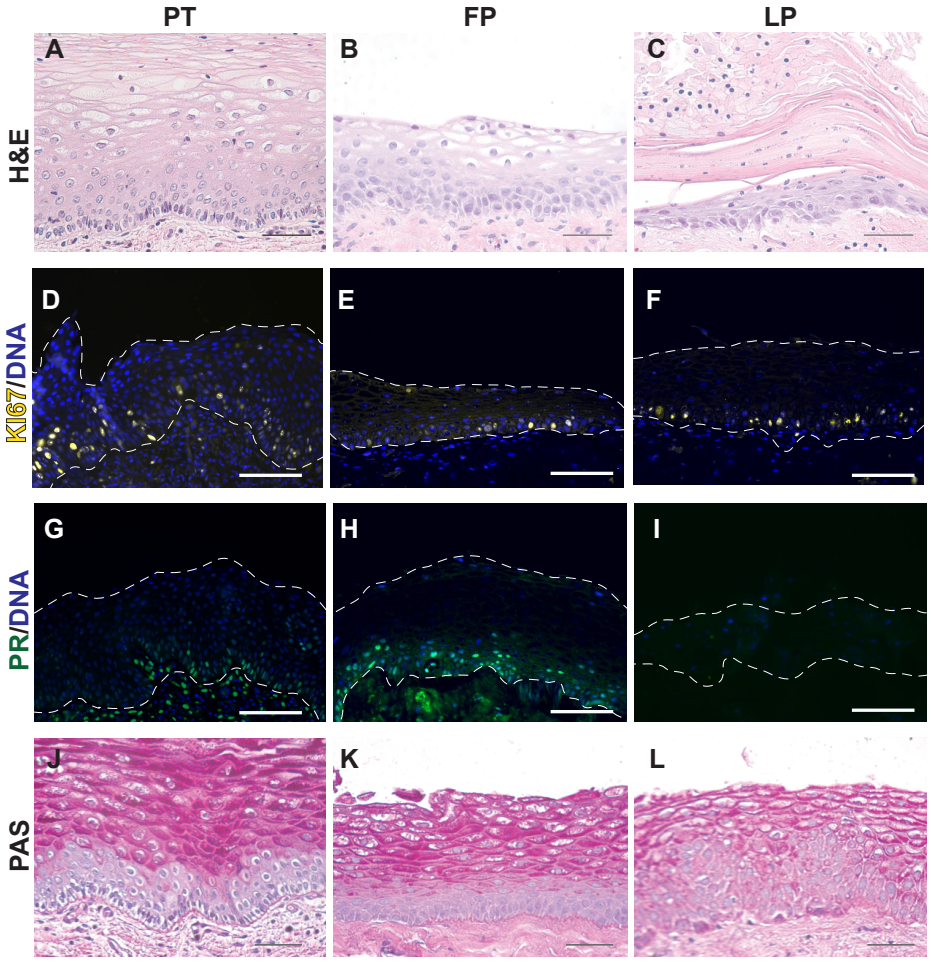

Figure 3.4 Viability, hormone response and glycogenation in ectocervical explants
H&E analysis of explant tissue revealed epithelial cells in different states of differentiation after follicular and luteal phase (FP and LP) hormones (B,C), similar to what is seen in native patient tissue (PT) (A). Immunofluorescence analysis of Ki67 expression revealed that similar to PT (D), cells in explant tissue basal and parabasal layers remained proliferative throughout the 28-day culture (D-F). To assess hormone responsiveness, PR expression was analyzed and revealed that FP explants expressed PR abundantly in basal and parabasal cells (H), while LP explants showed little to no PR expression (I).The presence of glycogenation/mucins was confirmed by PAS stain after FP and LP hormones, and similar to PT (J), intense staining in intermediate and superficial cells after FP and LP hormones was observed with highest intensity in the FP samples (K,L). Scale bars=50um.

After initial shedding and regrowth, H&E-stained sections from tissue harvested after FP (n=12) or LP (n=12) hormones showed that while overall epithelial thickness was decreased, the tissue architecture and epithelial differentiation of explant tissue closely resembled that of PT (n=7) (Figure 3.4A-C). To assess long-term viability of explants, we analyzed Ki67 expression in histological sections from samples harvested after FP (D7 or D14) and LP (D14 or D28) hormones, and found that similar to PT, Ki67 was expressed in basal and parabasal cells of explant tissue after both FP and LP hormones, indicating the tissue remained proliferative for at least 28 days *ex-vivo* (Figure 3.4D-F).

Increased expression of progesterone receptor (PR) is a well-documented physiological response to E2 in human reproductive tissues (*38, 48, 83*). To determine if static culture explants were responsive to E2, we analyzed PR expression in histological sections from samples harvested after FP and LP hormones and found abundant PR expression in basal and parabasal cells after FP hormones (high E2), similar to PT, and little to no expression of PR in explants after LP hormones (low E2, high P4) (Figure 3.4G-I). This suggests that E2 induced expression of PR in ectocervical explants, mimicking *in vivo* physiology. To evaluate glycogenation and mucin production, which are important components of barrier defense, PAS staining was performed. As in PT, we observed abundant glycogenation in intermediate and superficial layers of cells of explants after FP and LP hormones, with increased intensity after FP hormones (Figure 3.4J-L), further validating this physiologic model system. In summary, we found that cycling steroid hormones E2 and P4, from either endogenous or exogenous sources, were sufficient to induce physiologic responses to hormones in explants for at least 28 days *in vitro*.

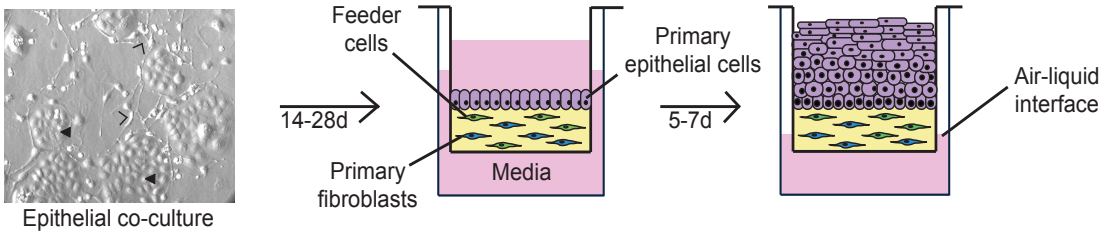

Figure 3.5 Development of engineered ectocervical tissue model
Primary ectocervical epithelial cells (closed arrowhead) were isolated and expanded on J2-3T3 feeder cells (open arrowheads) for 14-28 days. To generate a 3D stromal equivalent, fibroblasts and J2-3T3 cells were embedded in a collagen hydrogel on a cell culture insert. Epithelial cells were then seeded on the hydrogel and submerged in media for 5-7 days. Once a confluent monolayer formed, media was removed from above the cell insert, and cultured engineered ectocervical tissue at the air-liquid interface for 5-7 days to enable squamous differentiation.

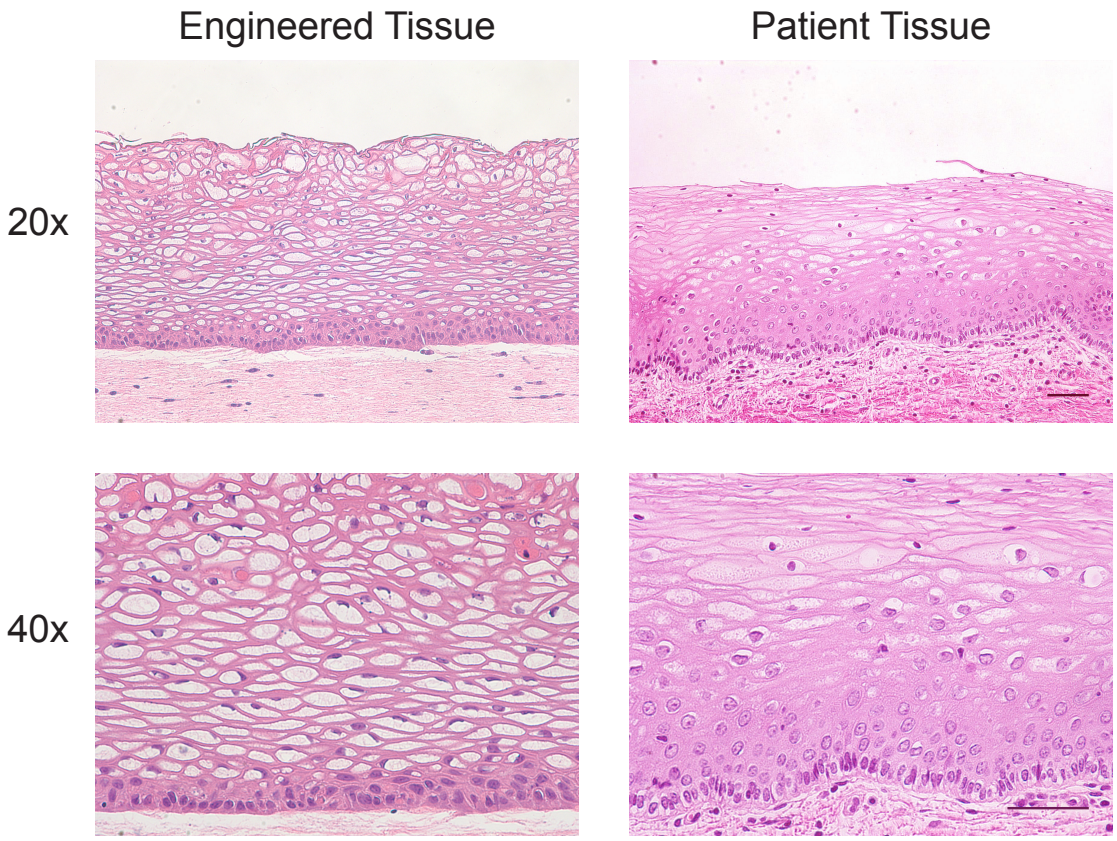

Figure 3.6 Engineered tissue mimics key aspects of normal ectocervical morphology Engineered cervical tissue was cultured at an air-liquid interface with ovarian hormone treatments. H&E staining of histological sections revealed engineered tissue matched the distinct morphology of native patient tissue with cells in multiple states of differentiation. Scale bars=50μm.

Development of engineered ectocervical tissue model

Advances in tissue-engineering such as hydrogel-encapsulation, 3D-printing, and differential cell layering allow reconstruction of complex tissues with compartmentalized cells, including stratified squamous and mucosal tissues, such as skin, cornea and esophagus (*80-82*). These methods rely on isolation/expansion of primary cells, increasing experimental scalability from a single donor. To mimic *in vivo* cervical physiology, we adapted these methods and added physiologic hormones and tissue-specific stroma. Primary ectocervical cells were isolated from benign patient hysterectomy tissue to engineer ectocervical tissue models consisting of well-differentiated epithelia on collagen hydrogel stromal-equivalents containing primary ectocervical fibroblasts and J2-3T3 feeders (Figure 3.5). Feeder cells secrete growth factors that support epithelial differentiation in many 2D and 3D cultures (*80, 84*). However, when only feeder cells were used in collagen hydrogels, epithelial cells in engineered tissue displayed different gene expression patterns than documented responses to E2 and what was observed in patient-matched hydrogels that included both feeder and primary cells. This supported our hypothesis that paracrine signaling from tissue-specific fibroblasts is necessary to model endocrine-signaling and highlighted the importance of the microphysiologic environment in ectocervical mucosa. However, when only primary fibroblasts were used, the collagen contracted, distorting tissue-architecture. To account for this, equal amounts of feeder cells and primary fibroblasts were used. Engineered tissue remained viable 28 days at an ALI and normal tissue architecture was observed. Similar to organotypic culture, endocrine support was provided by step-wise exogenous E2 and P4 over 14-28 days to represent

physiologic concentrations during the FP and LP (Figure 3.2B, C). After 7-28 days, H&E staining of histological sections revealed fully stratified epithelium with correct basal-apical polarization, and cells in different states of differentiation (n=6), recapitulating key features of patient morphology (n=7, Figure 3.6).

Differentiation in engineered cervical tissue

To further investigate differentiation in ECT, we performed IF analysis of differentiation-associated proteins CK13, CK14, P63 and ECAD in histological sections of engineered and patient tissue, and found that CK13, a marker of suprabasal cells in non-keratinized stratified squamous tissue, was expressed abundantly in suprabasal cells of ECT and PT, while basal cell-marker CK14 was expressed in only basal layers (Figure 3.7A-D), indicating basal and suprabasal differentiation. Previous cervical models that used immortalized cell lines resembled a neoplastic phenotype. To evaluate this in our model, we analyzed IF expression of stratification-driver P63, which is expressed in basal and parabasal cells of normal PT but can be expressed throughout the epithelium in neoplastic conditions (85, 86). We observed P63 expression in basal and parabasal cells of engineered tissue indicating epithelial cells maintained the normal differentiation phenotype of benign PT (Figure 3.8A,B). To determine if epithelial cells properly adhered to each other, we evaluated expression of adherens junction protein E-cadherin (ECAD) and observed strong ECAD expression in basal and parabasal cells of ECT, with decreasing intensity in intermediate and superficial layers.

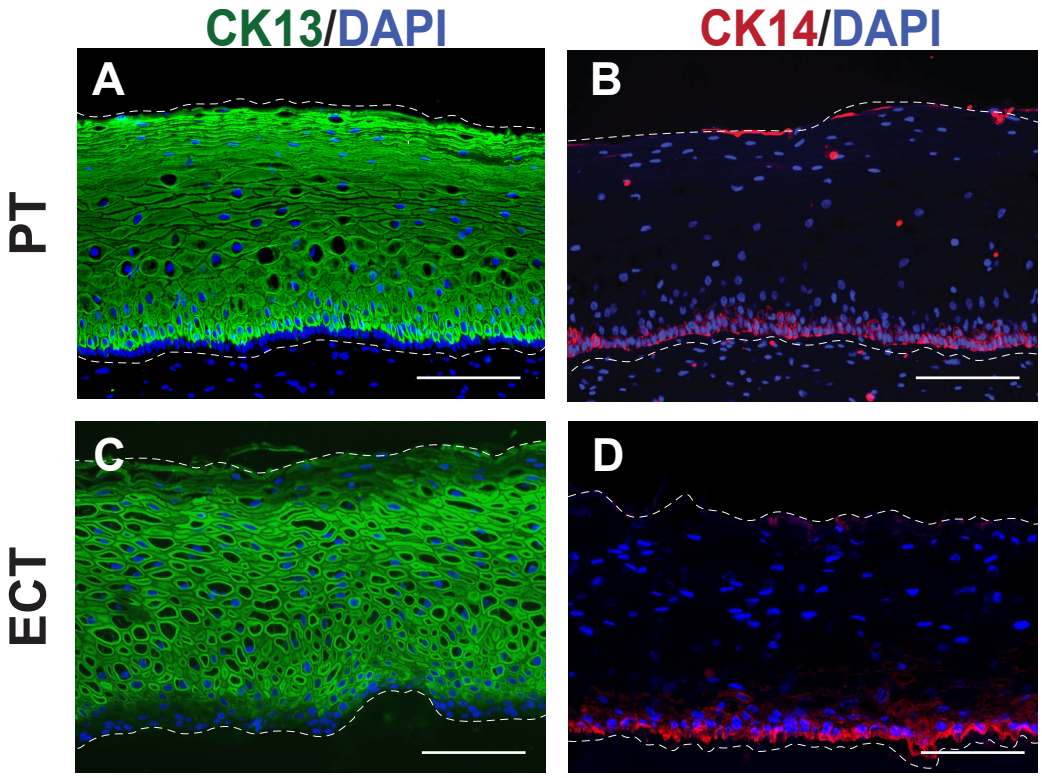

Figure 3.7 Cytokeratin expression in engineered cervical tissue
Engineered cervical tissue differentiated into multiple cell layers with distinct characteristics. Suprabasal cells expressed differentiation marker CK13 in both patient tissue PT and ECT, while basal cells expressed basal-marker CK14 (A-D). Scale bars=50μm.

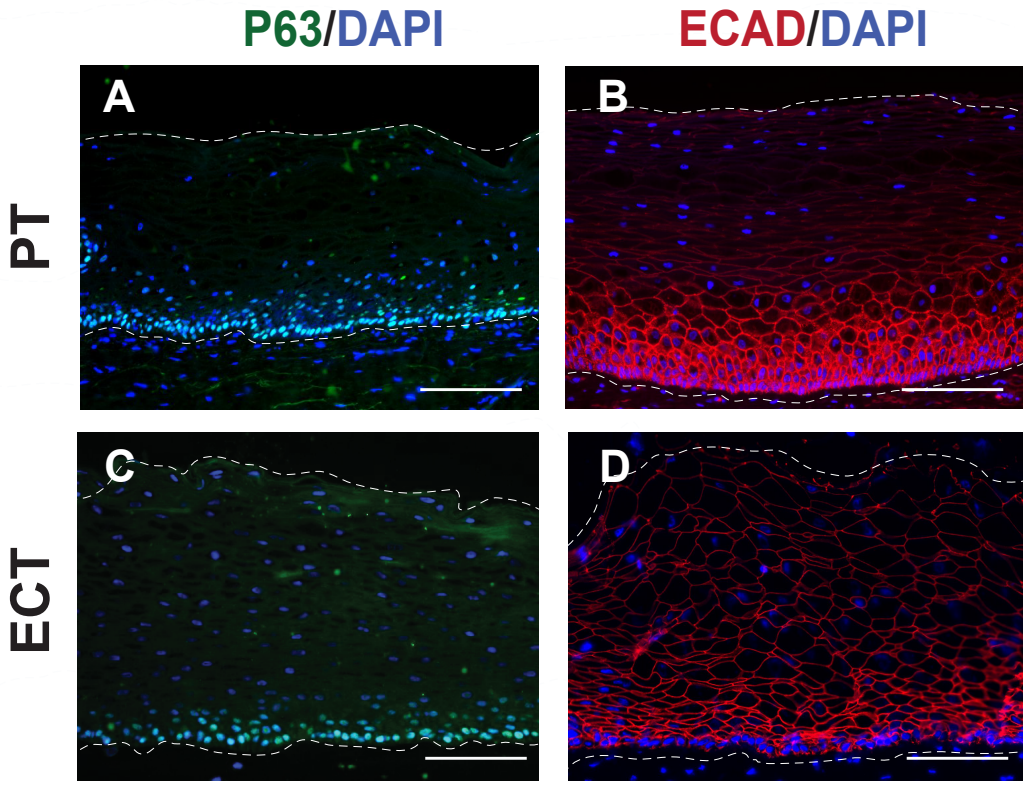

Figure 3.8 Differentiation-associated proteins in engineered ectocervical tissue. Immunofluorescence analysis of P63, a driver of stratification, revealed expression in the nuclei of basal and parabasal cells of ECT and PT (A,B), while analysis of adherens junction protein ECAD showed intense staining in basal and parabasal cell membranes with decreasing intensity in staining as cells become more differentiated in intermediate and superficial cells of ECT, phenocopying expression patterns seen in PT (C,D). Scale bars=50μm.

This is consistent with expression patterns observed in PT (Figure 3.8C,D), and a previous report by Blakewicz et al characterizing junctional protein localization in ectocervical biopsy tissue (4). However, H&E stained-sections showed that engineered tissue cultured without ovarian hormones resulted in a thinner, pseudo-stratified epithelium that appeared to lack intermediate, differentiated cells (Figure 3.9A,B). Immunofluorescence analysis of CK13 expression revealed patchy expression in engineered tissue cultured without hormone treatments, with only the most apical cells matching the staining intensity seen in suprabasal layers after FP hormones (Figure 3.9C, D). This suggested many cells maintained a more basal-like phenotype when cultured without E2 and P4, highlighting the role of endocrine signaling during differentiation. Indeed, ECT cultured at the A/L interface with both paracrine and endocrine support can establish normal cell-cell adhesion and reach terminal differentiation, closely mimicking normal, non-neoplastic ectocervical tissue.

Hormone Responsiveness in Engineered Cervical Tissue

To investigate hormone responsiveness of ECT, we characterized hormone receptor expression and localization through IF and qRT-PCR analysis of ECT during a 14-day exogenous hormone cycle or no hormone treatments (Figure 3.2B). We harvested tissue for analysis after FP (n=3) or LP (n=3) hormone treatments and compared with ECT cultured 7 (n=3) or 14 (n=3) days without hormones and with patient tissue obtained from women in late follicular phase (n=4), when E2 levels are highest, and late luteal phase (n=3), when E2 is low and P4 is high.

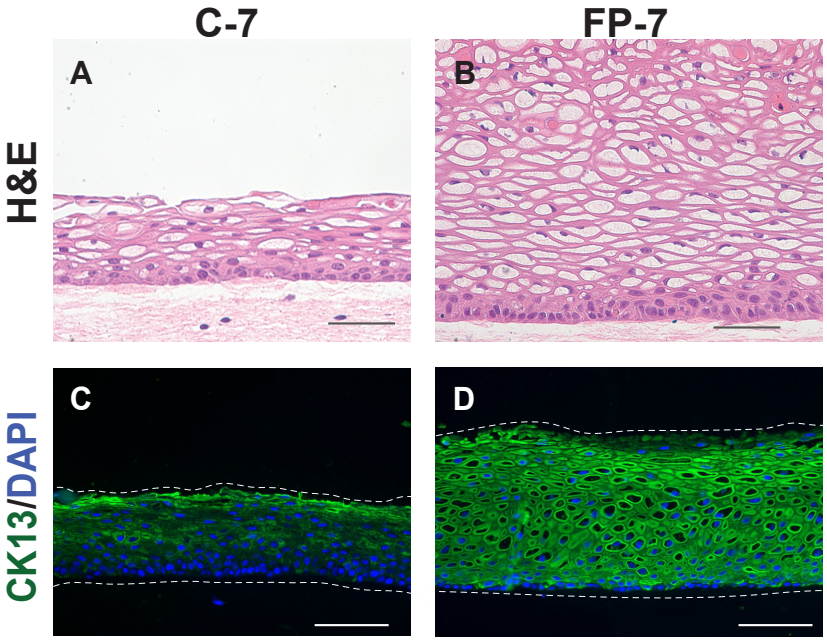

Figure 3.9 Endocrine support necessary for squamous maturation
Engineered cervical tissue (ECT) cultured without ovarian hormones (C-7) showed impaired differentiation compared to ECT cultured with follicular phase hormone treatments (FP-7) as demonstrated by tissue architecture, decreased thickness and lack of CK13-expressing intermediate cells (I-L).

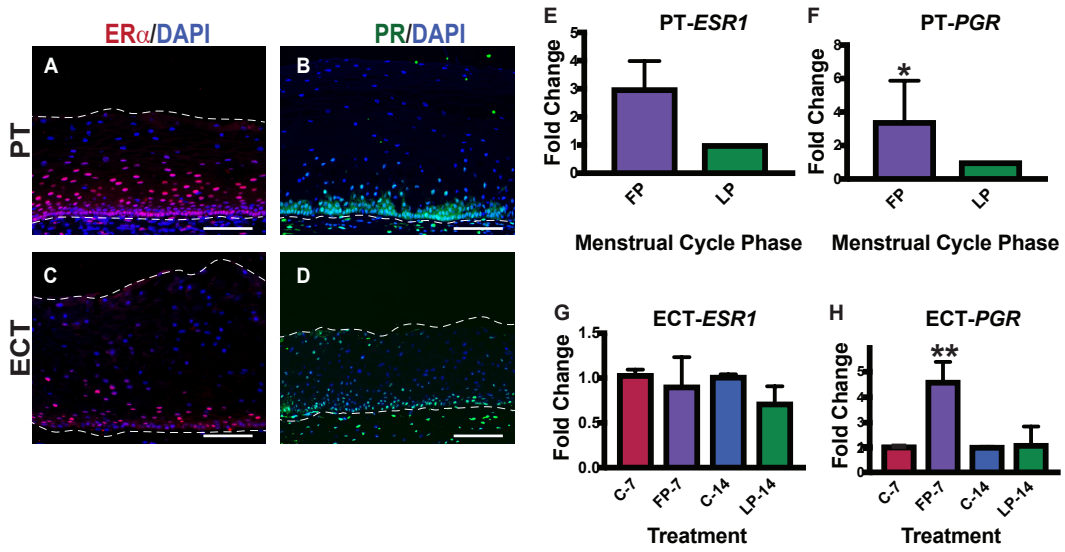

Figure 3.10 Hormone receptor expression in ectocervical tissue.
Immunofluorescence analysis of ERα and PR revealed abundant expression throughout the stroma and in basal and parabasal cells of both patient tissue (PT) and engineered cervical tissue (ECT) (A-D). Analysis of gene expression revealed upregulated PGR in response to FP hormones in engineered ectocervix similar to expression in FP compared to LP patient tissue, while ESR1 expression was not significantly different (E-H). Scale bar=50μm. *$P < 0.05$, **$P < 0.01$.

Immunofluorescence analysis revealed the localization of hormone receptors ERα and PR in engineered tissue phenocopied patient tissue with expression observed throughout the stroma and in the basal and parabasal cells of the epithelium (Figure 3.10A-D). ESR1 expression was not significantly different between follicular and luteal phase samples (Figure 3.10E,G). In contrast, engineered ectocervix harvested after FP hormone treatments showed significantly higher expression of PGR than in engineered tissue harvested after LP hormone treatments ($P = 0.0097$), which is consistent with the pattern seen in patient tissue in which FP expression of PGR was significantly higher than in LP patient tissue ($P = 0.0286$, Figure 3.10F, H). This indicates that ECT cultured *in vitro* with physiologic concentrations of cycling exogenous hormones mimics the physiological response to E2 signaling that occurs across the menstrual cycle *in vivo*.

Much less is known about P4 signaling in ectocervical tissue during the menstrual cycle. However, studies in non-human primate cervical tissue and human vaginal tissue have shown a decrease in epithelial thickness during the luteal phase (*62, 87*). To determine if ECT recapitulated this phenotype, we averaged measurements of epithelial thickness in H&E-stained sections along the entire length of ECT harvested after FP and LP hormone treatments or after 7-14 days without hormone treatments (Figure 5A,B). We observed a significant increase in thickness in FP ECT from day 7 (FP-7), compared to control ECT from day 7 (C-7) (P=0.0039), with FP-7 ECT having an average thickness of 164.7μm, and C-7 samples having an average thickness of 99.64μm. While there was little difference between control ECT from day 7 or 14 (C-7, C-14) and LP ECT from day 14 (LP-14), average epithelial thickness of LP-14 ECT was significantly thinner than FP-7 at 85.09μm

(P=0.0039) (Figure 3.11A,B). It remains unclear if the thinner epithelium in the LP ECT is a direct effect of P4 signaling, or an indirect effect due to low E2 in the LP. This serves as proof-of-concept that ECT is hormone-responsive and recapitulates menstrual cycle phase-specific phenotypes when cultured with physiological levels of ovarian hormones.

Mucin expression in engineered cervical tissue

Mucins are heavily glycosylated transmembrane or secreted proteins that provide lubrication and hydration and contribute to the chemical and physical barrier properties of mucosal tissues. Previously, Gipson et al and Ayehunie et al reported gene expression of mucins 1, 4, and L1 (MUC1, MUC4, MUCL1) in human ectocervical and vaginal tissue; however, protein expression and localization were not investigated (15, 27, 28). There is increasing interest in targeting mucins for drug delivery to treat infection and cancer of mucosal epithelium or through the mucosal epithelium (24, 88). We sought to characterize localization and hormone responsiveness of ectocervical mucins in order to guide future investigations of drug delivery targeting mucins based on cellular location and potential application. We investigated IF expression of MUC1, MUC4 and MUCL1 in histological sections from C-7 (n=3), FP-7 (n=3), C-14 (n=3) and LP-14 (n=3) ECT, and compared to PT from women in early FP (E-FP) (n=3), mid-cycle FP (M-FP) (n=4) and LP (n=3). We found that transmembrane MUC1 was abundantly expressed in intermediate cells in both PT and ECT and absent in other layers, while MUCL1 was abundantly expressed in the membranes of basal and parabasal cells in PT and ECT and absent in intermediate and superficial layers (Figure 3.12A-D).

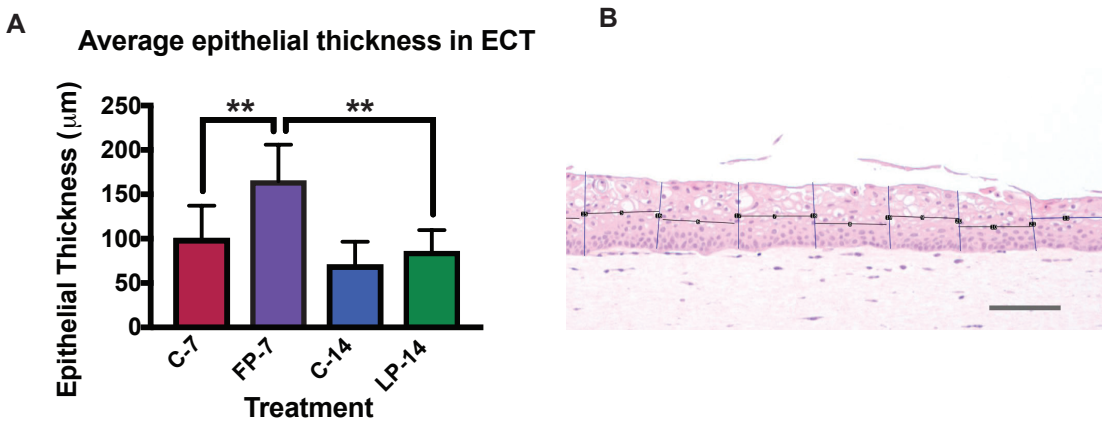

Figure 3.11 Epithelial thickness in engineered tissue
Epithelial thickness of engineered cervical tissue (ECT) from follicular and luteal phase treatments (FP-7, LP-14) or from control ECT (C-7, C-14) was measured and a significant increase in thickness was observed after FP treatments compared to C-7 or LP-14 (A,B). *Scale bar=100um, ** represents P < 0.01.*

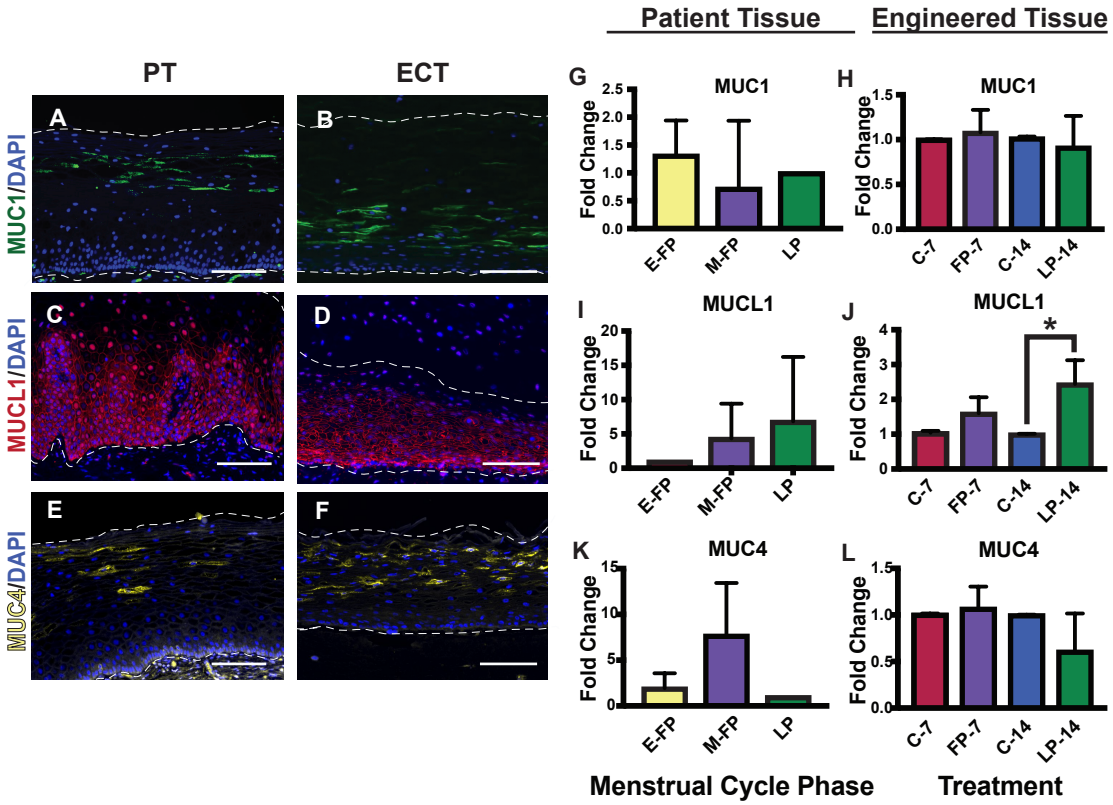

Figure 3.12 Mucin expression and localization in human ectocervical epithelium
Immunoflourescence analysis revealed that localization of ectocervical mucins MUC1, MUC4, and MUCL1 in engineered cervical tissue (ECT) mimicked patterns seen in patient tissue (PT), and expression was dependent on state of differentiation (A-F). Gene expression analysis of ECT revealed that while MUC1 was expressed constitutively across the menstrual cycle, MUCL1 was highly responsive to LP hormones, while MUC4 was not significantly different. Similar expression patterns were seen in PT from different phases of menstrual cycle, indicating ECT produces mucins in *in vivo*-like patterns during the menstrual cycle (G-L). Scale bars=50μm, $*P < 0.05$

In contrast, MUC4 was observed primarily in superficial and intermediate cell membranes (Figure 3.12E, F), but was also observed in parabasal cells of some patients. Interestingly, the proportion of cells staining positive for MUC4 was highly variable between patients in both PT and ECT, and this was not correlated to menstrual cycle phase. To quantify mucin gene expression, we performed qPCR analysis of MUC1, MUC4, and MUCL1 on RNA from C-7 (n=3), FP-7 (n=3), C-14 (n=3) and LP-14 (n=3) engineered ectocervix, and compared to PT from women in E-FP (n=3), M-FP (M-FP) (n=4) and LP (n=3). Expression of MUC1 was not dependent on hormones in patient or engineered tissue (Figure 3.12G, H). MUC4 expression decreased between FP and LP in both patient and engineered ectocervix; however, this did not reach statistical significance in either case (Figure 3.12I, J). MUCL1 in vaginal organotypic models was previously reported to be E2-responsive by microarray (*28*). Our data support this, as we saw an increase in the high-E2 FP of both PT and ECT, compared to low E2 in E-FP or no E2 in C-7 ECT. However, we saw a more significant increase in the LP of both PT and ECT, with approximately a 1.6-fold and 6.8-fold increase in LP compared to early or mid-cycle, respectively (Figure 3.12K). We observed a 2.4-fold increase in MUCL1 expression in LP-14 compared to C-14 engineered tissue ($P = 0.02$) and a 1.5-fold increase between FP and LP engineered ectocervix ($P = 0.02$) (Figure 3.12L). Collectively, we have determined the differentiation-dependent localization of mucins 1, 4 and L1 in human ectocervical tissue for the first time and demonstrated that engineered ectocervix produces mucins in patterns that mimic patient tissue, suggesting engineered ectocervical tissue could be a valuable tool to further our

understanding of the ectocervical mucosal barrier, with implications for infection and disease, drug development, and toxicology studies.

Discussion

In this chapter, we aimed to develop microphysiologic models of human ectocervical tissue for use in a wide range of biological applications. My hypothesis was that recapitulating the natural microenvironment of ectocervical tissue, with the endocrine and paracrine signaling that naturally take place *in vivo,* would enable squamous maturation, hormone response and long-term culture. To test this, we developed three distinct microphysiologic models. First, we considered the use of native cervical ECM as a scaffold for tissue growth. DeGregorio et al previously demonstrated that primary ectocervical epithelial cells could grow and differentiate on cell-specific regenerated ECM secreted by primary fibroblasts (*75*). However, the morphology and cell-cell adhesion differed from what is seen in native tissue. Building on the idea of using cell-specific stroma, we investigated if the native architecture of ECM from tissue that had been decellularized could guide epithelial differentiation in order to reach full maturation. While the cells were able to infiltrate and grow on the DCES, similar to DeGregorio's model, epithelial thickness was decreased compared to PT, and we were not able to recapitulate mature differentiation. Since our group is interested in developing research tools to study mechanisms of disease, we did not move forward with this model for our studies. However, it is worth noting that of the 3 models discussed here, the RCT has the most potential for clinical use. For example, it would be possible to remove diseased cells from a patient's

excised tissue, leaving behind the ECM, and then recellularize the ECM with the same patient's healthy cells, for transplantation or grafting. While additional research is necessary before this can become a reality, it is not beyond the realm of possibilities, as a similar method has been used for years to generate skin grafts for patient use (*89-91*), and more recently, to restore ovarian function (*92*), generate vessels (*93*), or support islet transplantation in mice (*94*). In all of these cases, when the scaffold was reintroduced to the niche environment *in vivo*, normal cell growth and function was resumed. In the case of cervical cancer and pre-cancer, in which the only treatment is to surgically remove affected tissue, the option to replace that tissue with the patient's own regenerated healthy tissue may help improve the negative consequences to fertility associated with these treatments.

Next, a microphysiologic organotypic model system of ectocervical tissue with endocrine support provided by co-culture with murine ovarian tissue or through a step-wise exogenous hormone cycle was developed. We found that similar to our previous *ex vivo* model of the FRT in microfluidic culture, this static culture method supported tissue viability for at least 28 days, and that while ovarian hormones were necessary, whether these came from ovarian tissue secretions or exogenous sources did not affect the results. The tissue responded to E2 by inducing PR expression, and maintained physiologic properties, such as glycogenation, throughout the culture. Some potential uses for this model include infection and toxicology studies, vaccine and drug development, or for basic research of tissue regeneration and differentiation. A benefit is that explant tissue can be used in experiments on the same day it is received, without the waiting period involved in

isolating and expanding cells for tissue reconstruction. However, we found the inconsistent epithelial shedding between patients, and even between samples from the same patient, made it difficult to study changes in proliferation and differentiation that occur over time. Since our goal is to understand how ovarian hormones regulate ectocervical epithelium throughout the menstrual cycle, consistency in the timing of epithelial regeneration is necessary. As such, we focused on a more engineering-based approach, in which we control the timing of epithelial differentiation.

To engineer cervical tissue, we adapted tissue reconstruction methods that have been successful in other stratified culture models, with the additions of tissue-specific stroma for paracrine support, and physiological levels of cycling ovarian hormones for endocrine support. A cervical stromal-equivalent was generated by embedding primary fibroblasts and growth-factor secreting feeder cells in a collagen hydrogel. This stromal equivalent was able to support epithelial proliferation and differentiation and remained viable for at least 28 days. We found that estradiol was necessary for differentiation, and without it, epithelium was thinner and absent of intermediate layers of cells. However, in the presence of hormones, engineered ectocervix reached full maturation, as demonstrated by the *in vivo*-like morphology and proper localization of differentiation proteins CK13, CK14, and P63. Additionally, engineered ectocervical tissue expressed hormone receptors in basal and parabasal layers, and responded to hormones in ways that mimic *in vivo* hormone action, such as E2-induced PR expression, mucin expression regulation, and LP epithelial thinning. Of the 3 models presented, this one was the most representative of *in vivo* biology. The isolation and expansion of cells allowed us to compare different

treatments on the same patient, rather than comparing between patients as in our explant system. This allowed us to identify significant results from a smaller sample size than would be necessary when comparing between samples from different patients. The ability to normalize experimental gene expression with control gene expression from the same patient decreased the standard deviation between experiments, and increased the significance as demonstrated by lower *P* values than what was observed when comparing PT, despite the higher number of samples.

Additionally, we confirmed the presence of ectocervical mucins MUC1, MUC4, and MUCL1 in ECT, and identified the differentiation-dependent localization of these mucins in patient cervical tissue for the first time, which is recapitulated in engineered cervical tissue. Mucins are a vital part of preventing infection and can inhibit the ability of microorganisms to breach the epithelial barrier. Mucins can also bind antibodies, acting as a reservoir of anti-microbial factors (*24, 31, 32*). In many cases, such as in some cancers (*95-97*), abundant mucin production has inhibited drug delivery to its target. However, increasingly, researchers are harnessing this natural defense mechanism for targeted immunotherapy and drug delivery to mucosal tissues, or to increase vaccine efficiency (*22, 33, 88, 98*). The identification of differentiation-dependent mucin localization in the ectocervix will help us develop more efficient drug delivery based on the application. For example, MUC1 appears to be expressed constitutively across the menstrual cycle in the intermediate layers of cells, and so targeting this mucin may increase efficiency of preventative treatments, as these cells come into contact with microorganisms in the vaginal vault. However, for treatment of HPV, it would be more logical to target MUCL1,

which is located in basal and parabasal layers, as HPV establishes infection in basal cells. Accordingly, if the goal is to target a hormone-responsive disease or cancer, we have identified hormonally-regulated mucins.

While engineered cervical tissue has many advantages over other types of culture for studying differentiation, hormone response, and barrier defense, there are also several limitations to this model system. The length of time from acquisition of tissue to completion of an experiment can take up to two months. Additionally, we were unable to recapitulate mature differentiation in cells that had been cryopreserved, which limited the timing of our experiments and number of experiments possible. Previously our group has developed protocols for standardized vitrification and warming and recovery of ovarian tissue for clinical research (*99*)Appendix B). Currently we are focused on adapting these methods to develop cryopreservation techniques for human ectocervix at both the tissue and cellular level that will enable regeneration of epithelium upon warming and recovery, which would exponentially increase the utility of this model. In conclusion, we have developed and validated three microphysiologic models of human ectocervical tissue, which include the endocrine and paracrine signaling that would be present *in vivo*, and outlined the benefits, limitations and potential uses for each. This serves as a useful resource for a number of disciplines, such as virology, toxicology, and oncology, and represents a significant achievement for the inclusion of women in biological research of infections or diseases that present different challenges in women than men, such as HPV-induced cancer. Indeed, this paves the way for a more personalized approach to

gynecological research and will propel much needed research on a critical tissue for women's health.

Acknowledgements

Thank you to Rhitwika Sensharma for help with IHC of patient tissue sections. Thank you to Chloe Williams for help with patient tissue PCR. Thank you to the Skin Disease Research Center and NU Ovarian Histology Core for histological processing and sectioning.

Chapter IV.

Distinct Transcriptional Profiles in Engineered Human Ectocervical Tissue Dependent on Menstrual Cycle Phase

The cervix responds to ovarian hormones throughout the menstrual cycle each month in order to optimize conditions for fertility, while maintaining a chemical and physical barrier against pathological infection. Recent evidence suggests that due to these somewhat opposing functions, there may be a critical window of time in which infection is more likely, as immune defenses are downregulated to increase chances of fertilization (*16, 29*). Additionally, many genes that have previously been shown to be involved in HIV infection (*21, 100, 101*) may be upregulated during the LP, as Yildiz-Arslan et al showed via microarray analysis of gene expression in endocervical tissue. As a primary entry point for HIV and many other sexually transmitted infections, it is important to understand how fluctuating steroid hormones may influence pathogenic infection, so that effective preventative and therapeutic treatments can be developed.

In chapter three, I demonstrated that engineered cervical tissue phenocopied native patient tissue (PT) morphology, responded to hormones, expressed properly localized differentiation-associated proteins and mucins, and remained viable up to 28 days in culture. Out of the 3 models developed in chapter three, the engineered tissue more closely represented *in vivo* biology, making it the best choice for RNA sequence analysis of genes expressed during different phases of the menstrual cycle. In this chapter, I present distinct

biological profiles for human ectocervix during the follicular and luteal phases of the menstrual cycle due to differential transcript-isoform and gene expression in response to ovarian hormones, providing critical insight into ovarian hormone action in ectocervical epithelium during homeostasis.

Materials and Methods

Next generation sequencing

RNA from eight engineered tissue samples analyzed in hormonal experiments in chapter 3 (2µg/sample) from two patients in four different conditions were submitted to the University of Chicago Genomics Facility – Knapp Center for Biomedical Discovery (KCBD) (Chicago, IL) for quality check by BioAnalyzer, generation of cDNA library, and high-throughput sequencing with Illumina HiSeq4000. Raw reads were provided by KCBD for downstream analysis.

Differential gene expression analysis

To map raw reads to the genome, open-source software Tophat2 was used through a UNIX command shell, as previously described (*102*). Reads for all 8 samples and a reference genome (hg_19) were loaded into TopHat2 to identify genomic positions for each fragment, and StringTie (ST) (*103*) was used to assemble mapped data into transcripts and quantify fragments per kilobase per million (FPKM) for each transcript detected. The 'gffcompare' function was used to determine the number of all known and novel

transcripts, genes, introns and exons in merged samples compared to reference genome, and to evaluate precision and sensitivity of alignment. StringTie output files for each sample were loaded into a dataframe in the Ballgown statistical analysis package in R (*104*). For primary analyses, data was filtered to include only genes in which the row variance between samples was greater than one. Genes of particular interest, such as mucins, were evaluated in the unfiltered data. A value of 1 was added to all FPKM values before log2 transformation to inspect distribution of FPKM values. The confounding patient variable was corrected for using the 'stattest' function in Ballgown with argument 'adjustvar=patient'. After filtering, genes found to be differentially expressed between sample groups ($P < 0.05$ by Kruskal-Wallis test) were used in cluster analysis. Each sample was analyzed as the fold change (FC) of FPKM value over the corresponding control FPKM value. ClustVis software (*105*) was used to perform unsupervised hierarchical cluster analysis on the resulting data, which grouped genes and samples by expression similarity.

Gene ontology and functional annotation

Genes that were differentially expressed ($P < 0.05$, FC > 1.5) between FP and LP treatments, and between each treatment and corresponding control (C-7, C-14), were used to compare ontology terms using WebGestalt software (*106*) and DAVID functional annotation software. Webgestalt software assigned genes into overall summary categories for cellular components, biological processes and molecular functions based on the number of genes associated with terms in each category. Resulting graphs are displayed as FC

between FP and LP treatments based on proportion of genes assigned to each category. To further investigate cycle-phase specific ontology, we performed a functional annotation analysis using the online DAVID bioinformatics database (*107, 108*) to compare gene ontologies, pathways, and key terms and group results of each into functional clusters. Genes most highly expressed in FP and LP treatments, as well as those up or downregulated by either FP or LP treatments relative to no hormone treatment control samples were compared. Gene ontology and pathway associations were considered significant when $P < 0.05$.

Quantitative RT-PCR

Quantitative real-time PCR was performed on previously isolated RNA from engineered tissue samples from 3 patients, in 4 conditions each (C-7, FP-7, C-14, FP-14). Two of the patients were the same patients used in RNAseq analysis. Reactions for each condition were run in triplicate using StepOnePlus real-time PCR system (Thermo Fisher) and IDT gene expression assays (Integrated DNA Technologies, IL) to determine relative expression of each gene. Cycle thresholds (Ct) were calculated and normalized with ribosomal 18S (18s rRNA) gene expression as a control. Ct was placed at approximate level where increases in amplification were parallel between samples. Gene expression in engineered tissue was calculated using the $-\log2(\Delta\Delta Ct)$ method, relative to corresponding control for each treatment. All reactions were run 40 cycles (95°C for 15 sec, 60°C for 1 min) after initial 3 min incubation at 95°C.

Results

Data inspection and differential expression analysis

To determine transcriptional changes induced by cycling E2 and P4, RNAseq was performed on 8 engineered cervical tissue (ECT) samples. Patient-matched conditions included: control ECT – no hormone treatment, day 7 (C-7) (n=2), day 7 of FP (FP-7) hormone treatments (n=2), control day 14 (C-14) (n=2), and day 14 of LP (LP-14) hormone treatments (n=2). FastQC was used for quality check of reads and revealed high quality scores across all bases, with approximately 27M human-specific mapping reads per sample. We used TopHat2 software to map raw reads for each condition to the reference genome, which was previously shown to have high precision and sensitivity of alignment at both the transcript and gene-level (*102, 109, 110*). Accurate transcript assembly is dependent on quality of the read alignments, so to determine alignment quality achieved with TopHat2, StringTie (ST) software (*103*) was used to merge the alignments of all samples and compare to reference genome hg_19 (UCSD). The 'gffcompare' was used to calculate base, exon, intron, intron chain, transcript and locus-level sensitivity and precision, as well as total matching, missed, and novel counts (Table 1). We found that samples aligned to the reference genome with 99.3%-100% sensitivity, and 95.2%-98.9% precision, indicating high-quality alignment data for downstream analysis. Additionally, 3756/622,240 exons identified were novel, and 2843/63,216 loci were novel.

Table 4.1 Read alignment summary data

Query mRNAs: 222323 in 63216 loci (192134 multi-exon transcripts)		
Reference mRNAs: 212354 in 60297 loci (185089 multi-exon)		
Matching intron chains	184,461	
Matching transcripts	211,657	
Matching loci	60,297	
Missed exons	0/611773	(0.0%)
Novel exons	3756/622,240	(0.6%)
Missed introns	2302/375,891	(0.6%)
Novel introns	201/377,672	(0.1%)
Missed loci	0/60,297	(0.0%)
Novel loci	2843/63,216	(4.5%)
	Sensitivity (%)	Precision (%)
Base level	100.0	96.9
Exon level	99.9	98.5
Intron level	99.3	98.9
Intron chain level	99.7	96.0
Transcript level	99.7	95.2
Locus level	100.0	95.3

Next, ST was used to compare the merged alignment with individual sample alignments and configure transcript assembly for each using the merged alignment as reference. StringTie output files for each sample were analyzed using Ballgown statistical software in R (*104*). Transcript and gene abundances were measured in fragments per kilobase per million (FPKM). Large differences in distribution of FPKM values between samples can indicate problematic transcript alignment or assembly. To inspect FPKM distribution, abundance values were plotted as log2(FPKM+1) for each. The resulting plot showed that all samples had a similar distribution (Figure 4.1A). Additionally, since most measurements fall below 5, this data suggest only a small fraction of transcripts are expressed at very high levels in these samples.

Ballgown was used to determine differential gene and transcript isoform expression, which automatically applies a log transformation to FPKM values to stabilize variance and fits standard linear models to detect differential expression (*104*). The confounding patient variable was accounted for using the 'stattest' function with the 'adjustvars' argument. We calculated fold change (FC) in gene and transcript FPKM values between treatments, including: C-7 and FP-7; C-14 and P-14; and between FP-7 and P-14 after normalization with the corresponding control for each. We found that 1,775 genes were differentially expressed with $P < 0.05$ between FP and LP treatments, of which 499 were novel. Significance was defined as $P < 0.05$ and FC > 1.5. Of the known genes with $P < 0.05$, 123 genes had a fold change (FC) greater than 1.5 between FP and LP hormone treatments, with 53% of these genes expressed more highly in the LP, and 47% in the FP (Figure 4.1B).

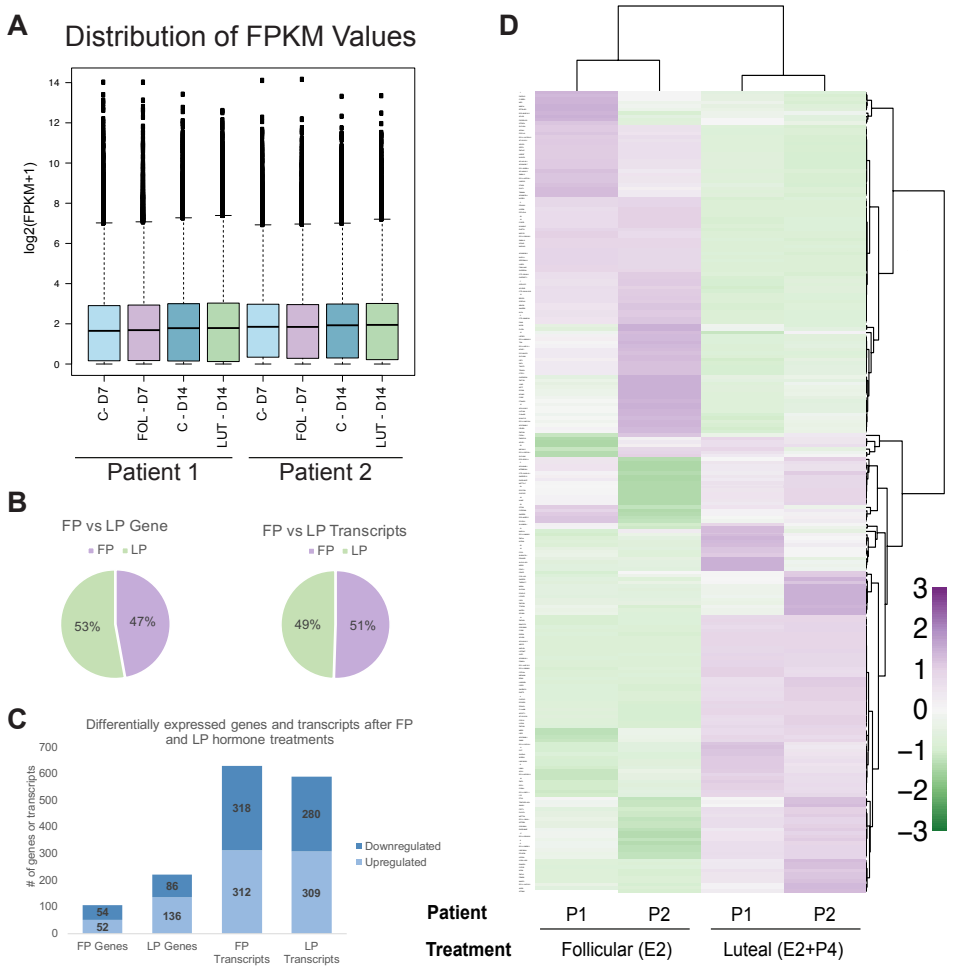

Figure 4.1 Distinct gene expression profiles after hormone treatments
RNA sequence analysis was performed on eight engineered cervical tissue samples exposed to follicular, luteal, or no hormone treatments. All samples showed consistent distribution of transcript fragments per kilobase per million (FPKM) counts, and the low median values demonstrate few very highly expressed genes (A). Of the 113 significant differentially expressed genes ($P < 0.05$, FC > 1.5), 47% were associated with FP treatments, and 53% with LP treatments, and at the transcript level 197 (49%) were associated with the FP, while 193 (51%) were associated with the LP (B). Comparing FP and LP ECT to no hormone treatments showed abundant up- and down-regulated genes and transcript isoforms in response to FP (E2) or LP (E2 + P4) (C). An unsupervised cluster analysis of differentially expressed genes between samples grouped genes and samples into clusters based on expression similarity and revealed two distinct, reciprocal gene expression profiles for follicular and luteal phase hormone treatments (D).

When comparing FP samples to C-7, we found 116 significant differentially expressed genes, of which 51% were down-regulated and 49% were upregulated (Figure 4.1C). LP hormone treatments compared to C-14 revealed 222 differentially expressed genes with $P<0.05$ and $FC>1.5$. Of those, 39% were downregulated and 61% upregulated (Figure 4.1C). At the transcript level we found 531 isoforms with significant differences in expression between FP and LP treatments, of which 139 were novel. Of the 390 known transcript isoforms, 51% were associated with FP and 49% with LP treatments (Figure 4.1B). Comparing FP and LP treatments with controls C-7 and C-14, we found 312 significantly upregulated and 318 significantly downregulated transcripts in response to FP treatments, while LP treatments resulted in 310 significantly upregulated and 281 significantly downregulated transcripts (Figure 4.1C). *Tables of all significant differentially expressed genes and transcripts available as supplementary data.*

Hierarchical clustering reveals two distinct gene profiles in ECT after follicular and luteal phase hormone treatments

To visualize gene expression data, ClustVis software (*105*) was used to perform an unsupervised cluster analysis of significant differentially expressed genes between FP and LP treatments. Samples and genes were clustered based only on expression similarity, which resulted in two distinct gene expression profiles for FP and LP hormone treatments. The results are shown as a heat map, with decreased expression represented by negative numbers in green, and increased expression represented by positive numbers in purple (Figure 4.1D). The heatmap shows striking differences in gene expression in FP and LP

treatments, with genes highly expressed in FP treatments down-regulated in LP treatments and vice versa. This demonstrates that there are two distinctly different genomic profiles in engineered ectocervix based on menstrual cycle phase and highlights the importance of considering physiologic endocrine signaling in the study of reproductive tissues. Additionally, this serves as proof-of-concept that patient-matched engineered tissue, cultured with precisely controlled hormone concentrations can enable the discovery of significant biological insights from small sample sizes.

Gene ontology analysis reveals differentially regulated cellular components, biological processes and molecular functions after follicular and luteal phase hormone treatments

To probe the phenotypes associated with differential gene expression after FP and LP treatments, we compared gene ontology (GO) terms associated with each gene set using Webgestalt online software (*106*), which assigned all significant genes into summary categories associated with cellular components (CCs), biological processes (BPs), and molecular functions (MFs). The proportions of genes assigned to each category after FP and LP treatments were compared, and results are reported as FC, highlighting the distinct differences in representation of genes associated with CCs, BPs, and MFs based on the presence of FP or LP hormones (Figures 4.2-4.4). Cellular components more highly represented in FP samples included endosome, chromosome, vesicle, vacuole, and extracellular matrix, while ribosomes, mitochondria, cell projections, and Golgi apparatus were more highly represented in LP ECT (Figure 4.2).

-

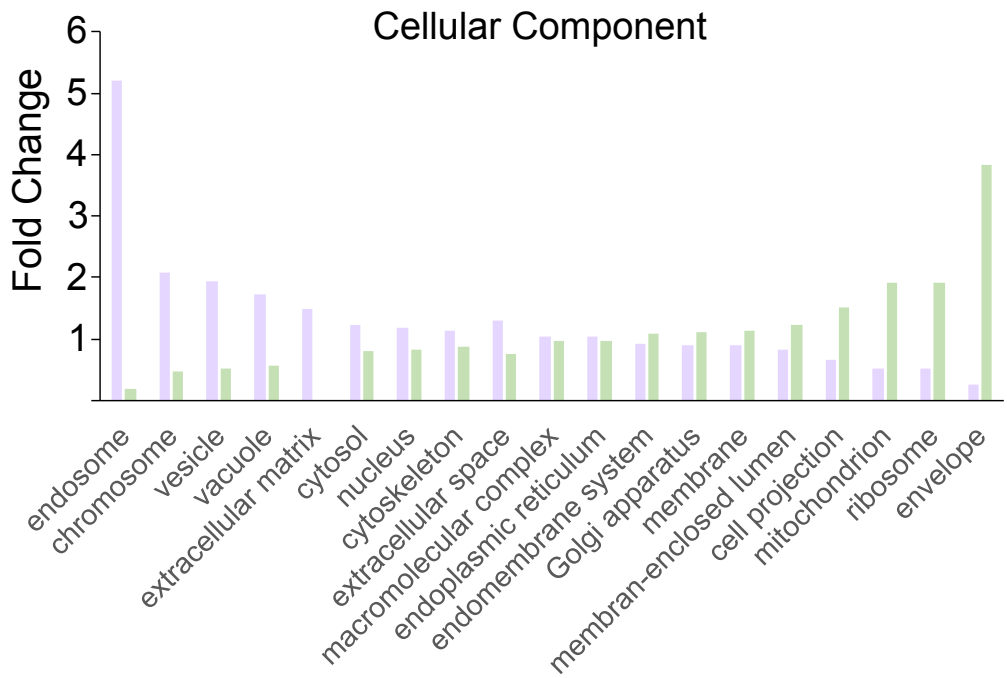

Figure 4.2 Enriched cellular components during follicular and luteal treatments
Comparing the proportions of genes assigned to cellular component ontology categories between follicular and luteal phase (FP, LP) samples revealed high expression of genes associated with endosome, chromosome, vesicle, vacuole, extracellular matrix, nucleus and cytoskeleton in FP samples. Highly expressed luteal phase genes were associated with envelope, ribosome, mitochondrion, and cell projection.

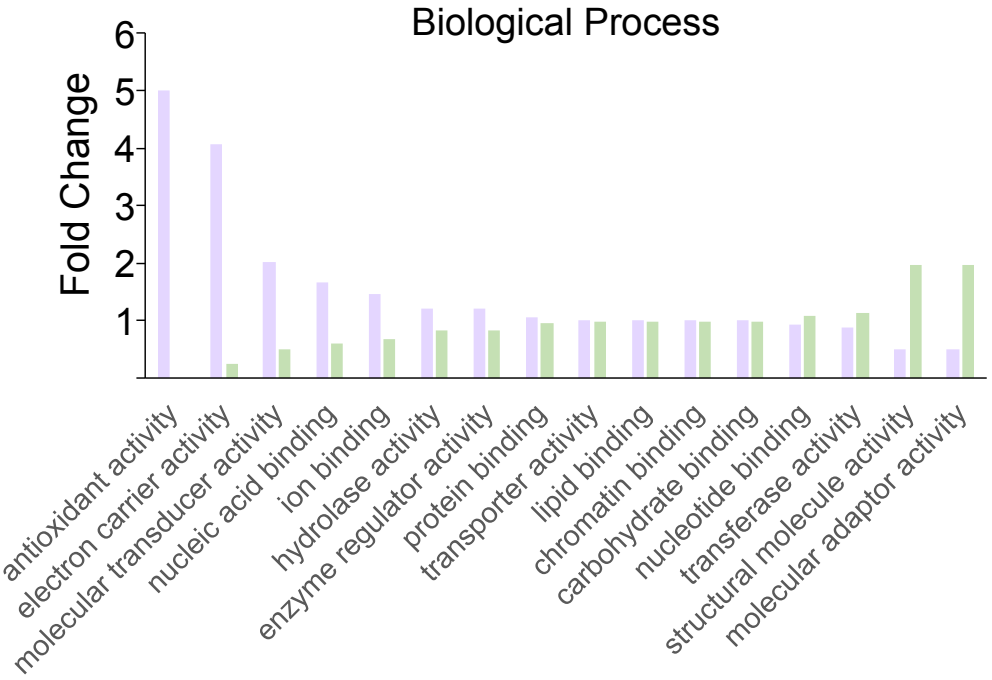

Figure 4.3 Enriched biological processes during follicular and luteal treatments
Comparing the proportions of genes assigned to biological process ontology categories between follicular and luteal phase (FP, LP) samples revealed high expression of genes associated with antioxidant activity, electron carrier activity, molecular transducer activity, and nucleic acid binding in the follicular phase samples, while biological processes enriched in the luteal phase included molecular adaptor activity and structural molecule activity.

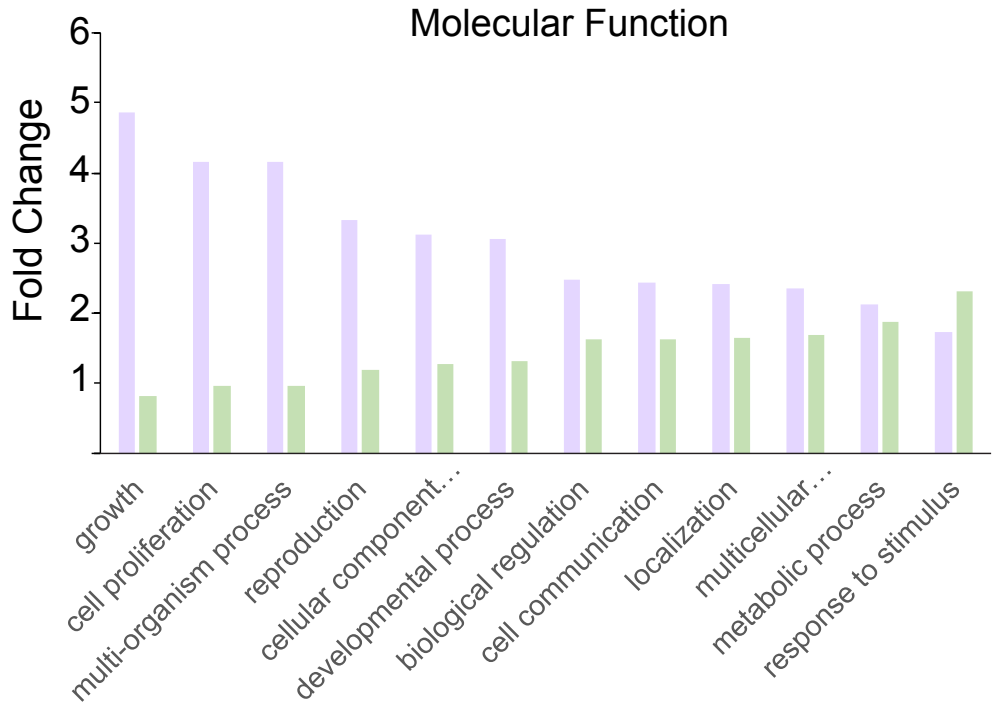

Figure 4.4 Enriched molecular functions during follicular and luteal treatments. Comparing the proportions of genes assigned to molecular function ontology categories between follicular and luteal phase (FP, LP) samples revealed high expression of genes associated with growth, cell proliferation, multi-organism process, reproduction, cellular component biogenesis, cell communication and localization, while molecular functions more highly enriched in the luteal phase included response to stimulus.

Biological processes highly associated with FP samples included antioxidant and electron carrier activity, nucleic acid binding, ion binding and enzyme regulator activity, while those most associated with LP included molecular adaptor, structural molecule and transferase activity (Figure 4.3). Molecular functions associated with FP samples included growth, proliferation, multi-organism process, reproduction, cellular component biogenesis, developmental process, biological regulation, cell localization and communication, and multicellular processes, while MFs associated with LP treatments included response to stimulus (Figure 4.4). These results indicate distinct differences in active CCs, BPs, and MFs in ECT dependent on menstrual cycle phase hormones.

Comparison of genes and functional clusters associated with follicular and luteal phase hormone treatments

To further investigate the profiles summarized by Webgestalt, a DAVID functional annotation analysis was performed, which grouped GO terms from CCs, BPs, and MFs, in addition to KEGG pathways, key processes, and protein-protein interactions into functional clusters most over-represented in each gene set. This resulted in significantly different functional clusters between the FP and LP treatment groups (Tables 4.2-4.3). The FP samples were characterized by genes associated with endosomes and protein transport, such as Solute Carrier Family 35 Member 6 (SLC35F6), Translocase of Inner Mitochondrial Membrane 44 (TIMM44), and Sequestosome 1 (SQSTM1).

Table 4.2 Functional gene clusters highly represented in follicular phase samples

	Functional Clusters	Genes
1	Lysosome, endosome, late endosome	LAMP2, SQSTM1, RAB17, RUFY1, AP5M1, SLC35F6
2	Endosome, protein transport, transport	LAMP2, SLC44A2, RAB17, RUFY1, PARP11, CNIH1, AP5M1, SLC35F6, FXYD5, TIMM44
3	Zinc finger, zinc iron binding, metal binding	ZC3H13, KDM2A, SQSTM1, SYTL4, RUFY1, LTA4H, HERC2, BAZ2B, FBXO11, NR2C1
4	GTPase activity, Nucleotide binding, GTP binding	GTPBP2, PSMC6, EIF5, RAB17, TUBA1A, TIMM44
5	Identical protein binding, chromatin binding, methylation	NONO, PSMC6, SQSTM1, RELA, HCFC1, STAT1, KLHDC3, WASF1, WDR74
6	Transcription regulation, host-virus interaction, and isopeptide bond	MDFIC, RELA, HCFC1, STAT1, NONO, ZC3H13, RPS20, BAZ2B, TUBA1A, RBM25, UIMC1, NR2C1, CCNK, KDM2A
7	Cell adhesion, adherens junctions, cadherin binding involved in cell-cell adhesion	EIF5, HCFC1, STAT1
8	Transit peptide, mitochondria	IMMT, TBRG4, HCFC1, SLC35F6, TIMM44
9	Membrane, glycoprotein, transmembrane helix	ORAI2, ZC3H13, SLC44A2, TMEM214, IMMT, RUFY1, FXYD5, TIMM44, LHFPL2, LAMP2, CFL1, RAB17, ULBP2, SYTL4, RAET1L, HBEGF, AP5M1, CNIH1, SLC35F6
10	Extracellular space, signal peptide, disulfide bond	LAMP2, SLC44A2, TMEM214, ULBP2, RAET1L, HCFC1, HBEGF, SLC35F6, FXYD5

Table 4.3 Functional gene clusters highly represented in luteal phase samples

	Functional Clusters	Genes
1	B-cell receptor signaling pathway, T-cell receptor signaling pathway, chemokine signaling pathway	SOS1, IKBKB, VAV1
2	Golgi apparatus, Golgi membrane	TGOLN2, NDFIP1, ATP8B1, SPPL2B, TRIP10, ITM2B, YKT6
3	Transit peptide, mitochondria	USP30, ECH1, MRPL49, ACAD8, C6ORF203, YKT6, MDH2, GLRX, DDX6, MTFR1
4	Hydrolase, protease, thiol protease	USP30, USPL1, SENP1, ATP8B1, SPPL2B, RNGTT, DDX6
5	Cell projection, cytoskeleton	CSPP1, ITGB1BP1, ABI2, CEP164, TRIP10, CENPJ, FMR1, ATP8B1,
6	Intracellular, transferase, proton acceptor, kinase, ATP-binding, protein phosphorylation	IRAK4, MAP4K5, ZNF738, SOS1, PIK3C3, EDA2R, ZNF816, IKBKB, VAV1, GYS1, YKT6, RNGTT, GLRX, FDFT1, ACAD8, MDH2, DDX6
7	Protein transport	SFT2D1, FMR1, ATP8B1, YKT6, NUP43, GLRX, ITGB1BP1
8	Nucleolus, poly(A) RNA binding, Ubl conjugation	USP30, SP100, FMR1, NDFIP1, IKBKB, UTP14A, DDX6
9	Membrane, transmembrane helix	TGOLN2, SFT2D1, USP30, TMEM187, NDFIP1, ATP8B1, SPPL2B, EDA2R, ZNF816, ITM2B, PAAF1, FDFT1
10	Secreted, extracellular region, glycoprotein	TGOLN2, EFEMP2, SPPL2B, EDA2R, PCYOX1, IGFBP2, ITM2B, MDH2, MIA, NDFIP1

Follicular phase genes also included many associated with zinc and metal binding, such as Bromodomain Adjacent to Zinc Finger Domain 2B (BAZ2B) and Zinc Finger CCCH-Type Containing 13 (ZC3H13). Zinc-binding is involved in transcription and cell cycle, so unsurprisingly many genes associated with chromatin binding and transcription were also highly expressed in FP samples, such as RELA Proto-oncogene NF-KB Subunit (RELA), Signal Transducer and Activator of Transcription 1 (STAT1), and MyoD Family Inhibitor Domain Containing (MDFIC). Genes that play a role in cell adhesion were also enriched, such as Eukaryotic Translation Initiation Factor 5 (EIF5), and Host Cell Factor C1 (HCFC1), as well as a number of glycoproteins and proteins localized to the membrane or extracellular space, such as Heparin-Binding EGF-Like Growth Factor (HBEGF), Transmembrane Protein 214 (TMEM214), and FXYD Domain Containing Ion Transport Regulator 5 (FXYD5).

Genes highly expressed in the luteal phase were associated with Golgi apparatus and mitochondria, such as Trans-Golgi Network Protein 2 (TGOLN), Integral membrane protein 2B (ITM2B), Malate dehydrogenase2 (MDH2) and YKT6 V-SNARE Homolog (YKT6). The Trans-Golgi Network sorts membrane and secreted proteins, many of which are also highly expressed after LP treatments, such as Transmembrane Protein 187 (TMEM187), Insulin-like Growth Factor Binding Protein 2 (IGFBP2) and Integral Membrane Protein 2B (ITM2B).

Table 4.8 Functional gene clusters upregulated by follicular phase E2

	Functional clusters	Upregulated genes
1	Metal-binding, zinc, zinc-finger	THAP7, POLI, POGZ, CNDP2, EPS15L1, ZNF669, ATP11C, NEK11, MAN2A2, ZNF706, RNF141, SLC25A25, ZNF146, ZSCAN32, NARFL, ZZZ3, GNAS, PGGT1B, PHF6, RNF13
2	Nucleus, DNA-binding, transcription regulation	THAP7, POLI, POGZ, TAF8, EPS15L1, ZNF669, COMMD9, NEK11, MSL3, ZNF706, STAT4, H2AFV, MED17, ZNF146, ZSCAN32, NELFA, RPP30, ZZZ3, PHF6, RNF13
3	Cell membrane, plasma membrane	SLC25A30, MAN2A2, RGMB, RNF141, SLC25A25, EPS15L1, GNAS, ATP11C, ADD3, SLC39A1, RNF13, RNF141, MED17, EPS15L1, HSPE1, GNAS, ADD3, SLC39A1
4	Transport, endoplasmic reticulum, transmembrane region	SLC25A30, MAN2A2, SLC25A25, SLC39A1, ATP11C, RNF13, RABEP1, COMMD9

Table 4.9 Functional gene clusters downregulated by follicular phase E2

	Functional clusters	Downregulated genes
1	Lipid degradation, lipid metabolism, hydrolase	DDHD2, LIPG, MUS81, PLA2G4D
2	Transcription, nucleus	CDK1, ANKRD54, KHDRBS3, GEMIN2, HOXA4, VHL, MUS81, FSTL3, HMG20B, GTF3C4, SUDS3, ATF7IP2, MLF1
3	Lipoprotein, cell membrane, plasma membrane	RAB3D, PDPN, IFITM2, LIN7B, ARAP3, ALDH3B1
4	Membrane, transmembrane helix	RAB3D, VHL, PDPN, IFITM2, MTX1, C17ORF62, LIN7B, TMEM42, ICMT, ALDH3B1, PRRG1, LRCH3, ROBO3, ARAP3, MANBAL, PLA2G4D
5	Extracellular region, secreted, glycoprotein	ANKRD54, PDPN, B9D1, LIPG, FSTL3, LRCH3, ROBO3, PRRG1

Additionally, the LP samples showed high expression of genes associated with hydrolase and protease activity, such as DEAD-box helicase 6 (DDX6), Ubiquitin-specific Peptidase L1 and 30 (USPL1, USP30), as well as transferase and kinase activity, such as Interleukin 1 Receptor-associated Kinase 4 (IRAK4), Glutaredoxin (GLRX), and Phosphatidylinositol 3-Kinase Catalytic Subunit Type 3 (PIK3C3). Genes associated with chemokine signaling and B and T-cell receptor signaling, such as SOS1, IKBKB and VAV1 were increased in LP samples. These data represent two distinctly different functional profiles in engineered tissue dependent on FP or LP hormones. However, it cannot be assumed that genes associated with the follicular phase are E2-regulated, as it is possible expression in LP samples was inhibited by P4 signaling, rather than induced by E2 signaling in FP samples, and vice versa.

To further investigate FP and LP gene and functional associations, categories of genes that were up or down-regulated by each treatment were compared relative to samples that were not exposed to hormones (Tables 4.6-7). The FP treatments (0.1nM-1nM E2) up-regulated genes involved in zinc and DNA-binding, such as Pogo Transposable Element Derived with ZNF Domain (POGZ), which plays a role in mitotic cell cycle, and Zinc Finger ZZ-Type Containing 3 (ZZZ3), a member of the chromatin-remodeling ATAC complex. Genes associated with transcription, such as TATA-Box Binding Proteins Associated Factor 8 (TAF8), and Signal Transducer and Activator of Transcription 4 (STAT4) were also upregulated. Additionally, genes associated with membrane components such as Adducin 3 (ADD3), and protein transport, such as Solute Carrier Family 25 Members 20 and 30 (SLC25A25, SLC25A30) were also upregulated.

Table 4.10 Functional gene clusters upregulated by luteal hormones E2 and P4

	Functional clusters	Genes
1	K Homology domain, RNA binding	FUBP3, SNRPA, QKI, CPSF4, AKAP1, JUNB
2	Kinase, transferase	SEPHS2, BCR, UBE2Z, DHDDS, AK1, EPHB2, CDKN1C, GALK2, POMT1, ASMTL, FUT2, AKAP1, POFUT1, LIPT1, MAP3K11
3	protein kinase binding, apoptosis, herpes simplex infection, hepatitis c	PEA15, UBE2Z, TICAM1, JTB, TP53, IGFBP3, TRAF3, SRSF8
4	Transcription, nucleus, DNA-binding	SNAPC5, SUPT3H, SSBP3, FUBP3, FOXK2, TP53, HMGA1, JUNB, CBFB, DVL1, ESRRA, MED25, RHOQ, RGMA, VEGFA, AGRN, SMARCA4, ZBTB47, ZNF282, ZNF646, ZNF35, PHC2
5	Oxidoreductase, NAD(P)-binding domain	GPD1L, RRM2, PHGDH, MICAL1, SESN2, BDH1, GFOD2
6	MAPK signaling pathway, neuron apoptotic process	IL1R1, TP53, TGFB2, MAP3K11
7	Poly(A) RNA binding, mRNA splicing, RNA processing	FUBP3, EFTUD2, SRSF8, FSCN1, SNRPA, QKI, CPSF4, UNK, MYH9, AKAP1, ZNF346, CDC42EP4, KAP1, JUNB
8	Lysosome, lysosomal membrane, endosome	TMEM175, LAMTOR1, ABCA2, KCNK1, TNFAIP1, TRAF3, FUCA1, MFSD12, AP1B1
9	Actin-binding, cadherin-binding	IMPACT, FSCN1, MICAL1, MYH9, EMD
10	Apoptosis	PEA15, UBE2Z, TICAM1, JTB, TP53, IGFBP3, TRAF3, TNFAIP1, ANAPC11, STUB
11	Pathways in cancer, positive regulation of gene expression	BCR, VEGFA, TP53, TGFB2, TRAF3, DVL1, FUBP3, QKI

Table 4.11 Functional gene clusters downregulated by luteal hormones E2 and P4

	Terms	Genes
1	Zinc, zinc-finger, transcription, metal binding, nucleus	GALNT3, KLF6, CNOT8, GEN1, PPM1A, ZNF25, RNF217, CLYBL, ZNF615, TRIM38, ZNF671, DNAJC24, ZSCAN32, ZIK1, NEK4
2	Mitochondrial translation termination, elongation	MRPL2, CKMT1B, PTCD3, CLYBL, DAP3, CBR4, SLC44A1
3	WD40 repeat	WRAP73, WDR77, WDR20
4	Mitosis, cell division, cell cycle	HAUS3, BUB1B, NEK4
5	cell junction, synapse	GRIP1, PSD3, LGI3, GID8
6	serine/threonine kinase, ATP-binding	ALPK1, CKMT1B, OPLAH, RFC2, BUB1B, NEK4
7	Membrane, transmembrane	GALNT3, SLC44A1, CKMT1B, GRIP1, FUT10, PSD3, PPM1A, TIRAP, RNF217, CLYBL, TMEM67, PRRG1, DNAJC24, HECTD4, ERC1, PLA2R1, CMTM4, MEST
8	Glycosylation, secreted, glycoprotein	GALNT3, TMEM67, OVGP1, FUT10, LGI3, TCTN1, PLA2R1, MEST, LGI3

In contrast, the E2 treatments down-regulated lipid metabolism and degradation genes, such as Lipase G (LIPG), and Phospholipase A2 Group IVD (PLA2G4D). Genes that repress transcription such as Activating Transcription Factor 7 Interacting Protein 2 (ATF7IP2) SDS3 Homolog and SIN3A Corepressor Complex Component (SUDS3) were also down-regulated, as were secreted glycoproteins Podaplanin (PDPN) and Follistatin-like 3 (FSTL3).

Luteal phase treatments (1nM-0.01nM E2 and 10nM-50nM P4) resulted in increased expression of genes involved in RNA binding, splicing and processing, such as Far Upstream Element Binding Protein 3 (FUBP3), and Elongation-factor TU GTO binding domain C2 (EFTUD2), and kinase activity, such as EPH Receptor B2 (EPHB2), Adenylate Kinase 1, and Galactokinase 2 (GK2). Genes associated with cytokine and MAPK signaling, such as Jun-B Proto-Oncogene, AP-1 TF Subtype (JUNB), Transforming Growth Factor Beta 2 (TGFB2) and Interleukin-1 Receptor Type 1 (IL1R1) were also up-regulated by LP hormones. Additionally, actin-binding genes involved in cytokinesis and cell motility were upregulated, such as Myosin Heavy Chain 9 (MYH9), Microtubule Associated Monooxygenase, Calponin and LIM Domain C1 (MICAL1) and Emerin (EMD). In contrast, LP treatments down-regulated genes associated with zinc-binding and transcription, such as Zinc Finger Proteins 25, 615 and 671 (ZFP25, ZFP615, ZFP671), and Kruppel Like Factor 6 (KLF6). Genes involved in serine/threonine kinase activity and ATP-binding were also down-regulated, such as Alpha Kinase 1 (ALPK1), 5-Oxoprolinase, ATP-Hydrolysing (OPLAH). Finally, glycosylated and secreted proteins OVGP1, Tectonic Family Member 1 (TCTN1) and others were down-regulated. These data

suggest the dynamic functional profiles for ECT across the menstrual cycle are a result of both complementary and contrasting hormone-receptor mediated events induced by E2 and P4.

Mucin expression in engineered tissue after follicular and luteal phase treatments

Mucins are heavily glycosylated proteins that are an important part of the chemical and physical barrier in ectocervical tissue during homeostasis and can also play a role in cancer progression and metastasis (*22, 95, 96*). Previously, MUC1, MUC4, and MUCL1 gene expression have been reported in ectocervical tissue (*27, 28*) , and we confirmed that ECT mimicked expression and localization patterns of mucins observed in patient tissue (manuscript 1). We examined read-data from RNA sequence analysis to identify other mucin genes expressed in ectocervical mucosa. We found that MUC15, MUC16 and MUC3A are abundantly expressed, while MUC12, MUC13, MUC19, MUC20, MUC22, MUC5B and MUC6 are expressed in low amounts in ECT epithelial cells. Additionally, this suggests many mucin genes may be regulated by ovarian hormones, as we observed higher FPKM values of MUC16, and MUC3A in FP samples, and higher FPKM values of MUC15 in LP samples. To our knowledge, this is the first time these 10 mucins have been identified in ectocervical epithelium. Differential expression suggests that dynamic expression of mucins across the menstrual cycle may result in specific mucosal functional characteristics, which has implications for both infection and reproduction.

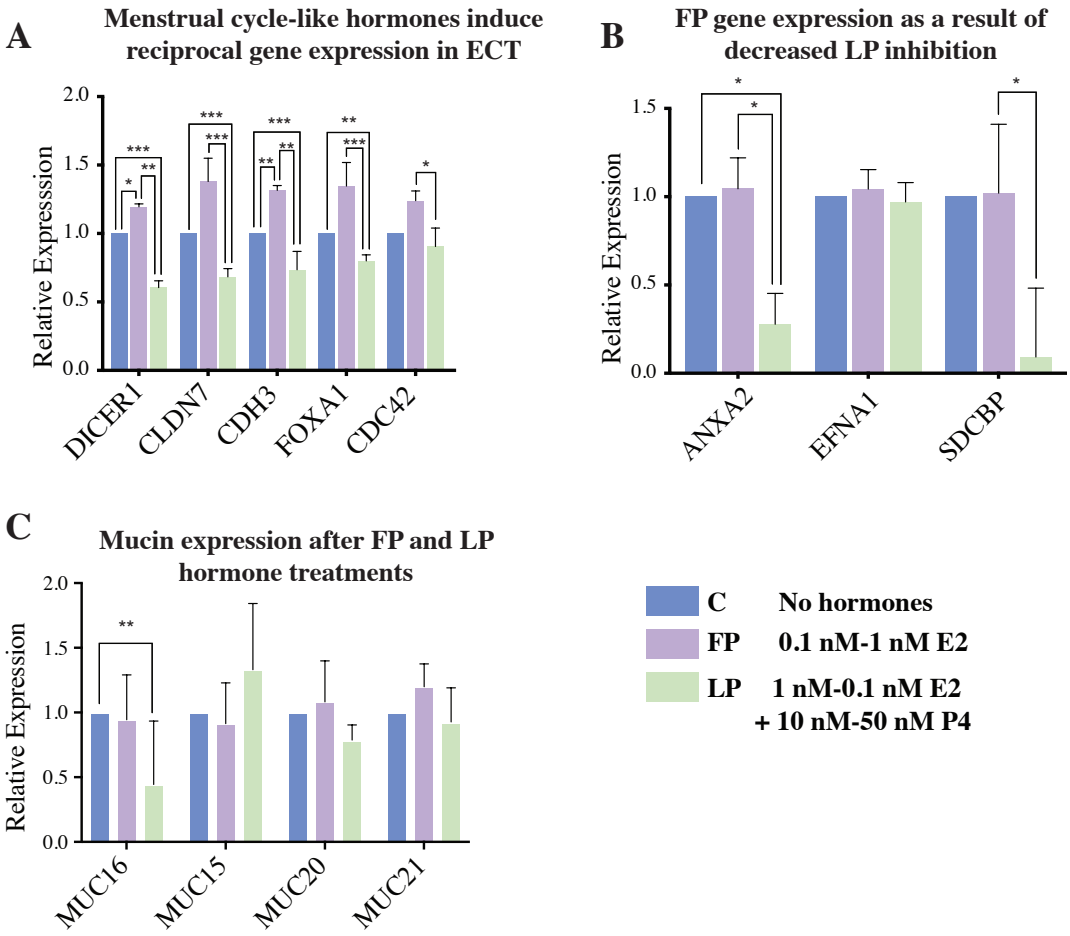

Figure 4.5 Reciprocal gene expression, luteal inhibition, and mucin expression after follicular and luteal phase hormone treatments

To validate RNAseq data, gene expression of selected genes in ECT was analyzed by qRT-PCR (n=3 per group). Resulting data is shown as expression relative to samples that received no hormone treatments. DICER1, CLDN7, CDH3, FOXA1 and CDC42 were upregulated in the follicular phase (FP) samples; in contrast, all were significantly downregulated in the luteal phase (LP) samples (A). Expression of ANXA2 and SDCBP did not seem to be estrogen-responsive but were significantly downregulated in the LP samples. EFNA1 on the other hand was not significantly different between the groups and the control (B). Expression of MUC21, MUC20, MUC15, and MUC16 was identified in RNAseq data. We confirmed by PCR and found that MUC 16 was significantly down-regulated in LP samples. MUC20 and 21 were also downregulated in LP samples, while MUC15 was upregulated, but this did not reach statistical significance. *(*P < 0.05, **P < 0.001, *** P < 0.0001).*

Validation of RNA sequence data by qRT-PCR

To validate RNA sequence data, qRT-PCR was performed probing expression of selected genes from differential expression analysis or genes of interest related to functional categories in ECT after FP (n=3) or LP (n=3) treatments compared to no hormone treatments C-7 (n=3) and C-14 (n=3). Previously, we had investigated CLDN1 and CDH1 expression in ECT, and found no significant difference in expression across the menstrual cycle (data not shown); however, since genes expressed more highly in FP samples were associated with cell adhesion, adherens junctions, and cell communication, we analysed read-data of genes previously shown to be expressed in the ectocervix involved in tight junction and adherens junctions, claudin 7 (CLDN7) and cadherin 3 (CDH3) that may interact with those genes identified in our analysis. Claudin7 and CDH3 (tight junctions, cell adhesion), FOXA1 (transcription), and DICER1 (RNA binding) were all significantly upregulated in FP and downregulated in LP ECT.

Mucin expression in ECT after FP and LP hormone treatments

Mucins are heavily glycosylated proteins that are an important part of the chemical and physical barrier in ectocervical tissue during homeostasis and can also play a role in cancer progression and metastasis (*22, 95, 96*). Previously, MUC1, MUC4, and MUCL1 gene expression have been reported in ectocervical tissue (*27, 28*) , and we confirmed that engineered tissue mimicked expression and localization patterns of mucins observed in patient tissue (Chapter 3). Read-data from RNA sequence analysis identified mRNA transcripts for additional mucins not previously reported in the cervix. We found that

MUC15, MUC16 and MUC3A were abundantly expressed in our samples, while MUC12, MUC13, MUC19, MUC20, MUC22, MUC5B and MUC6 were expressed in low amounts in ectocervical epithelial cells. Additionally, this data suggest many mucin genes may be regulated by ovarian hormones, as we observed higher FPKM values of MUC16, and MUC3A in FP samples, and higher FPKM values of MUC15 in LP samples. We validated expression of four mucin genes by qRT-PCR and found that MUC16 was significantly down-regulated in the luteal phase. To our knowledge, this is the first time mRNA transcripts for these 10 mucins have been identified in ectocervical epithelium. Differential expression suggests that dynamic expression of mucins across the menstrual cycle may result in specific mucosal functional characteristics, which has implications for both infection and reproduction.

Discussion

To determine changes occurring in ectocervical epithelium across the course of the menstrual cycle, we analyzed RNA sequence data of engineered ectocervical after follicular and luteal phase (FP, LP) hormone treatments, and compared to untreated ECT from the same patients. Genes and transcripts most highly associated with follicular and luteal phase treatments were identified enabling the distinct gene profiles for each phase of the cycle. Additionally, we further probed the role of each of the phase-specific hormone combinations (0.1-1nM E2, or 1-0.1nM E2 + 10-50nM P4) to investigate whether genes and functional clusters associated with each phase were expressed in response to the dominant steroid hormone associated with each phase (FP-E2, LP-P4), or simply a result

of decreased inhibitory signaling from the opposing receptor. Our studies indicate that hormone receptors in ectocervical epithelium act in complimentary and antagonistic ways to precisely regulate molecular and biological functions in response to cycling levels of E2 and P4. Indeed, many of the same genes and processes upregulated in the follicular phase are downregulated in the luteal phase and vice versa, highlighting the complementary signaling that occurs between the receptors to precisely regulate gene expression based on menstrual cycle phase.

As is the case in other female reproductive tissues, we found that follicular phase ECT samples were associated with genes involved in proliferation, transcription, chromatin-binding and cell cycle regulation. Additionally, genes associated with membrane components, cell adhesion, and secreted and transmembrane glycoproteins were also more highly expressed in FP samples. Interestingly, when we compared FP samples to control samples, we found that E2 seems to both upregulate and down-regulate the same categories of genes. For example, the four most upregulated functional clusters in response to E2 were: (1) Metal binding, zinc, zinc finger; (2) Nucleus, DNA-binding, transcription; (3) Membrane, cell membrane, plasma membrane; and (4) Transport and transmembrane region. The most highly down-regulated cluster by E2 was lipid degradation and metabolism. Other downregulated clusters included transcription and nucleus, membrane and transmembrane, as well as extracellular and secreted glycoproteins. However, upon further analysis of the genes associated with each category, we found that those which were upregulated had distinctly different functions from the genes in the same categories which were downregulated. For example, E2 downregulates Activating Transcription Factor 7

Interacting Protein 2 (ATF7IP2), which functions to repress transcription, thus E2 indirectly upregulates transcription in addition to the direct upregulation of many genes directly involved in transcription and DNA-binding.

In contrast, LP samples were more highly associated with RNA-binding and signaling. When comparing LP to FP samples, we found LP samples more highly expressed genes involved in insulin-like growth factor signaling, chemokine signaling, as well as B and T cell signaling. When comparing LP samples to control samples, a number of additional signaling pathways were found to be upregulated, such as MAPK, TGFB2, NFKB, and TNFα. LP gene expression also was highly associated with immune response and inflammation, as well as a number of genes involved in viral infection. For example, P4 upregulated expression of FOXK2, which can bind to HIV motifs and regulate viral transcription. The most enriched transcript in luteal vs. follicular phase samples was TLR3, a key component to host immune response. Additionally, IRF7 was found to be highly expressed in luteal phase samples and has been previously shown to play a role in activating transcription of virus-inducible genes.

Additionally, we report the expression of an additional 10 mucins not previously identified in ectocervical tissue, many of which appear to be hormonally-regulated. Mucins play a vital role in both the barrier and reproductive properties of cervical tissue and are increasingly becoming a target for drug delivery to mucosal tissues. Overall our data support the theory that there is a "window of vulnerability" in the ectocervix for infection based on menstrual-cycle phase, with the high progesterone luteal phase being the most vulnerable. This is the first study to characterize differential gene expression throughout

the menstrual cycle by RNAseq analysis in ectocervical tissue and has identified a number of new hormonally-regulated genes in this tissue that may influence susceptibility to infection or could potentially be used as targets for drug delivery or vaccines.

Acknowledgements

Thank you to the University of Chicago Genomics Facility – Knapp Center for Biomedical Discovery for next generation sequencing.

Chapter V.

Discussion and Future Directions

Summary

During each menstrual cycle human cervical mucosa undergoes dynamic changes in response to ovarian steroid hormones E2 and P4 in order to optimize conditions for fertilization during the fertile period, while providing a chemical and physical barrier against pathogenic infection. In order to maintain this barrier, human ectocervical epithelium must undergo constant regeneration. Thus, there must be a balance between proliferation in basal and parabasal cells and differentiation in intermediate and superficial cells to maintain homeostasis. Each of these cell subsets have distinct characteristics that contribute to the barrier defense of ectocervical epithelium, and the localization and expression of hormone receptors, mucins, and cell junctions is dependent on state of differentiation. As such, recapitulating human epithelial morphology and physiology *in vivo* or *in vitro* for the study of barrier defense, infection, or drug development has remained a challenge

Sexually transmitted infections can have devastating effects on women's health, leading to infertility and even cancer. While death from cervical cancer in the United States has continued to decline, Human Papillomavirus (HPV) and resulting neoplasia has remained a large problem. Unfortunately, the treatments available for HPV-induced neoplasia and early stage cervical cancer have not changed over the last few decades, and

surgical removal of affected tissue or total hysterectomy remains the standard of care for even early stage disease, and many women suffer from infertility or impaired fertility as a result (*49, 58-60*). Additionally, developing treatments and vaccines for Human Immunodeficiency Virus (HIV) remains an ongoing challenge. There are many hypotheses about mechanisms of HIV infection; for example, through immune cell recruitment to the stratified epithelium, or through viral entry into the stroma where the virus will encounter immune cells, or through the upper female reproductive tract, where epithelium is simple columnar and easier to penetrate than the lower FRT (*111-115*). Correlative studies suggest a link between progesterone use and increased rates of infection, such as during long-term contraceptive use (*20, 21, 101, 116, 117*), but mechanisms of hormone action during infection remain unclear.

Progress to develop better treatment options or preventative measures has been slow, due to our poor understanding of hormone action on ectocervical epithelium during homeostasis and disease, which is largely due to the lack of physiological models that adequately represent human tissue architecture, barrier properties, and endocrine and paracrine signaling, which all are important for maintain homeostasis. There is an increasing need for the development of 3D human tissue models to study mechanisms of hormone action during homeostasis, infection, and disease of the female reproductive tract. Based on the role of stromal cells in cervical endocrine function in mice (*38, 43, 46*), as well as more recent studies regarding the role of stromal cells in hormonally-regulated cancers (*118-124*), it is clear that in order to accurately model hormone action in ectocervical tissue, tissue-specific stromal cells are crucial. I hypothesized that engineering

the microphysiologic environment, including endocrine and paracrine signaling, would support differentiation, hormone response and long-term culture of human ectocervical tissue. To test this hypothesis, I developed three microphysiologic culture systems of human ectocervical tissue with ovarian hormone signaling and paracrine support from stromal fibroblasts. These models were validated and used for downstream characterization and analysis, as outlined below, and will be a valuable tool for use in future studies.

Discussion and conclusions

Development of 3D human ectocervical tissue models with physiologic endocrine signaling

To model normal cervical morphology during homeostasis, I developed a tissue-engineered stromal equivalent with differentiated epithelial cells and cycling exogenous hormones. This model supports endocrine signaling, and paracrine signaling between epithelium and stroma, and can last at least 28 days in culture. The advantages of this system are the build-from-scratch method, which allows different concentrations of hormones, collagen, and cell type. This would also be valuable for gene deletion or overexpression studies, in which only stromal cells or only epithelial cells are targeted in order to study paracrine signaling. Additionally, this model allows treatment comparisons without the burden of patient variability. While there will always be a high amount of variability between patients, I have shown that when cells are isolated, expanded, and used to regenerate multiple cervical tissues, we can compare controlled concentrations of

treatments between the same patient's tissue, which effectively normalizes for patient variability. Secondly, human ectocervical tissue explants were used in connection with other reproductive tract tissues, including the ovary, which supplied endocrine support over a 28-day menstrual cycle. This system supports tissue-tissue interactions and cross-talk between the entire female reproductive tract in real time, which will be crucial for understanding mechanisms of hormone-regulated diseases in the female reproductive tract, such as endometriosis, fibroids and cervical cancer.

These new model systems are an improvement over previously developed cervical models (*75-77*) as they include both endocrine and paracrine signaling, which supports more *in vivo*-like physiology. However, there are limitations to each of these systems. For example, in the ex vivo FRT model, the ectocervical explants shed their suprabasal epithelial cells after 1-2 weeks in culture. While the tissue is able to regenerate the entire epithelium from the remaining basal cells, it is difficult to study differentiation or barrier properties this way due to the inconsistent timing when this shedding occurs.

The engineered cervical tissue more accurately differentiates, because even though the epithelium is regenerated from only the basal cells, the timing is controlled and stable across experimental conditions, enabling valuable comparisons of differentiation under different hormonal treatments or other factors. However, we are still limited by the need for fresh tissue in this model system. Indeed, cells that have been isolated, expanded, and cryopreserved fail to accurately differentiate upon thawing, resembling a more menopausal-like phenotype in 3D culture. Additionally, we have not yet determined effective methods for cryopreserving intact cervical tissue, so that cells can be isolated at

a later time. Recently, Fox et al described methods for the cryopreservation of cervical tissue explants (*125*), and showed explant cultures could be recovered and cultured up to 14 days; however, cell isolation from the recovered tissues was not investigated. The ability to isolate cells from previously frozen tissue would vastly improve experimental designs and reproducibility and allow the banking of more tissue. Thus, efforts should be made to identify new cryopreservation techniques for ectocervical tissue, such as vitrification, which we and others have previously shown supports ovarian tissue vitrification and recovery (see Appendix B) (*99, 126-128*).

Hormonal regulation of proliferation and differentiation in human ectocervical epithelium

After comparing and validating our microphysiologic systems with native ectocervical epithelium, I asked if normal, pre-menopausal cycling levels of E2 and P4 affected differentiation or barrier properties in this tissue. Histological analysis showed impaired differentiation without the presence of E2 in culture media, and cervical epithelium was thinner, indicating decreased proliferation. Additionally, I performed gene enrichment and pathway analysis comparing luteal and follicular phase genes and found that genes over-represented in the follicular phase were associated with proliferation, growth, differentiation, and cell-cycle, further supporting the role of E2 in these processes. This is consistent with previous studies in animals that showed E2 regulates proliferation and differentiation in the FRT (*38, 40, 43, 46*); however, the hormone receptor-mediated mechanisms of these properties remain unclear in human ectocervical epithelium.

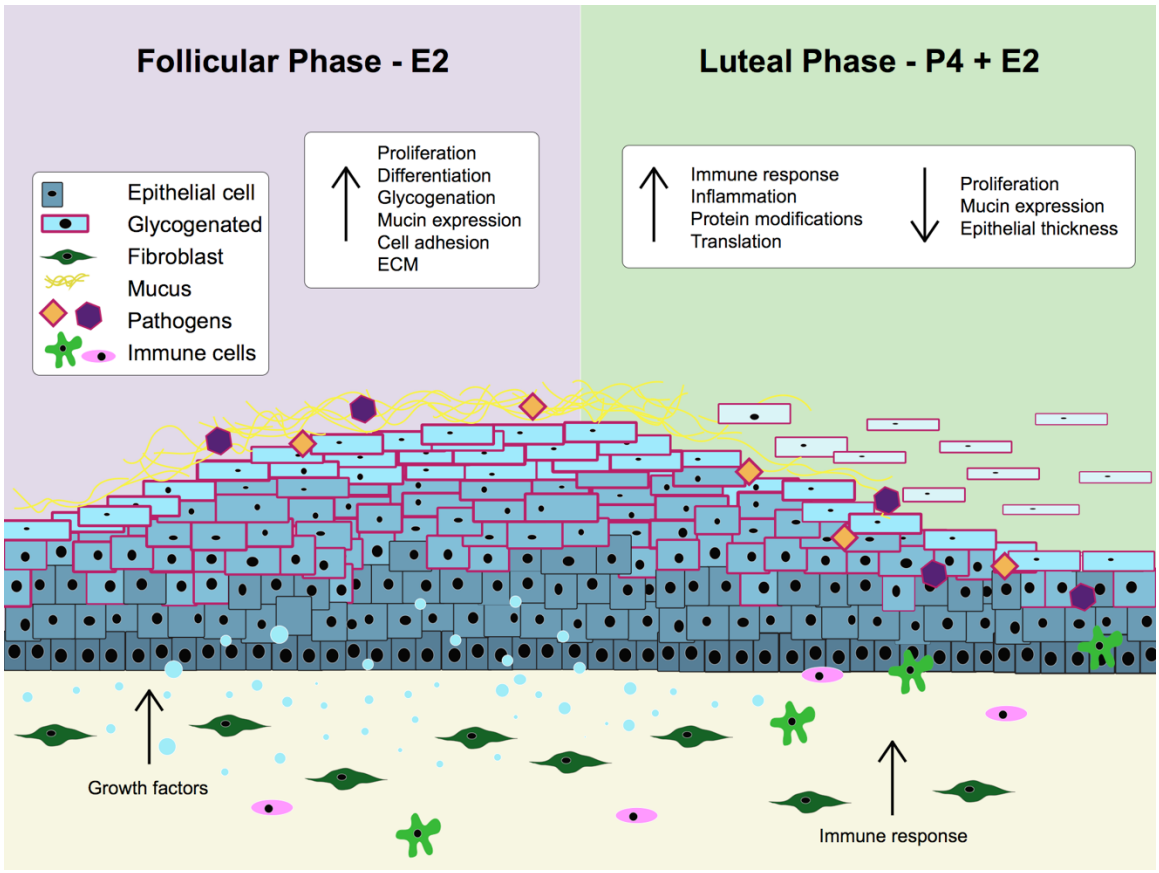

Figure 5.1 Working model of hormonal regulation in ectocervical epithelium across the menstrual cycle.
Our studies demonstrate that a number of barrier properties are upregulated during the follicular phase of the menstrual cycle, including proliferation, differentiation, glycogenation, mucin expression, adhesion, and growth factor signaling. Luteal phase treatments were characterized by increased immune response, inflammation, protein modifications, and decreased proliferation, mucin expression and epithelial thickness, indicating ectocervical tissue may be more vulnerable to infection in the luteal phase of the menstrual cycle.

In the luteal phase, gene ontology analysis showed that in contrast to the follicular phase, growth and proliferation were down-regulated. Additionally, epithelium was significantly thinner than in the follicular phase, more closely resembling the control samples that had not been exposed to hormones. This thinner phenotype in the luteal phase is consistent with studies on the effect of progesterone-based contraceptives on patient biopsy ectocervical and vaginal tissue (*20, 28, 129*), and may increase risk of infection in the luteal phase by allowing microorganisms more proximal access to their target cell types. Figure 5.1 demonstrates our working model moving forward taking these results in to account. Future studies looking at the roles of each receptor and downstream signaling are necessary to further elucidate hormone-regulated differentiation pathways important in homeostasis and disease of human ectocervical tissue.

Mucin expression in human ectocervical epithelium throughout the menstrual cycle

Localization of mucin expression may help determine best therapeutic targets for future medical interventions. While MUC1, MUC4, and MUCL1 gene expression was previously shown in the ectocervix (*1, 27, 28*), localization and hormone response were not investigated. I characterized localization and expression patterns across the menstrual cycle and observed that expression is dependent on level of differentiation, with MUCL1 in the basal and parabasal cells, MUC1 in the intermediate cells, and MUC4 in both superficial and intermediate layers of cells (chapter 4). Moving forward, we can use this knowledge to design more targeted approaches to mucin-bound treatments, based on proximity to therapeutic target cells for individual conditions.

In initial PCR studies, we did not observe a significant difference in mucin expression across the menstrual cycle, though there was a trend of decreased expression of MUC1 and MUC4 in the luteal phase. However, RNA sequencing revealed an additional 10 mucin genes expressed in the ectocervix. MUC15, MUC16, MUC20, and MUC21 were validated by PCR; and all except for MUC15 were down-regulated in the luteal phase, consistent with what we observed in MUC1 and MUC4 expression in our models. This suggests the ectocervical mucosal barrier may be more vulnerable to infection during the luteal phase, when mucins are down-regulated. Additional studies will be necessary to elucidate the role of individual mucins in ectocervical tissue throughout the menstrual cycle.

Gene expression profiles for ectocervical epithelium in the follicular and luteal phases of the menstrual cycle during homeostasis

Charles Wira et al previously showed that ovarian hormones can affect immune cell populations and secreted immune factors in the female reproductive tract, with E2 down-regulating important antimicrobial peptides and immune factors, suggesting a "window of vulnerability," when E2 levels are highest (*3, 16, 17, 29, 130, 131*). In contrast, our studies suggest that E2 enhances many other barrier properties of ectocervical tissue in the follicular phase, such as mucin production, glycogenation, proliferation, and cell adhesion, potentially providing balance to the decrease in barrier defense as a result of decreased immune factors. However, in the P4-dominant luteal phase, we observed

decreased proliferation, mucin expression, and decreased epithelial thickness, along with increased inflammation, and immune response (chapter 4).

Collectively, these results suggest that women in the luteal phase of their cycle, and more broadly, women exposed to high levels of progesterone, may be at higher risk for infection. However, the development of 3D microphysiologic model systems enable an increased understanding of how barrier mechanisms are regulated by ovarian hormones in the cervix and will allow more targeted research for both prevention and intervention of infection and cervical disease in women. The powerful tools described in these chapters will be used to propel research on women's health issues that have for far too long been neglected. To achieve this, it will be necessary to take a multi-faceted approach, which includes hypothesis-based, development-based, and application-based approaches as outlined below.

Future Directions

Define mechanisms of hormone action in ectocervical epithelium

Estradiol and progesterone are key regulators of growth, differentiation and function in a variety of tissues. Estrogen receptor alpha (ERα), estrogen receptor beta (ERβ) and progesterone receptor (PR) are expressed in the human cervix, in both the stroma (ERα, PR) and epithelium (ERα, ERβ, PR). Mouse studies support a role for ERα in proliferation and differentiation of ectocervical and vaginal epithelium (*40, 43, 46*), but

differentiation-dependent roles of ERβ and PR were not investigated. Additionally, mouse ERβ differs from human ERβ in the DNA binding domain, with the murine version more closely resembling ERα, suggesting redundant functions in the cervix. However, in many human epithelial tissues, ERα and ERβ have distinct transcriptional activities, with ERα promoting proliferation, and ERβ promoting differentiation and apoptosis (*132-138*). Additionally, post-menopausal cervical epithelium is characterized by lack of differentiated intermediate layers, and lack of ERβ expression, further suggesting a role for ERβ in differentiation of human ectocervical epithelium.

Additionally, our bioinformatics analysis of recent RNAseq data suggest that in addition to hormone receptors being differentially expressed at the gene level, they may also be differentially expressed at the transcript level. Indeed, preliminary analysis showed differential expression in transcript isoforms dependent on menstrual cycle phase, including estrogen and progesterone receptors. Rigorous, hypothesis-based, mechanistic studies of fundamental biology and signaling will be necessary to tease apart the complex hormone signaling that occurs in this tissue through endocrine and paracrine mechanisms in order to target these pathways therapeutically. I have developed a validated system for investigating these mechanisms, as well as reference profiles for hormone signaling, which will enable a variety of biological, mechanistic and pharmacological research to improve women's health.

Develop resources to increase access to rare tissue

To increase availability of a rare tissue in which many researchers are not able to access, we must develop a renewable resource of reproductive tissue that can easily be shared with other researchers across the country. Differentiating ectocervix-like epithelial cells from induced pluripotent stem cells will act as a critical starting point by providing insight into the common differentiation path through which all FRT cells will progress. Tissue specific factors and decellularized ECM can be used to direct differentiation and known morphology and expression profiles identified in chapter 4 can be used to validate the end product. To achieve this, a three-step approach should be followed: (1) Drive mesodermal lineage through established culture techniques, (2) transfect transcription factors that control the characteristic mechanisms of ectocervix epithelial cells (HOXA13, RUNX1, MSX2), (3) instruct further differentiation through tissue-specific ECM cues, using decellularized extracellular matrix as a tissue scaffold (Figure 5.1). At each step, known lineage and/or tissue-specific markers should be examined, as well as verifying negative results of unintended lineages and tissues. Mullerian duct epithelial markers should be verified (*LIM1, PAX2, PAX8*), and the final cells will express *TP63, CDH1, K13*, *ESR1, PR*, and have a stratified squamous morphology, characteristic of ectocervical epithelium. Cells and protocols can then be shared to exponentially increase the power of women's health research.

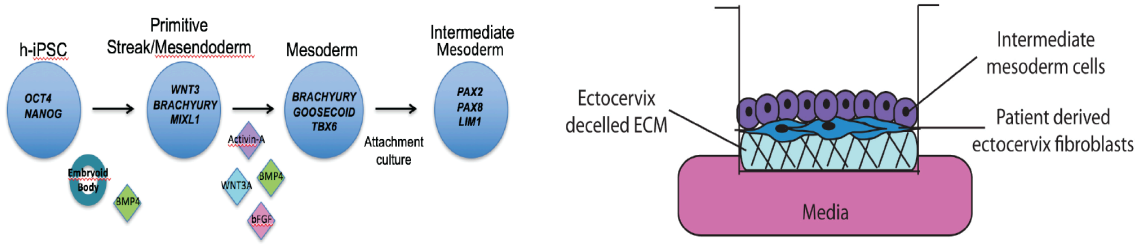

Figure 5.1 Differentiation protocol for iPS derived cervical cells.
Established protocols will be used to establish intermediate mesoderm iPS cells, which can then be cultured on decellularized ectocervical tissue to promote further differentiation.

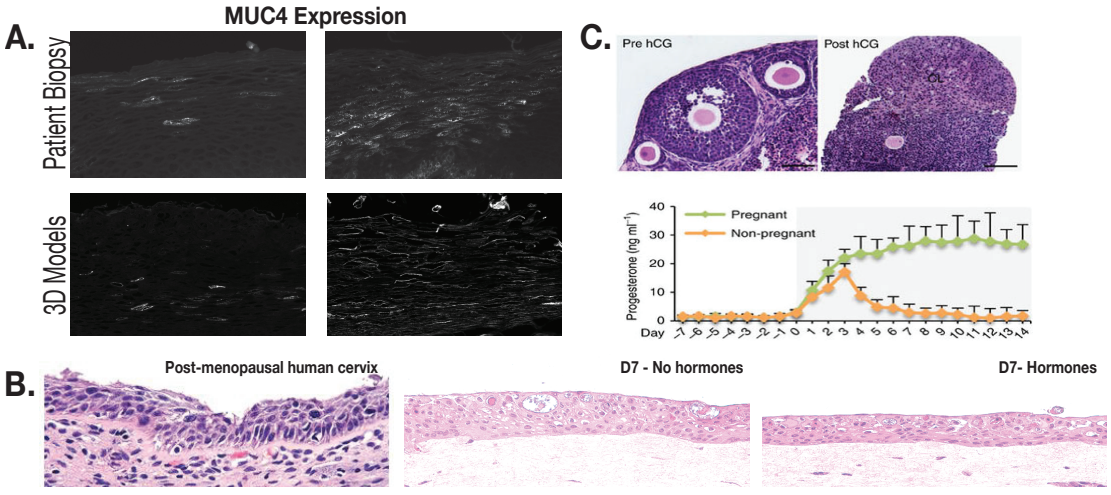

Figure 5.2 Engineered cervical tissue cycles for personalized medicine.
We are now closer than ever to the development of personalized disease and drug studies. Here we show proof-of-concept that 3D cervical models retain MUC4 expression patterns of the patient tissue from which they were obtained (A). Additionally, post-menopausal cells in 3D culture maintained a post-menopausal phenotype even in the presence of pre-menopausal levels of hormones (B). And finally, we've shown in chapter 3 we can simulate pregnancy levels of hormones in the murine ovary (C), these methods could also be applied in co-culture with human ectocervical tissue model to study changes occurring in the cervix during pregnancy.

Personalized disease models for precision medicine

As microphysiologic culture conditions and technology continue to improve, we are becoming closer than ever to personalized medicine, which will allow precise, patient-specific treatments. We have previously shown that engineered ectocervical tissue maintains the phenotype of the person from whom the cells were isolated, even though cervical tissue is completely regenerated from only the basal cells. For example, some patients highly expressed MUC4, while others hardly expressed MUC4 at all, and the same patterns returned in the regenerated epithelium (Figure 5.2A). Additionally, cells isolated from post-menopausal women that were used in the 3D models, maintained the undifferentiated phenotype associated with menopause, even in the presence of cycling ovarian hormones (Figure 5.2B). My hypothesis is that cells isolated from cervical cancer epithelial biopsies, or biopsies of cervical intraepithelial neoplasia will also maintain their phenotype as we have observed so far in this system. This would represent a major milestone for women's health, as the options for disease modeling are endless. Improved treatments could prevent the morbidity associated with infections and progressive cervical disease, preserving fertility and preventing invasive surgical procedures.

Additionally, we have previously engineered the human menstrual cycle in mouse ovaries and can also engineer pregnancy-like levels of hormones (*73*), to study the changes that occur in reproductive tissues during pregnancy (Figure 5.2 C). Connecting the pregnant ovary mimic to engineered ectocervical tissue with microfluidics will allow the study of early pregnancy-related changes in the cervix. Our validated model systems are valuable tools for identification of novel hormone responsive factors and pathways that

regulate cervical epithelium and could lead to new targets for therapeutic intervention against STIs, infertility, as well as cervical cancer, or in the development of new contraceptives. Additionally, future studies will provide insight into how these mechanisms are altered in response to disrupted hormone cycles, such as during pregnancy, menopause, and hormonal contraceptive use, having the potential to significantly impact women's health.

Closing thoughts

As mentioned previously, death from cervical cancer in the United States has continued to decline. However, it should be noted this is not the case for all women. In fact, LGBT women, women of color, and low-income women are much more likely to develop HPV-induced cervical cancer due to not having access to or avoiding preventative screening (*139-142*). Of course, these minority populations are not more biologically susceptible to HPV. However, due to mistreatment or mistrust, or lack of access to preventative healthcare for financial/geographical reasons, these women avoid getting screened for pre-cancerous lesions. They are more likely to not know of their pathology until later stages of cancer, which are characterized by higher morbidity and mortality (*139, 140, 143*). Additionally, minorities are more likely to smoke, use illicit drugs, binge drink, or have poor nutrition, all of which have been shown to correlate with increased risk of HPV-induced cervical cancer (*117*). This is where the disciplines of social science and life science intersect, and creative solutions are needed.

Thus, it is clear that in addition to the scientific aims listed above, increased educational outreach and increased access to reproductive care is deeply needed for women in minority communities. The educational outreach can be achieved through developing online resources and engaging the community through social media, blogging, or other platforms. Additionally, community outreach events promoting women's health will bring real research that matters to women in the community, while establishing a trust between citizens and scientists. In this hyper-political environment, it's increasingly important to be a non-biased authoritative source of scientific information for the community, about issues that affect them.

Similar to the endocrine loops that occur between pituitary and ovary, ovary and cervix, and the paracrine loops between fibroblasts and epithelial cells, all of this is connected. Complex signaling networks regulate homeostasis in the cervix – and complex, nuanced signaling between scientists, educators, policy makers, and the public regulate homeostasis in the community. I hypothesize that both can be achieved and maintained through the interdisciplinary approach I outlined above.

References

1. I. K. Gipson, Mucins of the human endocervix. *Front Biosci* **6**, D1245-1255 (2001).
2. C. L. Sentman, C. R. Wira, M. Eriksson, NK cell function in the human female reproductive tract. *Am J Reprod Immunol* **57**, 108-115 (2007).
3. C. R. Wira, J. V. Fahey, C. L. Sentman, P. A. Pioli, L. Shen, Innate and adaptive immunity in female genital tract: cellular responses and interactions. *Immunol Rev* **206**, 306-335 (2005).
4. C. D. Blaskewicz, J. Pudney, D. J. Anderson, Structure and function of intercellular junctions in human cervical and vaginal mucosal epithelia. *Biol Reprod* **85**, 97-104 (2011).
5. C. T. Capaldo, A. Nusrat, Cytokine regulation of tight junctions. *Biochim Biophys Acta* **1788**, 864-871 (2009).
6. L. Shen, C. R. Weber, J. R. Turner, The tight junction protein complex undergoes rapid and continuous molecular remodeling at steady state. *J Cell Biol* **181**, 683-695 (2008).
7. G. I. Gorodeski, Estrogen decrease in tight junctional resistance involves matrix-metalloproteinase-7-mediated remodeling of occludin. *Endocrinology* **148**, 218-231 (2007).
8. M. E. Cuevas *et al.*, Estrogen-dependent expression and subcellular localization of the tight junction protein claudin-4 in HEC-1A endometrial cancer cells. *Int J Oncol* **47**, 650-656 (2015).
9. M. Hata *et al.*, Estrogen decreases the expression of claudin-5 in vascular endothelial cells in the murine uterus. *Endocr J* **61**, 705-715 (2014).
10. M. Someya *et al.*, Regulation of tight junctions by sex hormones in normal human endometrial epithelial cells and uterus cancer cell line Sawano. *Cell Tissue Res* **354**, 481-494 (2013).
11. C. Cunniffe, B. Brankin, H. Lambkin, F. Ryan, The role of claudin-1 and claudin-7 in cervical tumorigenesis. *Anticancer research* **34**, 2851-2857 (2014).
12. J. Hernandez-Monge *et al.*, Papillomavirus E6 oncoprotein up-regulates occludin and ZO-2 expression in ovariectomized mice epidermis. *Experimental cell research* **319**, 2588-2603 (2013).
13. E. R. Boskey, R. A. Cone, K. J. Whaley, T. R. Moench, Origins of vaginal acidity: high D/L lactate ratio is consistent with bacteria being the primary source. *Human reproduction (Oxford, England)* **16**, 1809-1813 (2001).
14. E. R. Boskey, K. M. Telsch, K. J. Whaley, T. R. Moench, R. A. Cone, Acid production by vaginal flora in vitro is consistent with the rate and extent of vaginal acidification. *Infect Immun* **67**, 5170-5175 (1999).
15. I. K. Gipson, S. Spurr-Michaud, A. Tisdale, B. B. Menon, Comparison of the Transmembrane Mucins MUC1 and MUC16 in Epithelial Barrier Function. *PLOS ONE* **9**, e100393 (2014).
16. C. R. Wira *et al.*, Epithelial cell secretions from the human female reproductive tract inhibit sexually transmitted pathogens and Candida albicans but not Lactobacillus. *Mucosal Immunol* **4**, 335-342 (2011).
17. C. R. Wira, M. V. Patel, M. Ghosh, L. Mukura, J. V. Fahey, Innate immunity in the human female reproductive tract: endocrine regulation of endogenous antimicrobial protection against HIV and other sexually transmitted infections. *Am J Reprod Immunol* **65**, 196-211 (2011).
18. A. J. Quayle *et al.*, Gene expression, immunolocalization, and secretion of human defensin-5 in human female reproductive tract. *Am J Pathol* **152**, 1247-1258 (1998).
19. J. F. Tomee, P. S. Hiemstra, R. Heinzel-Wieland, H. F. Kauffman, Antileukoprotease: an endogenous protein in the innate mucosal defense against fungi. *J Infect Dis* **176**, 740-747 (1997).
20. A. Tjernlund *et al.*, Progesterone-based intrauterine device use is associated with a thinner apical layer of the human ectocervical epithelium and a lower ZO-1 mRNA expression. *Biol Reprod* **92**, 68 (2015).

21. J. Deese *et al.*, Injectable Progestin-Only Contraception is Associated With Increased Levels of Pro-Inflammatory Cytokines in the Female Genital Tract. *Am J Reprod Immunol* **74**, 357-367 (2015).
22. A. Amini, S. Masoumi-Moghaddam, D. L. Morris, in *Utility of Bromelain and N-Acetylcysteine in Treatment of Peritoneal Dissemination of Gastrointestinal Mucin-Producing Malignancies,* A. Amini, S. Masoumi-Moghaddam, D. L. Morris, Eds. (Springer International Publishing, Cham, 2016), pp. 43-61.
23. B. Sperandio, N. Fischer, P. J. Sansonetti, Mucosal physical and chemical innate barriers: Lessons from microbial evasion strategies. *Seminars in Immunology* **27**, 111-118 (2015).
24. A. Chen *et al.*, Transient Antibody-Mucin Interactions Produce a Dynamic Molecular Shield against Viral Invasion. *Biophysical Journal* **106**, 2028-2036 (2014).
25. A. L. Radtke, A. J. Quayle, M. M. Herbst-Kralovetz, Microbial products alter the expression of membrane-associated mucin and antimicrobial peptides in a three-dimensional human endocervical epithelial cell model. *Biol Reprod* **87**, 132 (2012).
26. I. K. Gipson *et al.*, MUC4 and MUC5B transcripts are the prevalent mucin messenger ribonucleic acids of the human endocervix. *Biol Reprod* **60**, 58-64 (1999).
27. I. K. Gipson *et al.*, Mucin genes expressed by human female reproductive tract epithelia. *Biol Reprod* **56**, 999-1011 (1997).
28. S. Ayehunie *et al.*, Characterization of a Hormone-Responsive Organotypic Human Vaginal Tissue Model: Morphologic and Immunologic Effects. *Reproductive sciences (Thousand Oaks, Calif.)* **22**, 980-990 (2015).
29. D. K. Hickey, M. V. Patel, J. V. Fahey, C. R. Wira, Innate and adaptive immunity at mucosal surfaces of the female reproductive tract: stratification and integration of immune protection against the transmission of sexually transmitted infections. *J Reprod Immunol* **88**, 185-194 (2011).
30. M. M. DeSouza *et al.*, MUC1/episialin: a critical barrier in the female reproductive tract. *J Reprod Immunol* **45**, 127-158 (1999).
31. B. Gunn *et al.*, Enhanced binding of antibodies generated during chronic HIV infection to mucus component MUC16. *Mucosal Immunol* **9**, 1549-1558 (2016).
32. K. M. Fahrbach, O. Malykhina, D. J. Stieh, T. J. Hope, Differential binding of IgG and IgA to mucus of the female reproductive tract. *PLoS One* **8**, e76176 (2013).
33. H. Zhang *et al.*, MUC1 and survivin combination tumor gene vaccine generates specific immune responses and anti-tumor effects in a murine melanoma model. *Vaccine* **34**, 2648-2655 (2016).
34. T. Kimura, O. J. Finn, MUC1 immunotherapy is here to stay. *Expert opinion on biological therapy* **13**, 35-49 (2013).
35. T. L. Cherpes, S. L. Hillier, L. A. Meyn, J. L. Busch, M. A. Krohn, A delicate balance: risk factors for acquisition of bacterial vaginosis include sexual activity, absence of hydrogen peroxide-producing lactobacilli, black race, and positive herpes simplex virus type 2 serology. *Sex Transm Dis* **35**, 78-83 (2008).
36. H. Wang, H. Eriksson, L. Sahlin, Estrogen receptors alpha and beta in the female reproductive tract of the rat during the estrous cycle. *Biol Reprod* **63**, 1331-1340 (2000).
37. G. Pelletier, M. El-Alfy, Immunocytochemical localization of estrogen receptors alpha and beta in the human reproductive organs. *The Journal of clinical endocrinology and metabolism* **85**, 4835-4840 (2000).
38. T. Kurita *et al.*, Paracrine regulation of epithelial progesterone receptor by estradiol in the mouse female reproductive tract. *Biol Reprod* **62**, 821-830 (2000).
39. D. L. Buchanan *et al.*, Tissue compartment-specific estrogen receptor-alpha participation in the mouse uterine epithelial secretory response. *Endocrinology* **140**, 484-491 (1999).
40. D. L. Buchanan *et al.*, Role of stromal and epithelial estrogen receptors in vaginal epithelial proliferation, stratification, and cornification. *Endocrinology* **139**, 4345-4352 (1998).
41. S. Yildiz-Arslan, J. S. Coon, T. J. Hope, J. J. Kim, Transcriptional Profiling of Human Endocervical Tissues Reveals Distinct Gene Expression in the Follicular and Luteal Phases of the Menstrual Cycle. *Biol Reprod* **94**, 138 (2016).
42. M. F. Rubio *et al.*, TNF-alpha enhances estrogen-induced cell proliferation of estrogen-dependent breast tumor cells through a complex containing nuclear factor-kappa B. *Oncogene* **25**, (2006).

43. T. Kurita, Normal and abnormal epithelial differentiation in the female reproductive tract. *Differentiation; research in biological diversity* **82**, 117-126 (2011).
44. T. Kurita, Developmental origin of vaginal epithelium. *Differentiation; research in biological diversity* **80**, 99-105 (2010).
45. T. Kurita, P. S. Cooke, G. R. Cunha, Epithelial-stromal tissue interaction in paramesonephric (Mullerian) epithelial differentiation. *Developmental biology* **240**, 194-211 (2001).
46. G. R. Cunha, P. S. Cooke, T. Kurita, Role of stromal-epithelial interactions in hormonal responses. *Archives of histology and cytology* **67**, 417-434 (2004).
47. L. Ye *et al.*, Generation of human female reproductive tract epithelium from human embryonic stem cells. *PLoS One* **6**, e21136 (2011).
48. T. Kurita *et al.*, Stromal progesterone receptors mediate the inhibitory effects of progesterone on estrogen-induced uterine epithelial cell deoxyribonucleic acid synthesis. *Endocrinology* **139**, 4708-4713 (1998).
49. G. Jin, Z. LanLan, C. Li, Z. Dan, Pregnancy outcome following loop electrosurgical excision procedure (LEEP) a systematic review and meta-analysis. *Archives of Gynecology and Obstetrics* **289**, 85-99 (2014).
50. M. J. Trepka *et al.*, Deaths Due to Screenable Cancers Among People Living With HIV Infection, Florida, 2000-2014. *Am J Prev Med* **53**, 705-709 (2017).
51. G. Van Kriekinge, X. Castellsague, D. Cibula, N. Demarteau, Estimation of the potential overall impact of human papillomavirus vaccination on cervical cancer cases and deaths. *Vaccine* **32**, 733-739 (2014).
52. K. P. Maniar, R. Nayar, HPV-related squamous neoplasia of the lower anogenital tract: an update and review of recent guidelines. *Adv Anat Pathol* **21**, 341-358 (2014).
53. A. C. Attia, J. Wolf, A. E. Nunez, On surmounting the barriers to HPV vaccination: we can do better. *Ann Med*, 1-17 (2018).
54. N. J. Nonzee, S. B. Baldwin, Y. Cui, R. Singhal, Disparities in parental human papillomavirus (HPV) vaccine awareness and uptake among adolescents. *Vaccine*, (2017).
55. M. Barnard, P. George, M. L. Perryman, L. A. Wolff, Human papillomavirus (HPV) vaccine knowledge, attitudes, and uptake in college students: Implications from the Precaution Adoption Process Model. *PLoS One* **12**, e0182266 (2017).
56. L. M. Niccolai, M. M. Pettigrew, The Role of Cognitive Bias in Suboptimal HPV Vaccine Uptake. *Pediatrics* **138**, (2016).
57. K. A. So *et al.*, The Impact of High-Risk HPV Genotypes Other Than HPV 16/18 on the Natural Course of Abnormal Cervical Cytology: A Korean HPV Cohort Study. *Cancer Res Treat* **48**, 1313-1320 (2016).
58. Y. Tanaka *et al.*, Predictors for recurrent/persistent high-grade intraepithelial lesions and cervical stenosis after therapeutic conization: a retrospective analysis of 522 cases. *Int J Clin Oncol* **22**, 921-926 (2017).
59. R. M. Ehsanipoor *et al.*, The relationship between previous treatment for cervical dysplasia and preterm delivery in twin gestations. *J Matern Fetal Neonatal Med* **27**, 821-824 (2014).
60. N. Santesso *et al.*, Systematic reviews and meta-analyses of benefits and harms of cryotherapy, LEEP, and cold knife conization to treat cervical intraepithelial neoplasia. *Int J Gynaecol Obstet* **132**, 266-271 (2016).
61. C. E. Wood, Morphologic and Immunohistochemical Features of the Cynomolgus Macaque Cervix. *Toxicologic Pathology* **36**, 119S-129S (2008).
62. E. S. E. Hafez, S. Jaszczak, Comparative anatomy and histology of the cervix uteri in non-human primates. *Primates* **13**, 297-314 (1972).
63. S. S. Suarez, Mammalian sperm interactions with the female reproductive tract. *Cell Tissue Res* **363**, 185-194 (2016).
64. J. Lamy *et al.*, Regulation of the bovine oviductal fluid proteome. *Reproduction (Cambridge, England)* **152**, 629-644 (2016).
65. J. Zhu *et al.*, Human fallopian tube epithelium co-culture with murine ovarian follicles reveals crosstalk in the reproductive cycle. *Mol Hum Reprod* **22**, 756-767 (2016).

66. E. V. Garcia *et al.*, Bovine embryo-oviduct interaction in vitro reveals an early cross talk mediated by BMP signaling. *Reproduction (Cambridge, England)* **153**, 631-643 (2017).
67. M. Ferraz *et al.*, Improved bovine embryo production in an oviduct-on-a-chip system: prevention of poly-spermic fertilization and parthenogenic activation. *Lab Chip* **17**, 905-916 (2017).
68. M. A. M. M. Ferraz, H. H. W. Henning, T. A. E. Stout, P. L. A. M. Vos, B. M. Gadella, Designing 3-Dimensional In Vitro Oviduct Culture Systems to Study Mammalian Fertilization and Embryo Production. *Annals of biomedical engineering* **45**, 1731-1744 (2017).
69. T. Hiraoka *et al.*, STAT3 accelerates uterine epithelial regeneration in a mouse model of decellularized uterine matrix transplantation. *JCI insight* **1**, (2016).
70. M. Hellstrom *et al.*, Bioengineered uterine tissue supports pregnancy in a rat model. *Fertility and sterility* **106**, 487-496.e481 (2016).
71. H. Campo *et al.*, De- and recellularization of the pig uterus: a bioengineering pilot study. *Biol Reprod* **96**, 34-45 (2017).
72. S. A. Olalekan, J. E. Burdette, S. Getsios, T. K. Woodruff, J. J. Kim, Development of a Novel Human Recellularized Endometrium that responds to a 28 day Hormone Treatment. *Biol Reprod*, (2017).
73. S. Xiao *et al.*, A microfluidic culture model of the human reproductive tract and 28-day menstrual cycle. *Nat Commun* **8**, 14584 (2017).
74. E. A. Partridge *et al.*, An extra-uterine system to physiologically support the extreme premature lamb. *Nat Commun* **8**, 15112 (2017).
75. V. De Gregorio *et al.*, An Engineered Cell-Instructive Stroma for the Fabrication of a Novel Full Thickness Human Cervix Equivalent In Vitro. *Advanced healthcare materials* **6**, (2017).
76. A. Karolina Zuk, X. Wen, S. Dilworth, D. Li, L. Ghali, Modeling and validating three dimensional human normal cervix and cervical cancer tissues in vitro. *J Biomed Res* **31**, 240-247 (2017).
77. T. W. Ridky, J. M. Chow, D. J. Wong, P. A. Khavari, Invasive three-dimensional organotypic neoplasia from multiple normal human epithelia. *Nature medicine* **16**, 1450-1455 (2010).
78. W. Zhang *et al.*, KLF13 regulates the differentiation-dependent human papillomavirus life cycle in keratinocytes through STAT5 and IL-8. *Oncogene* **35**, 5565-5575 (2016).
79. S. Heuser *et al.*, The levels of epithelial anchor proteins beta-catenin and zona occludens-1 are altered by E7 of human papillomaviruses 5 and 8. *J Gen Virol* **97**, 463-472 (2016).
80. C. L. Simpson, S.-i. Kojima, S. Getsios, in *Epidermal Cells: Methods and Protocols,* K. Turksen, Ed. (Humana Press, Totowa, NJ, 2010), pp. 127-146.
81. S. Wang *et al.*, In vitro 3D corneal tissue model with epithelium, stroma, and innervation. *Biomaterials* **112**, 1-9 (2017).
82. N. H. Green, B. M. Corfe, J. P. Bury, S. MacNeil, Production, Characterization and Potential Uses of a 3D Tissue-engineered Human Esophageal Mucosal Model. *J Vis Exp*, e52693 (2015).
83. E. R. Vazquez-Martinez *et al.*, Estradiol differentially induces progesterone receptor isoforms expression through alternative promoter regulation in a mouse embryonic hypothalamic cell line. *Endocrine* **52**, 618-631 (2016).
84. A. Barreca *et al.*, In vitro paracrine regulation of human keratinocyte growth by fibroblast-derived insulin-like growth factors. *Journal of Cellular Physiology* **151**, 262-268 (1992).
85. T. Kurita, G. R. Cunha, S. J. Robboy, A. A. Mills, R. T. Medina, Differential expression of p63 isoforms in female reproductive organs. *Mechanisms of development* **122**, 1043-1055 (2005).
86. R. A. Romano *et al.*, DeltaNp63 knockout mice reveal its indispensable role as a master regulator of epithelial development and differentiation. *Development (Cambridge, England)* **139**, 772-782 (2012).
87. D. L. Patton *et al.*, Epithelial cell layer thickness and immune cell populations in the normal human vagina at different stages of the menstrual cycle. *American journal of obstetrics and gynecology* **183**, 967-973 (2000).
88. C. V. Rao, N. B. Janakiram, A. Mohammed, Molecular Pathways: Mucins and Drug Delivery in Cancer. *Clin Cancer Res* **23**, 1373-1378 (2017).
89. E. O. Terino, Alloderm acellular dermal graft: applications in aesthetic soft-tissue augmentation. *Clin Plast Surg* **28**, 83-99 (2001).

90. B. M. Achauer, V. M. VanderKam, B. Celikoz, D. G. Jacobson, Augmentation of facial soft-tissue defects with Alloderm dermal graft. *Ann Plast Surg* **41**, 503-507 (1998).
91. D. J. Wainwright, Use of an acellular allograft dermal matrix (AlloDerm) in the management of full-thickness burns. *Burns* **21**, 243-248 (1995).
92. M. M. Laronda *et al.*, Initiation of puberty in mice following decellularized ovary transplant. *Biomaterials* **50**, 20-29 (2015).
93. M. M. Wong, X. Hong, E. Karamariti, Y. Hu, Q. Xu, Generation and grafting of tissue-engineered vessels in a mouse model. *J Vis Exp*, (2015).
94. K. Wang, X. Wang, C. S. Han, L. Y. Chen, Y. Luo, Scaffold-supported Transplantation of Islets in the Epididymal Fat Pad of Diabetic Mice. *J Vis Exp*, (2017).
95. C. V. Rao *et al.*, Small-Molecule Inhibition of GCNT3 Disrupts Mucin Biosynthesis and Malignant Cellular Behaviors in Pancreatic Cancer. *Cancer research* **76**, 1965-1974 (2016).
96. Z. Z. Liu, X. D. Xie, S. X. Qu, Z. D. Zheng, Y. K. Wang, Small breast epithelial mucin (SBEM) has the potential to be a marker for predicting hematogenous micrometastasis and response to neoadjuvant chemotherapy in breast cancer. *Clinical & experimental metastasis* **27**, 251-259 (2010).
97. E. G. Munro *et al.*, Upregulation of MUC4 in cervical squamous cell carcinoma: pathologic significance. *International journal of gynecological pathology : official journal of the International Society of Gynecological Pathologists* **28**, 127-133 (2009).
98. M. Alkholief, R. B. Campbell, Investigating the role of mucin in the delivery of nanoparticles to cellular models of human cancer disease: an in vitro study. *Nanomedicine* **12**, 1291-1302 (2016).
99. M. M. Laronda *et al.*, Good manufacturing practice requirements for the production of tissue vitrification and warming and recovery kits for clinical research. *J Assist Reprod Genet* **34**, 291-300 (2017).
100. A. R. Thurman *et al.*, Comparison of Follicular and Luteal Phase Mucosal Markers of HIV Susceptibility in Healthy Women. *AIDS research and human retroviruses* **32**, 547-560 (2016).
101. S. C. Irvin, B. C. Herold, Molecular mechanisms linking high dose medroxyprogesterone with HIV-1 risk. *PLoS One* **10**, e0121135 (2015).
102. D. Kim *et al.*, TopHat2: accurate alignment of transcriptomes in the presence of insertions, deletions and gene fusions. *Genome Biol* **14**, R36 (2013).
103. M. Pertea *et al.*, StringTie enables improved reconstruction of a transcriptome from RNA-seq reads. *Nat Biotechnol* **33**, 290-295 (2015).
104. A. C. Frazee *et al.*, Ballgown bridges the gap between transcriptome assembly and expression analysis. *Nat Biotechnol* **33**, 243-246 (2015).
105. T. Metsalu, J. Vilo, ClustVis: a web tool for visualizing clustering of multivariate data using Principal Component Analysis and heatmap. *Nucleic Acids Res* **43**, W566-570 (2015).
106. J. Wang, S. Vasaikar, Z. Shi, M. Greer, B. Zhang, WebGestalt 2017: a more comprehensive, powerful, flexible and interactive gene set enrichment analysis toolkit. *Nucleic Acids Res*, (2017).
107. W. Huang da, B. T. Sherman, R. A. Lempicki, Systematic and integrative analysis of large gene lists using DAVID bioinformatics resources. *Nat Protoc* **4**, 44-57 (2009).
108. W. Huang da, B. T. Sherman, R. A. Lempicki, Bioinformatics enrichment tools: paths toward the comprehensive functional analysis of large gene lists. *Nucleic Acids Res* **37**, 1-13 (2009).
109. S. Ghosh, C. K. Chan, Analysis of RNA-Seq Data Using TopHat and Cufflinks. *Methods Mol Biol* **1374**, 339-361 (2016).
110. C. Trapnell *et al.*, Differential gene and transcript expression analysis of RNA-seq experiments with TopHat and Cufflinks. *Nat Protoc* **7**, 562-578 (2012).
111. R. Shen, H. E. Richter, P. D. Smith, Early HIV-1 target cells in human vaginal and ectocervical mucosa. *Am J Reprod Immunol* **65**, 261-267 (2011).
112. C. Fraser *et al.*, Virulence and Pathogenesis of HIV-1 Infection: An Evolutionary Perspective. *Science* **343**, (2014).
113. A. Nazli *et al.*, Exposure to HIV-1 directly impairs mucosal epithelial barrier integrity allowing microbial translocation. *PLoS Pathog* **6**, e1000852 (2010).
114. A. Burgener, I. McGowan, N. R. Klatt, HIV and mucosal barrier interactions: consequences for transmission and pathogenesis. *Current Opinion in Immunology* **36**, 22-30 (2015).

115. G. Maartens, C. Celum, S. R. Lewin, HIV infection: epidemiology, pathogenesis, treatment, and prevention. *The Lancet* **384**, 258-271 (2014).
116. E. H. Byrne *et al.*, Association between injectable progestin-only contraceptives and HIV acquisition and HIV target cell frequency in the female genital tract in South African women: a prospective cohort study. *Lancet Infect Dis* **16**, 441-448 (2016).
117. A. Gadducci, C. Barsotti, S. Cosio, L. Domenici, A. Riccardo Genazzani, Smoking habit, immune suppression, oral contraceptive use, and hormone replacement therapy use and cervical carcinogenesis: a review of the literature. *Gynecological endocrinology : the official journal of the International Society of Gynecological Endocrinology* **27**, 597-604 (2011).
118. M. M. Kumar *et al.*, Role of estrogen receptor alpha in human cervical cancer-associated fibroblasts: a transcriptomic study. *Tumour Biol* **37**, 4409-4420 (2016).
119. J. A. den Boon *et al.*, Molecular transitions from papillomavirus infection to cervical precancer and cancer: Role of stromal estrogen receptor signaling. *Proceedings of the National Academy of Sciences of the United States of America* **112**, E3255-3264 (2015).
120. P. F. Yu *et al.*, TNFα-activated mesenchymal stromal cells promote breast cancer metastasis by recruiting CXCR2+ neutrophils. *Oncogene* **36**, 482 (2016).
121. C. Katanov *et al.*, Regulation of the inflammatory profile of stromal cells in human breast cancer: prominent roles for TNF-α and the NF-κB pathway. *Stem Cell Research & Therapy* **6**, 87 (2015).
122. A. Tsuyada *et al.*, CCL2 mediates cross-talk between cancer cells and stromal fibroblasts that regulates breast cancer stem cells. *Cancer research* **72**, (2012).
123. Z. Mi *et al.*, Osteopontin promotes CCL5-mesenchymal stromal cell-mediated breast cancer metastasis. *Carcinogenesis* **32**, (2011).
124. R. Romieu-Mourez *et al.*, Mesenchymal stromal cells expressing ErbB-2/neu elicit protective antibreast tumor immunity in vivo, which is paradoxically suppressed by IFN-gamma and tumor necrosis factor-alpha priming. *Cancer research* **70**, (2010).
125. J. M. Fox *et al.*, Methodology for reliable and reproducible cryopreservation of human cervical tissue. *Cryobiology* **77**, 14-18 (2017).
126. M. Ramezani, M. Salehnia, M. Jafarabadi, Vitrification and in vitro culture had no adverse effect on the follicular development and gene expression of stimulated human ovarian tissue. *J Obstet Gynaecol Res*, (2018).
127. A. Dalman *et al.*, Slow freezing versus vitrification technique for human ovarian tissue cryopreservation: An evaluation of histological changes, WNT signaling pathway and apoptotic genes expression. *Cryobiology* **79**, 29-36 (2017).
128. A. Y. Ting *et al.*, Morphological and functional preservation of pre-antral follicles after vitrification of macaque ovarian tissue in a closed system. *Human reproduction (Oxford, England)* **28**, 1267-1279 (2013).
129. C. M. Mitchell *et al.*, Long-term Effect of Depot Medroxyprogesterone Acetate on Vaginal Microbiota, Epithelial Thickness and HIV Target Cells. *The Journal of Infectious Diseases* **210**, 651-655 (2014).
130. C. R. Wira *et al.*, Sex hormone regulation of innate immunity in the female reproductive tract: the role of epithelial cells in balancing reproductive potential with protection against sexually transmitted pathogens. *Am J Reprod Immunol* **63**, 544-565 (2010).
131. C. R. Wira, K. S. Grant-Tschudy, M. A. Crane-Godreau, Epithelial cells in the female reproductive tract: a central role as sentinels of immune protection. *Am J Reprod Immunol* **53**, 65-76 (2005).
132. Y. Zhou, J. Ming, Y. Xu, Y. Zhang, J. Jiang, ERbeta1 inhibits the migration and invasion of breast cancer cells through upregulation of E-cadherin in a Id1-dependent manner. *Biochem Biophys Res Commun* **457**, 141-147 (2015).
133. P. Christoforou, P. F. Christopoulos, M. Koutsilieris, The role of estrogen receptor beta in prostate cancer. *Mol Med* **20**, 427-434 (2014).
134. H. Gao, K. Dahlman-Wright, Implications of estrogen receptor alpha and estrogen receptor beta for adipose tissue functions and cardiometabolic complications. *Horm Mol Biol Clin Investig* **15**, 81-90 (2013).

135. T. P. Le, M. Sun, X. Luo, W. L. Kraus, G. L. Greene, Mapping ERbeta genomic binding sites reveals unique genomic features and identifies EBF1 as an ERbeta interactor. *PLoS One* **8**, e71355 (2013).
136. P. Mak, C. Chang, B. Pursell, A. M. Mercurio, Estrogen receptor beta sustains epithelial differentiation by regulating prolyl hydroxylase 2 transcription. *Proceedings of the National Academy of Sciences of the United States of America* **110**, 4708-4713 (2013).
137. M. Zuguchi *et al.*, Estrogen receptor alpha and beta in esophageal squamous cell carcinoma. *Cancer Sci* **103**, 1348-1355 (2012).
138. L. Yafang *et al.*, Role of Estrogen Receptor-alpha in the Regulation of Claudin-6 Expression in Breast Cancer Cells. *J Breast Cancer* **14**, 20-27 (2011).
139. B. Brown, T. Poteat, L. Marg, J. T. Galea, Human Papillomavirus-Related Cancer Surveillance, Prevention, and Screening Among Transgender Men and Women: Neglected Populations at High Risk. *LGBT Health* **4**, 315-319 (2017).
140. M. McDowell *et al.*, Cervical Cancer Screening Preferences Among Trans-Masculine Individuals: Patient-Collected Human Papillomavirus Vaginal Swabs Versus Provider-Administered Pap Tests. *LGBT Health* **4**, 252-259 (2017).
141. A. Ojeaga, E. Alema-Mensah, D. Rivers, I. Azonobi, B. Rivers, Racial Disparities in HPV-related Knowledge, Attitudes, and Beliefs Among African American and White Women in the USA. *J Cancer Educ*, (2017).
142. E. M. Rettig *et al.*, Race is Associated With Sexual Behaviors and Modifies the Effect of Age on Human Papillomavirus Serostatus Among Perimenopausal Women. *Sex Transm Dis* **43**, 231-237 (2016).
143. A. R. Karuri *et al.*, Disparity in rates of HPV infection and cervical cancer in underserved US populations. *Front Biosci (Schol Ed)* **9**, 254-269 (2017).
144. F. Pampaloni, E. G. Reynaud, E. H. K. Stelzer, The third dimension bridges the gap between cell culture and live tissue. *Nat Rev Mol Cell Bio* **8**, 839-845 (2007).
145. M. Dickson, J. P. Gagnon, Key factors in the rising cost of new drug discovery and development. *Nat Rev Drug Discov* **3**, 417-429 (2004).
146. D. J. Ward, O. I. Martino, S. Simpson, A. J. Stevens, Decline in new drug launches: myth or reality? Retrospective observational study using 30 years of data from the UK. *Bmj Open* **3**, (2013).
147. J. Z. Huang *et al.*, Down-regulation of TRPS1 stimulates epithelial-mesenchymal transition and metastasis through repression of FOXA1. *J Pathol* **239**, 186-196 (2016).
148. M. Hay, D. W. Thomas, J. L. Craighead, C. Economides, J. Rosenthal, Clinical development success rates for investigational drugs. *Nature biotechnology* **32**, 40-51 (2014).
149. C. Heylman, A. Sobrino, V. S. Shirure, C. C. Hughes, S. C. George, A strategy for integrating essential three-dimensional microphysiological systems of human organs for realistic anticancer drug screening. *Experimental Biology and Medicine* **239**, 1240-1254 (2014).
150. M. B. Esch, G. J. Mahler, T. Stokol, M. L. Shuler, Body-on-a-chip simulation with gastrointestinal tract and liver tissues suggests that ingested nanoparticles have the potential to cause liver injury. *Lab on a Chip* **14**, 3081-3092 (2014).
151. C. Oleaga *et al.*, Multi-Organ toxicity demonstration in a functional human in vitro system composed of four organs. *Scientific reports* **6**, (2016).
152. C. Zhang, Z. Zhao, N. A. A. Rahim, D. van Noort, H. Yu, Towards a human-on-chip: culturing multiple cell types on a chip with compartmentalized microenvironments. *Lab on a Chip* **9**, 3185-3192 (2009).
153. J. H. Sung *et al.*, Microfabricated mammalian organ systems and their integration into models of whole animals and humans. *Lab on a Chip* **13**, 1201-1212 (2013).
154. A. Agarwal, J. A. Goss, A. Cho, M. L. McCain, K. K. Parker, Microfluidic heart on a chip for higher throughput pharmacological studies. *Lab on a Chip* **13**, 3599-3608 (2013).
155. I. Maschmeyer *et al.*, A four-organ-chip for interconnected long-term co-culture of human intestine, liver, skin and kidney equivalents. *Lab on a Chip* **15**, 2688-2699 (2015).
156. I. Wagner *et al.*, A dynamic multi-organ-chip for long-term cultivation and substance testing proven by 3D human liver and skin tissue co-culture. *Lab on a Chip* **13**, 3538-3547 (2013).
157. D. Huh *et al.*, Reconstituting organ-level lung functions on a chip. *Science* **328**, 1662-1668 (2010).

158. M. Xu, P. K. Kreeger, L. D. Shea, T. K. Woodruff, Tissue-engineered follicles produce live, fertile offspring. *Tissue engineering* **12**, 2739-2746 (2006).
159. S. Xiao *et al.*, Size-specific follicle selection improves mouse oocyte reproductive outcomes. *Reproduction* **150**, 183-192 (2015).
160. R. M. Skory, Y. M. Xu, L. D. Shea, T. K. Woodruff, Engineering the ovarian cycle using in vitro follicle culture. *Hum Reprod* **30**, 1386-1395 (2015).
161. J. S. Jeruss, T. K. Woodruff, Preservation of fertility in patients with cancer. *The New England journal of medicine* **360**, 902-911 (2009).
162. N. P. Groome *et al.*, Detection of dimeric inhibin throughout the human menstrual cycle by two-site enzyme immunoassay. *Clinical endocrinology* **40**, 717-723 (1994).
163. T. K. Woodruff *et al.*, Inhibin A and inhibin B are inversely correlated to follicle-stimulating hormone, yet are discordant during the follicular phase of the rat estrous cycle, and inhibin A is expressed in a sexually dimorphic manner. *Endocrinology* **137**, 5463-5467 (1996).
164. T. K. Woodruff, J. D'Agostino, N. B. Schwartz, K. E. Mayo, Dynamic changes in inhibin messenger RNAs in rat ovarian follicles during the reproductive cycle. *Science* **239**, 1296-1299 (1988).
165. T. Mahmood, E. Saridogan, S. Smutna, A. M. Habib, O. Djahanbakhch, The effect of ovarian steroids on epithelial ciliary beat frequency in the human Fallopian tube. *Human reproduction (Oxford, England)* **13**, 2991-2994 (1998).
166. T. Nakahari *et al.*, The regulation of ciliary beat frequency by ovarian steroids in the guinea pig Fallopian tube: interactions between oestradiol and progesterone. *Biomedical research (Tokyo, Japan)* **32**, 321-328 (2011).
167. M. F. Erickson-Lawrence, T. T. Turner, T. S. Thomas, G. Oliphant, Effect of steroid hormones on sulfated oviductal glycoprotein secretion by oviductal explants in vitro. *Biology of reproduction* **40**, 1311-1319 (1989).
168. H. G. Verhage, P. A. Mavrogianis, M. L. Boice, W. Li, A. T. Fazleabas, Oviductal epithelium of the baboon: hormonal control and the immuno-gold localization of oviduct-specific glycoproteins. *The American journal of anatomy* **187**, 81-90 (1990).
169. W. Yuan, X. N. Wang, G. S. Greenwald, Follicle-stimulating hormone, human chorionic gonadotropin, and prolactin receptors in hamster corpora lutea or dispersed luteal cells during pregnancy. *Biology of reproduction* **52**, 313-319 (1995).

APPENDIX A: 28-day Menstrual Cycle Hormone Control of Human Reproductive Tract Function in a Microphysiologic, Dynamic, and Microfluidic Culture System

Shuo Xiao[1,*], Jonathan R. Coppeta[2,*,**], Hunter Rogers[1,*], Brett C. Isenberg[2,*], Jie Zhu[1,*], Susan A. Olalekan[1,*], Kelly E. McKinnon[1,*], Danijela Dokic[1], Alexandra S. Rashedi[1], Daniel J. Haisenleder[3], Saurabh S. Malpani[1], Chanel Arnold-Murray[1], Kuanwei Chen[1], Mingyang Jiang[1], Lu Bai[1], Catherine T. Nguyen[1], Jiyang Zhang[1], Monica M. Laronda[1], Thomas Hope[1], Mary Ellen Pavone[1**], Michael J. Avram[4]; Elizabeth C. Sefton[1]; Spiro Getsios[5**], Joanna Burdette[6**], J. Julie Kim[1**], Jeffrey T. Borenstein[2], Teresa K. Woodruff[1,**,†]

[1]Department of Obstetrics and Gynecology, Feinberg School of Medicine, Northwestern University, Chicago, IL, 60611, USA; [2]The Charles Stark Draper Laboratory, Cambridge, MA, 02139, USA; [3]Ligand Assay and Analysis Core, Center for Research in Reproduction, University of Virginia, Charlottesville, VA, 22908, USA; [4]Department of Anesthesiology, Feinberg School of Medicine, Northwestern University, Chicago IL, 60611, USA; [5]Department of Dermatology, Feinberg School of Medicine, Northwestern University, Chicago IL, 60611, USA; [6]Department of Medicinal Chemistry and Pharmacognosy, University of Illinois at Chicago, Chicago, IL 60607, USA;

*Denotes equal first author contribution, **denotes sub-team leaders

ABSTRACT

The endocrine system dynamically controls tissue differentiation and homeostasis but has not been studied using microfluidic tissue culture paradigms. A microfluidic system stimulated murine follicles to produce the human 28-day menstrual cycle hormone control, which controlled human female reproductive tract and peripheral tissue homeostasis in single, dual, and multiple unit microfluidic platforms (Solo-MFP™, Duet-MFP™, and Quintet-MPF™, respectively). For the first time, this system demonstrated endocrine loops between organ modules for the ovary, fallopian tube, uterus, cervix and liver, with an unprecedented sustained circulating flow between all tissues. The integrated reproductive tract in microfluidic platform termed EVATAR, represents a powerful new *in vitro* tool that allows organ-organ integration of hormonal signals as a phenocopy of menstrual-like endocrine loops.

INTRODUCTION

Methods used to grow mammalian cells outside the body have not fundamentally changed in the last 50 years. Pre-clinical studies often begin with individual cells, separated from cellular and physical contacts that are important for biological function(*144*). These dispersed cells must be propagated through weekly reduction divisions and maintained on flat plastic; however, these cells are missing the cell physicochemical microenvironment, three-dimensional (3D) tissue-specific architecture, and blood flow perfusion found in natural tissues. Typical media composition is based on basal nutrients, bovine serum, and a few specialized factors that are placed in a static setting with random mixing. As a consequence, cell-cell and tissue-level cytokine and endocrine signals are not integrated into signaling pathways. As a consequence, fewer drugs are emerging to address many unmet needs, including cardiovascular disease, cancer, Alzheimer's and immune diseases, and new contraceptives(*145-147*). Despite large investments in research funding, only about 8% of drugs for which Investigational New Drug Application (IND) have been filled will be approved by the FDA(*148*). Innovative methods to culture cells *in vitro* to test new compounds are badly needed to reinvigorate the drug pipeline. Organ-on-a-chip and human-on-a-chip technologies have recently garnered much interest and offer promising approaches to test the efficacy and toxicity of new drugs *in vitro*(*149-157*). Here an integrated microfluidic platform that enables dynamic and precisely controlled interaction between organs is demonstrated during operation over month-long experiments and represents that next step forward in fundamental and applied toxicology, therapeutic

discovery as well as the deployment to address a wide range of biological problems and fill our drug pipeline.

RESULTS

Microfluidic technology enabled dynamic flow and multiple tissue integration

The Solo-MFP™ and Duet-MFP™ systems are based on pneumatic actuation technology, by which the individual systems are supplied with positive and negative air pressure via a system dock that is connected to a 5-channel pressure controller manifold (Fig. 1 a and b, refer to Supplementary Table 1 for nomenclature). The pressure of individual channels is switched between a vacuum or pressure source using an electromagnetic three-way valve controlled via a personalized pump program created in LabVIEW using a computer interface. The Solo-MFP™ and Duet-MFP™ systems use a common universal pneumatic plate that distributes positive and negative air pressure to specific valve or pump membranes clamped between the pneumatic and fluidic plates. Sequential application of pressure and vacuum to valve and pump membranes create a peristalsis causing fluid to move through individual microfluidic paths within or between modules. Four valves arranged in North, South, East, West positions about a central pump chamber create a four-port pump enabling multiple bi-direction flows in each fluidic circuit. The fluidic plates are specifically designed for either the Solo-MFP™ or Duet-MFP™ modules configuration. Solo-MFP™ systems consist of 4 replicates of a fluidic circuit with 2 connected modules: a coupled donor/acceptor module and a module for tissues (Fig. 1a). Duet-MFP™ systems consist of a single set of 4 modules: a donor module,

2 modules for tissues, and a separate acceptor module (Fig. 1b). Pneumatic actuation manipulates the membranes, generating pressure-driven flow in the fluidic paths, in order to transport fresh media from the donor to tissues, remove older media and secreted factors to the acceptor, or (in the case of Duet-MFP™ systems) move fluid from the upstream tissue to the downstream tissue to enable *in vitro* communication between cultured tissues.

Advancing beyond two tissues to capture the tissue diversity and interaction complexity of the female reproductive tract would require a larger number of pneumatic air lines. Integrating five tissues in Quintet-MFP™ system, a more practical and scalable approach was used for microfluidic control of tissue interaction (Fig. 1c). This was accomplished by embedding electromagnetically actuated micro-pumps within the platform, obviating the need to address the platform with independent airlines for each pneumatic actuator (Fig. 1d). This design approach allowed each of the 58 actuators of the Quintet-MFP™ to be individually controlled thus enabling precise flow control over a wide dynamic range. Modules were redesigned to include additional flow ports for the introduction of recirculation within each module, to ensure that the system was well mixed and to enable homogenous exposure of cultured tissues to factors within the media. In addition to recirculation within individual modules, the fluidic path design allowed for whole-system recirculation (Fig. 1c). The combination of whole-system and inter-module recirculation enabled a well-mixed system within and across all modules of the Quintet-MFP™. Each fluidic path between modules was controlled by two sets of 3 actuators. This redundancy acted as a fail-safe in the event of actuator failure. A total of 12 modules, including 1 donor,

1 acceptor, 5 blank, and 5 tissue-specific modules were developed for the Quintet-MFPTM (Fig. 1c). As with the Solo-MFP™ and Duet-MFP™ systems, the modules were secured on a fluidic plate that contains the microfluidic flow channels. The fluidic plate was placed atop the actuator plate that contains the electromagnetic actuators, and the two plates were separated by a Viton membrane. A fan-cooled heat sink was also added to the system to remove excess heat from the actuator plate. The actuator plate was connected to a controller box via 2 ribbon cables. This controller box acted as the intermediate between the Quintet-MFP™ system and the PC running the custom LabVIEW pump program.

For all Solo-MFP™ and Duet-MFP™ experiments, the empirically derived nominal thru-system flow rate was set to 40 μl/h to create physiologic concentrations of estradiol and progesterone. The average thru-system flow rates across 28-day for each system is shown in Fig. 2a and 2b. For Quintet-MFP™ experiments, the nominal of the empirically derived thru-system flow rate was set to 100 μl/h to create physiologic concentrations of estradiol and progesterone as well as to minimize the concentration lag between sequential modules (Supplementary Note 1 and Supplementary Fig. 1-3). The average thru-system flow rates across 28-day for the Quintet-MFP™ are shown in Fig. 2c. The thru-system flow rates for all 3 systems were found to consistently pump at flow rates close to the target flow rate value for the entirety of 28-day experiments and in the case of the Quintet-MFP™, capable of maintaining these flow rates for more than 100 days. In addition, the stroke volumes (i.e. the fluid volume displaced in a single pump stroke) were found to exhibit little variation across all pump pathways during a month-long pump cycle (Fig. 2d).

The status of actuator function was periodically evaluated *in situ* by monitoring the voltage pulse using an oscilloscope (Fig. 2e). The actuation time is defined as the amount of time required to completely open the actuator after the application of current to the electromagnet of the actuator (Fig. 2f). From empirical data, actuation times within the range of 250 – 625 μs were considered indicative of long term stability of mechanical function; actuation times below the lower limit indicates incomplete opening of the valve while actuation times longer than the upper limit indicates the actuation distance may be too long for reliable actuation. *In situ* actuator monitoring together with daily flow measurements enabled consistent pumping over month long studies. The timeline for the microfluidic platform setting up and tissue preparation and culture were shown in Fig. 2g.

Microfluidic culture supported follicle growth, maturation, and differentiation

In vitro follicle growth (IVFG) is a well-established model to study ovarian function *in vitro*(*158-160*). To test whether the microfluidic system supports follicle growth, we initially performed follicle cultures in Solo-MFP™ using primary mouse follicles (Fig. 3ai-iii). Mouse gonadal tissue was used throughout these studies because healthy ovaries are never removed from women except under extraordinary circumstances such as in the case of a sterilizing cancer diagnosis(*161*). As has been demonstrated previously, murine and human primary follicles are similar in static culture(*160*). For the microfluidic cultures, follicle-stimulating hormone (FSH) was provided at a concentration of 10 mIU/ml through the first 14 days of culture (day -14 to day 0) to mimic follicular phase gonadotropin levels (Fig. 2g). To phenocopy the LH surge, we created an algorithm

called ‘purge surge’ that generated peak human chorionic gonadotropin (hCG) on day 0 (Fig. 2g). Hormones were then brought to baseline for the remaining days in culture (day 1 to day 14) (Fig. 2g). All data is presented with the hCG surge as day 0 to permit comparison of follicular and luteal phase patterns to human menstrual cycle data (Fig. 2g). Follicle architecture and the spatial relationship of germ cells and their supporting somatic cells were maintained in Solo-MFP™. Moreover, follicle growth was supported from primary/early secondary stage to antral stage (Fig. 3aiv-vi). After hCG stimulation, follicles released good quality metaphase II (MII) oocytes with extruded first polar bodies with barrel-shaped bipolar spindles and tightly aligned chromosomes, which was termed MFP-ovulation (Fig. 3avii-viii). Once MFP-ovulation occurred, the granulosa cells differentiated into luteal cells as indicated by the granulosa cell hypertrophy and the significantly reduced number of cell nuclei in a defined area (Fig. 3b). These results demonstrate that a microfluidic environment was capable of supporting individual ovarian follicle growth, maturation, MFP-ovulation, and granulosa cell luteinization.

28-day menstrual cycle hormone production in Solo-MFP™

Follicle hormone secretion was next examined within microfluidic culture. During the follicular phase, 17β-estradiol (E2) production gradually increased and peaked on day 0 (14 days culture) when follicles reached maturation (Fig. 3c). During the luteal phase, the progesterone (P4) concentrations were significantly increased and peaked 2 days after the hCG treatment (Fig. 3c). Compared to steroid hormones secreted in static culture, follicles with dynamic flow in the microfluidic culture had significantly higher of E2 and

P4 production (pg/follicle/day) (Fig. 3e and f). We next examined two peptide hormones that are known to be secreted in the follicular phase to assess non-steroidal patterns of follicular function. Inhibin A is a member of the TGFβ superfamily and had a secretion pattern similar to that of E2, peaking when follicles reached maturation and subsequently decreasing and remaining low during the luteal phase (Fig. 3d). The secretion of inhibin B gradually increased until day -2 of the follicular phase, and then decreased and remained low in the later stage of the luteal phase (Fig. 3d). Taken together, these patterns of inhibin A and inhibin B, as well as E2 and P4 are consistent with healthy ovarian follicle performance(*162-164*). This human-like patterns were entirely controlled by our exogenous hormones; these data show what has long been suspected, that pituitary hormones set the tempo of each reproductive cycle both *in vivo* and now in microfluidics.

Ovarian explant cultures in Solo-MFP™ and Duet-MFP™

Based on the success of our follicle cultures in Solo-MFP™, we next tested whether ovarian explants could be cultured in the microfluidic system. Ovaries from day 12 CD-1 mice were collected; these tissues included pre-matured follicles from all classes (primordial, primary, and secondary). Ovaries were cut into 4 pieces and 2 pieces were placed in one cell culture insert and cultured in both Solo-MFP™ and Duet-MFP™ for 28 days. The treatment strategies of the pituitary hormones FSH and hCG were similar to those of the follicle microfluidic culture (Fig. 4a and b). Both Solo-MFP™ and Duet-MFP™ supported follicle growth from primary/early secondary to multilayer and antral stages within the ovarian explants (Fig. 4c). After hCG stimulation, mature follicles had

cumulus-oocyte complex (COC) expansion and released MII oocytes, and the granulosa cells differentiated into luteal cells (Fig. 4c). Both steroid (E2 and P4) and peptide hormones (inhibin A and B) had secretion patterns similar to those in the follicle microfluidic culture (Fig. 4d-g), suggesting that ovarian tissue is a good proxy for individual follicles and that Solo-MFP™ and Duet-MFP™ support each of the follicular endpoints described above.

Integration of human reproductive tract tissues with murine ovary in Quintet-MFP™

To create a hormonally-coupled *ex-vivo* female reproductive tract, we cultured the murine ovary, with human fallopian tube, endometrium, ectocervix, and liver tissues for 28 days in Quintet-MFP™, which was termed EVATAR. Quintet-MFP™ maintained consistent pituitary hormone circulation and recapitulated human 28-day menstrual cycle pituitary hormone control (Fig. 5a). E2 and P4 peaked in follicular and luteal phases, respectively (Fig. 5b). However, the absolute concentrations for both steroid and peptide hormones were significantly decreased compared to hormone concentrations in both Solo-MFP™ and Duet-MFP™ (60-fold decreased for E2, 10-fold decreased for P4, 20-fold decreased for inhibin A, and 60-fold decreased for inhibin B) (Fig. 5b and c). Since all materials are the same between platforms and there was no hormone binding to the microfluidic module materials (Fig. 5d), these data suggest the multiple tissue integration changed the upstream ovarian hormone expression patterns, or downstream reproductive tissues consumed hormones secreted by the ovary.

Microfluidic culture of human fallopian explants in Quintet-MFP™

A co-culture system between murine follicles and human fallopian tissue has previously been established in our laboratory (in press). Our work confirmed that the cultured human fallopian tube epithelium, including ciliated and secretory cells, could be regulated by exogenous steroid hormones from co-cultured ovarian tissues. Indeed, cilia length and cilia beating status and oviduct-specific glycoprotein 1 (OVGP1) secretion provided hallmarks of the functional change in the human fallopian epithelium during menstrual cycle(*165-168*). In the current study, fallopian explants were adapted into the Quintet-MFP™ to create a more complex co-culture environment beyond the simple static cultures. Histology confirmed that tissues were viable and cilia beating continued after 21 days of culture (Fig. 5e, supplementary Fig. 4). Moreover the thickness of the fallopian epithelium taken from day 0 prior to hCG stimulation was greater than tissues from day 7, and OVGP1 expression was higher following follicular phase E2 stimulation (Fig. 5e).

Microfluidic culture of human endometrium in Quintet-MFP™

Human uterine endometrial tissue is difficult to culture *in vitro*, and we tested a number of systems and found that the culture of fresh human endometrial explants consisting of both glands and stroma on decellularized uterine scaffolds were the most successful model for static and microfluidic cultures (Fig. 5f). Stromal and epithelial cells within the recellularized scaffolds were delineated by immunohistochemical staining of vimentin and cytokeratin, respectively (Fig. 5f). The stromal cells stained positively for Ki-67, and had nuclear estrogen receptors (ER) and progesterone receptors (PR) at the end

of the 28 days culture, indicative of active cell proliferation and uterine stromal cell characteristics (Fig. 5f).

Microfluidic culture of human ectocervix explants in Quintet-MFP™

To model hormone response in human ectocervix tissue *in vitro,* 3 mm biopsy punches of human ectocervix explants were cultured without hormones for 2-5 days before integration in Quintet-MFP™. Tissue was harvested throughout the entire 28-day cycle for histological analysis. The cultured ectocervix maintained its stratified squamous epithelial tissue architecture with proliferative potential as assessed by histology and Ki67 immunoreactivity, respectively (Fig. 6a). At the end of follicular phase, when estradiol concentrations peaked, the ectocervix explants prominently expressed PR in both epithelium and stroma, while this receptor was undetecable at the end of the hormone cycle (cycle day 14; 28 days culture), when estradiol concentrations decreased (Fig. 6a). These findings suggest that ectocervix tissue responded to E2 secreted from the upstream ovarian tissue in this microfluidic system.

Microfluidic culture of human liver microtissues in Quintet-MFP™

Human liver microtissues were also included in Quintet-MFP™ to explore non-reproductive tissue stability within our culture system and because this organ will be an important tool in future metabolic studies. Over 28 days of microfluidic culture, liver microtissues retained their structure, as measured by the tight cellular contacts and nuclear

staining before and after hCG stimulation (Fig. 6b). In addition, albumin secretion was stable throughout the 28-day culture period (Fig. 6c).

Cytokines expression in Quintet-MFP™

A variety of other factors are made at constitutive levels by reproductive tract tissues and are not hormonally controlled. We examined two such cytokines, Interleukin 8 (IL8) and Vascular endothelial growth factor (VEGF) in Quintet-MFP™. IL8 and VEGF peaked in the follicular phase and remained relatively constant through the end of the luteal phase (Fig. 6d), suggesting the integrated system is healthy throughout culture and supports reproductive and non-reproductive secretions.

Microfluidic culture supported pregnant-like hormone condition in Quintet-MFP™

To challenge the reproductive tissues in a different way, we asked whether we could prolong luteal phase function using the physiological cues associated with pregnancy. Briefly, once ovulation occurs, the mature egg is released into the fallopian tube where, if sperm are available, will be fertilized before moving into the uterus to implant. The fertilized embryo and newly developing placenta produce hCG and prolactin at high levels which rescues the corpus luteum to support an ongoing pregnancy(*169*). We mimicked this 'pregnancy' like state and maintained the corpus luteum (CL) for the full 14 days of the luteal phase after MFP-ovulation in Quintet-MFP™ (Fig. 6e). Moreover, as predicted the 'pregnant' luteal tissue produced significantly higher levels of P4 compared to the 'non pregnant' system (Fig. 6f). This experiment demonstrates the power of the integrated

EVATAR in Quintet-MPF™ to elucidate fundamental mechanisms of reproductive function and opens the door to drug discovery and toxicological studies in an entirely new way.

DISCUSSION

There are limited ways to effectively study whole tissues and tissue-tissue interactions. The female reproductive organs are especially dynamic as they respond to fluctuating hormonal concentrations driven by the pituitary gland and ovary in preparation for ovulation, fertilization, embryo implantation, and placentation. Our work provides evidence that the female reproductive tract and many peripheral organs can be integrated into the microphysiologic, dynamic, and microfluidic culture system termed EVATAR. This powerful tool that allows organ-organ integration of hormonal signals in a manner which phenocopies the human menstrual cycle and pregnancy. The Solo-MFP™, Duet-MFP™, and Quintet-MFP™ were invented to investigate of both single tissue response and multi-tissue interactions in a manner that maintains the 3D architecture of each tissue. These systems produce highly-controllable, stable flow patterns for up to 105 days. Due to the reconfigurable nature inherent in the design of these systems, the Solo-MFP™, Duet-MFP™, and Quintet-MFP™ can be used to investigate numerous combinations of tissue-tissue interactions beyond the female reproductive tract opening up a brand new method for *in vitro* tissue culture that is expected to improve the pace and quality of a whole range of biological and pharmacological research.

ACKNOWLEDGMENTS: We thank all patients who donated their reproductive tissues through the Gynecological Tissue Library in Northwestern University, A.J. Spencer and J.Q. Santos for assistance with fabrication and testing of microfluidic devices, and R. N. Shah and A. Rutz kindly provided the 3D printed scaffold for liver microtissue culture. This work was supported by NIEHS-ORWH-UH2ES022920; NCATS-NIEHS-NICHD-ORWH-UH3TR001207, and the NIH Common Fund.

AUTHOR CONTRIBUTION: T. K. Woodruff conceived of the microfluidic reproductive tract project. S. Xiao, H. Rogers, and T. K. Woodruff worked on the follicle/ovary team and the integration of multiple tissue culture in Quintet-MFP™, J. R. Coppeta, H. Rogers, B. C. Isenberg, and J. T. Borenstein worked on the microfluidic platform design, J. Zhu and J. Burdette worked on the fallopian tube team, S. A. Olaekan and J. J Kim worked on the endometrium team, K. E. McKinon and S. Getsios worked on the ectocervix team. All co-first authors and sub-team leaders designed the microfluidic system, performed the experiments, collected the data, and wrote the manuscript. E. C. Sefton managed the project and coordinated the teamwork. A. S. Rashedi, D. Dokic, K. Chen, M. Jiang, L. Bai, C. T. Nguyen, and J. Zhang helped on sample collection, microfluidic system set up and management, and ELISA assays. D. J. Haisenleder conducted the immunoassays. ME. Pavone, S. S. Malpani and C. Arnold-Murray helped on IRB approval, human gynecological tissue collection, and histology. M. M. Laronda, T. Hope, and M. J. Avram helped on the experiment design and data interpretation. All subteam leaders and corresponding author approved the manuscript.

COMPETING FINANCIAL INTERESTS: The authors declare no competing financial interests.

FIGURE LEGENDS

Figure 1. Microfluidic platforms design. Digital images and flow diagrams illustrating the pump pathways of (a) Solo-MFP™, (b) Duet-MFP™, and (c) Quintet-MFP™. (d) Illustration of the pump mechanism of the electromagnetic Quintet-MFP™. DO: donor module, T: tissue module, AC: acceptor module.

Figure 2. The pumping exhibition of microfluidic platforms and experimental procedures. The average flow rates of (a) Solo-MFP™ (n=19), (b) Duet-MFP™ (n=23), and (c) Quintet-MFP™ (n=10). (d) Average stroke volume for each pump pathway in Quintet-MFP™ over the course of 33 days normalized with respect to the initial value. (e) Example oscilloscope reading illustrating how the actuation time was measured to determine the status of actuator function. (f) A plot of Quintet-MFP™ actuator status at the beginning of an experiment with the upper and lower bounds of 625 μs and 250 μs, respectively. (g) Timeline for microfluidic platforms setting up and tissue preparation and culture. Graphs in a-d displayed average ± standard deviation.

Figure 3. Microfluidic platform supported follicle maturation and hormone secretion in Solo-MFP^{TM}. (a) Multiple follicle culture in Solo-MFP^{TM} (i-iii), microfluidic culture supported the follicle growth from primary stage to antral stage (iv-vi), and oocyte completed the first meiosis after hCG stimulation with well-organized microtubule fibers (green), tightly aligned chromosomes (blue), and round shape of F-actin (red) (vii-viii). (b) Follicles showed morphological changes as luteinization *in vivo* with granulosa cell hypertrophy and decreased nucleus to cytoplasm ratio. (c-d) Ovarian hormone secretions of estradiol (E2) and progesterone (P4) (c) and inhibin A and inhibin B (d) over 28 days in Solo-MFP^{TM}. (e-f) Comparison of E2 (e) and P4 (f) secretion rates between microfluidic and static cultures. Graphs in b-f display average ± standard deviation. *$p<0.05$ comparison of number of nuclei/mm^3 in follicles before and after hCG treatments (b), and hormone secretion rates between microfluidic and static cultures (e and f). Scale bar: 50 μm in a and 10 μm in b. N=3-6 replicates for the microfluidic and static culture.

Figure 4. Ovarian explant cultures supported follicle development, oocyte maturation, and hormone secretion in Solo-MFP^{TM} and Duet-MFP^{TM}. (a-b) Concentrations of pituitary hormones follicle-stimulating hormone (FSH) and human chorionic gonadotropin (hCG) in the acceptor module during 28-day microfluidic culture. (c) Ovarian explants were cultured in Solo-MFP^{TM} and Duet-MFP^{TM}, and follicles developed from pre-antral to antral stage, and extruded metaphase II (MII) oocytes after hCG stimulation. (d-e) Secretion of estradiol (E2) and progesterone (P4) in Solo-MFP^{TM} and Duet-MFP^{TM}. (f-g) Secretion of inhibin A and inhibin B in Solo-MFP^{TM} and Duet-MFP^{TM}.

Graphs in a-b and d-f display average + standard deviation. Scale bar: 50 μm. N=3-5 replicates for the Solo-MFP™ and Duet-MFP™ microfluidic cultures.

Figure 5. Quintet-MFP™ supported the integration of female reproductive and non-reproductive tissues (ovary, fallopian tube, and endometrium). (a) Concentrations of pituitary hormone follicle-stimulating hormone (FSH) and human chorionic gonadotropin (hCG) during 28-day culture in Quintet-MFP™. (b-c) Ovarian hormone secretion during 28-day microfluidic culture with E2 and progesterone (P4) in b and inhibin A and inhibin B in c. (d) Dynamic E2 concentrations in donor and acceptor modules over 48 h. (e) Histology of the fallopian epithelium, cilia image, and OVGP1 expression of the fallopian epithelium after 14 and 21 days microfluidic culture in Quintet-MFP™. (f) Human endometrium tissue before and after the decellularization, after recellularization, and immunohistochemistry staining of vimentin, cytokeratin, Ki67, estrogen receptor (ER), and progesterone receptor (PR) in Quintet-MFP™. Graphs of a-d display average + standard deviation. Scale bar: 100 μm for fallopian epithelium histology and 10 μm for cilia images (e), and 50 μm in f. OVGP1: oviduct-specific glycoprotein 1 and α-tubulin as internal control. N=3 replicates for the integrated tissue culture in Quintet-MFP™.

Figure 6. Quintet-MFP™ supported the integration of female reproductive and non-reproductive tissues (ectocervix and liver) and pregnant-like hormone condition. (a) Ectocervix histology, Ki67 and progesterone receptor (PR) staining at the end of follicular and luteal phases. (b) Histology of liver microtissues before (day -14) and after hCG

treatment (day 14). (c) Human albumin production over 28 days microfluidic culture. (d) Production of IL8 and VEGF over 28 days microfluidic culture. (e) Histology of ovarian tissue in Quintet-MFP™ on day 0 (pre hCG) and day 8 (continuously cultured with hCG). (f) Ovarian progesterone secretion with and without hCG treatments. Graphs in c, d, and f display average + standard deviation. Scale bar: 10 μm in a, 25 μm in b, and 100 μm in e. IL8: Interleukin 8, VEGF: vascular endothelial growth factor, CL: corpus luteum. N=3 replicates for the integrated tissue culture Quintet-MFP™.

This work originally appeared in *Nature Communications* (2017).

APPENDIX B: Good manufacturing practice for the production of vitrification and warming and recovery media for use on human tissue

Authors: Monica M. Laronda1, Kelly E. McKinnon1, Alison Y. Ting3, Ann V. LeFever2, Mary B. Zelinski3,4, Teresa K. Woodruff1*

Affiliations:

1 Division of Reproductive Biology, Department of Obstetrics and Gynecology, Feinberg School of Medicine, Northwestern University, Chicago, Illinois

2. Mathews Center for Cellular Therapy, Northwestern Memorial Hospital, Chicago, Illinois

3. Division of Reproductive & Developmental Science, Oregon National Primate Research Center, Oregon Health & Science University, Beaverton, Oregon

4. Department of Obstetrics & Gynecology, Oregon Health & Science University, Portland, OR

Abstract

Products that are manufactured for use in a clinical trial, with the intent of gaining US Food and Drug Administration (FDA) approval for clinical use, must be produced under an FDA approved investigational new drug (IND) application. We describe work done toward generating reliable methodology and materials for preserving ovarian cortical tissue through a vitrification kit and reviving this tissue through a warming and recovery kit. We have described the critical steps, procedures and environments for manufacturing products with the intent of submitting an IND. The main objective was to establish an easy-to-use kit that would ensure standardized procedures for quality tissue preservation and recovery across the 117 Oncofertility Consortium sites around the globe. These kits were developed by breaking down the components and steps of a research protocol and recombining them in a way that considers component stability and use in a clinical setting. The kits were manufactured utilizing current good manufacturing practice (cGMP) requirements and environment, along with current good laboratory practices (cGLP) techniques. Components of the kit were tested for sterility, endotoxicity and morphological endpoint release criteria was established. We worked with the intended down-stream users of these kits for development of the kit instructions. Our intention is to test these initial kits, developed and manufactured here, for submission of an IND and to begin clinical testing for preserving the ovarian tissue that may be used for future restoration of fertility and/or hormone function in women who have gonadal dysgenesis from gonadotoxic treatment regimens or disease.

Purpose

Current Good Manufacturing Practice (cGMP) regulations are enforced by the US Food and Drug Administration in order to ensure the quality of manufactured drug products. These guidelines are listed in the 21 Code of Federal Regulations (CFR) part 211 [1]. cGMPs include a set of guidelines for facility standards, proper documentation, and implementation of procedures. Additionally, equipment within facilities used for drug manufacturing must be monitored and calibrated under cGMP guidelines and personnel must be properly trained and proficient in the facility procedures in order to be compliant. Current good laboratory practices (cGLPs) are additional guidelines that ensure that the data generated by testing the manufactured products has been collected in a scientifically sound manner and is reliable to support the product application. Taken together, these guidelines and training requirements are constructed to protect the consistency and sterility of the materials throughout the manufacturing process and ensure a quality, standardized product.

We sought to create Vitrification and Warming & Recovery kits for use by our Oncofertility® Consortium members and partners for preserving and reviving ovarian cortical tissue. This tissue would be isolated under institutional review board (IRB)-approved procedures for preserving tissue in patients at risk for gonadal dysgenesis due to chemotherapy, radiation and/or disease. We hope to gain approval of these kits as an Investigational New Drug (IND) through the FDA, and therefore, defining the production and manufacturing of quality medias for this approval are achieved by adhering to the cGMP guidelines [2]. Standard operating procedures (SOPs) for formulating Vitrification

and Warming and Recovery medias that have been made for research purposes must be converted to fulfill the manufacturing and release guidelines put forth by the FDA with the goal of submitting the IND and performing clinical trials for establishing this procedure in clinical practice. Clinical use of this vitrified and recovered tissue could include autotransplant of the tissue back into the patient or isolation of specific cell types within the vitrified tissue for cytotherapy for restoring fertility and hormone production as previously reported [3]. An easy-to-follow kit would ensure standardized procedures for quality tissue preservation and recovery across our 117 sites around the globe [oncofertility.northwestern.edu].

Choosing the vitrification protocol

Other laboratories have created ovarian tissue vitrification formulations with common cryoprotectants, mainly ethylene glycol (EG) and dimethyl sulfoxide (DMSO), developed from embryo and oocyte cryopreservation protocols and generally involves plunging the tissue directly into liquid nitrogen. Table 1 displays examples of these vitrification solutions in which bovine, non-human primate or human ovarian tissue was used to test the vitrification protocol. An additional method was developed within the Oncofertility Consortium to investigate a closed system of vitrification that may reduce cross-contamination between samples and from the environment, with intended clinical use. Synthetic polymers such as polyvinylpyrrolidone (PVP), a polyvinyl alcohol and vinyl acetate copolymer (Super cool X-1000) and a polyglycerol (Super cool Z-1000) were used to bind nucleators and prevent ice formation and de-vitrification in an ethylene glycol based

cryoprotectant solution [4,5]. These synthetic polymers were chosen over others because they have been shown to decrease crystallization, and improve functionality of tissues warmed and recovered after vitrification when compared to solutions without these polymers, and did not increase tissue toxicity [6,7].

Methods

GMP manufacturing of kit reagents

Environmental requirements

These procedures were performed at the Northwestern Memorial Hospital (NMH) Mathews Center for Cellular Therapy (MCCT) under the direction of Ann LeFever. The MCCT is a fully operational current Good Tissue Practice (cGTP) and cGMP compliant clinical facility dedicated to manufacturing support of human cellular and tissue-based products intended for human use and is an FDA registered establishment for such manufacturing. The facility has a Quality Assurance/Quality Control (QA/QC) Laboratory, receiving area, control room, library and classified areas (International Organization for Standardization (ISO) Class 5, ISO Class 7 and ISO Class 8). The ISO Class 8 areas consist of separate material staging, material airlocks for passage of materials in and out of the facility and gowning and de-gowning areas. An ISO Class 7 clean corridor connects the work suites with the gowning, de-gowning and material staging areas. The classified areas of the facility are cleanrooms, and they are supplied with high efficiency particulate air (HEPA) filtered air. The Building Automation System (BAS) with an integral

Environmental Monitoring System (EMS) continuously monitors the MCCT including critical parameters such as temperature, humidity and differential pressure. The system also monitors critical parameters of dedicated laboratory equipment, including incubators and refrigerators. The BAS is equipped with an emergency callout system for off-site and off-hours personnel notification.

Personnel

Three key personnel were given the authority for approving the SOPs developed for manufacturing these media kits, as well as overseeing the production of the kit under cGMP. This approval was given in writing by Teresa K Woodruff (Research Director), Ann V LeFever (Laboratory Director) and Monica M Laronda (Quality Assurance Officer).

Appropriate hygiene is essential for the personnel involved in the manufacturing of sterile media. Appropriate personal protective equipment (PPE) is required for the use of the MCCT GMP facility, which included gloves, face mask, bouffant cap, hood, jump suit, booties and long surgical gloves for the ISO 7 work suites. These items are put on carefully in an order outlined by the MCCT Gowning Procedure SOP, in which each person using the suit had demonstrated proficiency. Only the minimum number of personnel should be present during the production of materials. For our media production, 1 person pipetted or weighed the ingredients while the second person noted the progress of large quantities and reviewed all work and calculations to minimize measuring errors. Each person involved initialed the SOPs at the completion of a task.

Kit components

The media created for Oncofertility Consortium Vitrification and Oncofertility Consortium Warming and Recovery kits were based on a previously established protocol for rhesus macaque ovarian tissue with modifications for ease of use as a kit and conversion to what would be needed for a clinical lab receiving human tissue [7,8]. The list of solutions for each kit and the components within each solution are for research use only. The Equilibration Solution 1 (ES1) contained glycerol (Sigma G9021), Sage OFC Holding Media (Origio ART-8040) and Quinn's AdvantageTM Serum Protein Substitute (SPS, ART-3011). The CryoMedium (CM) contained Sage OFC Holding Media, and SPS. The Vitrification Solution (VS) contained glycerol, ethylene glycol (Sigma 03750), Sage OFC Holding Media, and SPS, and the Vitrification Solution with Polymers (VS+PXZ) contained Poly(N-vinylpyrrolidone), MW 2500 (PVP-25, Polysciences 16693), Super cool X-1000 (21st Century Medicine) and Super Cool Z-1000 (21st Century Medicine) in addition to the VS base components. The Warming Solution (WS1) contained sucrose (Sigma ARK2195B), SAGE OFC Holding Media and SPS. The CM for the Warming and Recovery kit is the same formulation as the Vitrification kit. The L-ascorbic acid 2-phosphate sesquimagnesium salt hydrate (AA2P, Sigma A8960) would be added to each medium by the end user and was kept as a lyophilized powder for a prolonged media shelf-life. All reagents were vetted through the cGMP Supply Management protocols, Certificates of Analysis reviewed to confirm specifications met kit requirements and additional sterility testing was conducted to confirm sterility and endotoxin levels in the individual kit components.

The containers for these media were PETG Certified Clean Containers in the appropriate volumes of 30, 60, 125, 250 or 500 ml (Nalgene, 2019) and sealed with the appropriate shrink band (Nalgene 312160) sealed with a 1500 watt Dual Temperature Heat Gun (Drill Master). The AA2P in each kit was packaged in amber serum tubing bottles (Wheaton 223693) and ultra-pure straight plug stoppers (Wheaton 224100-400) and capped securely with aluminum seals (Wheaton 224182-01). The original kits also included individually wrapped, high security 2 ml tissue straws (IMV Technologies 018960). Single-use, disposable, sterile supplies were used throughout.

Sterility and endotoxin testing

The MCCT and the Clinical Microbiology Laboratories of Northwestern Memorial Hospital (both are CAP/CLIA certified), provide quality assurance and quality control support of products manufactured within the MCCT.

Suitability of kit reagents for tissue vitrification and revival of tissue

To establish the suitability of the various cGMP manufactured buffers for tissue vitrification and revival of tissue function, a series of processes were conducted utilizing bovine ovarian tissue. These non-clinical evaluations were not done within the GMP facility.

Preparation of test tissue

Two shipments of 4-5 bovine ovaries each were obtained young cows at the Aurora Packing Company (Aurora, IL) and transported to the lab in BoviPro Oocyte Holding Medium (1182/1210). The single best ovary, based on size and appearance (lack of cysts and with smooth even surface epithelium) was chosen from the two shipments. Upon arrival the ovaries are rinsed in fresh medium and the excess fat was removed. Ovaries were first bisected along the hilus and cut into quarters. Ovarian tissue was processed into 500 μm–thick sections of ovarian cortex using a Thomas Stadie-Riggs Tissue Slicer. The first slice was considered cortex tissue and was used for our experiments. Tissue was sliced into 5 x 5 mm square pieces and pieces that did not contain visible corpus luteum were used. This experiment was performed 2 separate times. For each experiment, 5 cortical pieces were not put through the vitrification protocol but were fixed in 10% neutral buffered formalin to represent fresh tissue. 20 cortical pieces were vitrified per experiment.

Vitrification procedure

The vitrification procedure was performed as written in the kit instructions (Suppl. Fig. 1). The vial of AA2P was dissolved in 2 ml of CM to make a 100 □M AA2P solution. The AA2P solution was added to ES1, CM, VS and VS+PXZ at 1:1000 to create a concentration of 100 nM AA2P per solution. 70 ml each of Equilibration Solution 2 and 3 (ES2, ES3) were made in sterile Nalgene bottles by combining 17.5 ml VS with 52.5ml CM for ES2 and 35 ml VS with 35 ml CM for ES3. In a biosafety cabinet, 5 60 mm petri dishes were arranged on a slide warmer set to 37 °C and 10 ml each of ES1, ES2, ES3, VS and VS+PXZ were mixed thoroughly, aliquoted into each dish and allowed to warm for 15

minutes. A vitrification validation test was performed to ensure that the VS+PXZ would solidify without forming crystals when held in liquid nitrogen vapors for 10 min in a 2 ml high security straw. The remainder of the straws needed were sealed on one side, labeled and pre-loaded with 2 ml of VS+PXZ. Up to 10 pieces of ovarian tissue were placed in 1 petri dish starting with ES1. Tissue was incubated in ES1 for 7 minutes. The contents of the dish were agitated by swirling the dish 2 times every 30 seconds. Tissue was then transferred to the dish with ES2 solution, ES3 and VS solution and incubated in the same way as with ES1. The tissue was then transferred to VS+PXZ for 30 seconds, swirled twice and immediately loaded into the straws containing 2 ml of VS+PXZ each. 1 or 2 pieces of tissue were loaded into the straw at a time and either pushed down with a sterile pipet tip or left alone until the pieces settled before loading the rest of the tissue, up to 10 pieces. The straw was then sealed and placed into liquid nitrogen vapor for 10 or more minutes before plunged into the liquid nitrogen. The straws were stored in liquid nitrogen inside pre-chilled canisters until ready to warm and recover. The location and quantity of tissue in storage was noted. Of note, the preferred method for incubating the tissue in each solution is by constant shaking at 37 °C, as stated in the original article describing this vitrification method [7]. However, our lab and the consulting fertility clinic lab were not equipped to do this within our sterile hood and therefore, swirled the dish at regular intervals. Further analysis will be done to compare these two methods.

Warming and recovery procedure

The AA2P for this kit was prepared in the same way with 2 ml of CM to create a 100 □M solution. AA2P solution was added at 1:1000 in WS1 and CM. 70 ml each of Warming Solutions 2, 3, and 4 (WS2, WS3, WS4) were made in sterile bottles by combining 52.5 ml WS1 with 17.5 ml CM for WS2, 35 ml of WS1 and 35 ml with 35 ml of CM for WS3 and 17.5 ml of WS1 with 52.5 ml of CM for WS4. In a biosafety cabinet, 6 60 mm petri dishes were arranged on a slide warmer and 10 ml each of WS1, WS2, WS3, WS4 and 2 plates of CM. Straws were removed from storage into a dewar flask with liquid nitrogen. Straws were removed 1 at a time with forceps and not touched at an area with the vitrification solution. The straw was held at room temperature for 1 minute then plunged into and stirred in a 45□C water bath for 30 seconds. The contents were poured into an empty 100 mm petri dish, then the tissue was immediately transferred to the warm WS1. The contents from each straw were put into a separate set of dishes. The tissue was incubated in WS1, WS2, WS3 and WS4 for 5 minutes each and swirling 2 times every 30 seconds. The tissue was then transferred to CM and incubated 2 times for 10 minutes each, swirling 2 times every 30 seconds. Media from the first CM plate was reserved for anaerobic, aerobic, fungal sterility and endotoxin testing. The tissue was fixed in 10% neutral buffered formalin to represent vitrified, warmed and recovered tissue.

Histological analysis of tissue

All tissue processing and hematoxylin and eosin (H&E) staining was performed by the Northwestern University Center for Reproductive Sciences Histology Core. Fixed tissue was processed using an automated tissue processor (Leica) and embedded in

paraffin. Serial sections were cut 5 μm thick and stained with H&E using a Leica Autostainer XL (Leica Microsystems). TUNEL analysis was performed using the DeadEnd™ Fluorometric TUNEL System (Promega, G3250) and following kit instructions. Controls for detection of TUNEL-positive cells were created by digesting fresh bovine tissue sections with DNase I (Promega, M6101; Suppl. Fig. 2). Negative controls were created by performing all steps in the kit instructions and excluding the Images were obtained using a Nikon E600 fluorescent microscope and Metamorph software and analyzed using ImageJ software (NIH). Sections from 4-5 pieces per group were analyzed in duplicate from different slides. Over 10,000 individual cells were counted as positive or negative for GFP (TUNEL) expression for each group (fresh or vitrified/recovered) and the data is represented as a percent of positive cells detected within each piece of tissue.

Premises and equipment

The MCCT is constructed with appropriate lighting, ventilation and sufficient space in accordance with cGMP CFR title 21 guidelines [2]. The facility is also constructed with clean surfaces for easy testing and decontamination. The work suite used for manufacturing this media had undergone a complete sanitization and analysis of sterility prior to manufacturing to prevent the introduction, transmission or spread of contaminants. This required the use of preapproved cleaning agents, such as 70% isopropyl alcohol, and documentation of cleaning and sanitization on the MCCT log sheet. Additionally, all equipment used was calibrated according to MCCT standards prior to manufacturing, and

included laminar flow hoods, scales and pipets. Data was analyzed using a two-tailed Student's t-test.

Storage instructions and stability

Written procedures were established to describe the process for testing and accepting materials, including chemical components, for media manufacturing and are described in more detail below. The components were kept sealed and treated as containing potential contaminants until it was determined that they met our endotoxin and sterility standards. The Human Ovarian Tissue Vitrification Kit and Human Ovarian Tissue Warming & Recovery Kit were stored at 4 °C and are stable until the date listed. Expiry date was dictated by the expiry date of the components and, in this case, was determined by the shelf life of the OFC Holding Media which was listed as expiring 1 year following production. AA2P was not added until the day of vitrification. The solutions should be used within 24 hours following addition of AA2P.

Results

Development of media kits to be used in clinical labs

A flow chart for this process is illustrated in Fig. 1. Vitrification of ovarian tissue has already been tested as a potential way to preserve and restore quality ovarian tissue in rhesus monkeys and humans [7-12]. The goal for developing the Human Ovarian Tissue Vitrification Kit and Human Ovarian Tissue Warming & Recovery Kit were to maintain consistent media formulations and sets of instructions for handling the human ovarian

tissue for establishing ovarian tissue vitrification as a way to preserve and restore quality ovarian tissue in future clinical trials. These kits must consider the down-stream users, and strong communication with the clinical labs that would use the kits for the first human trials was established and maintained throughout this process.

The instructions considered the equipment within the lab of the down-stream user. The medias within each kit were designed to require only simple dilutions, and therefore, the components that were consistent within each medium was created as the diluent, here called CM. Additionally, the volumes chosen also considered the amount of ovarian tissue received from each participant in the trial as the kits are designed to be used for 1 participant only. The AA2P required in each medium is quickly degraded, and therefore, we decided to include this in its most stable form, lyophilized powder in a light-block container, and instruct the down-stream user to add AA2P to each medium within 24 hours of use. We began production once we had determined the quantity of materials required for each kit and scaled to create 10 kits for use by the clinical lab for human tissue, with an additional 4 kits for testing the media under our SOP for release criteria and ease-of-use.

Production

Establishing SOPs for each point of production

SOPs were written and approved by the Research Director, Laboratory Director and Quality Assurance Officer. These were written in a standard format that included, the location of production (MCCT), protocol number, version number, implementation and

revision date and author. They consisted of the "principal" or reason for creating the SOP, the "scope" or to whom this document applies, a list of reagents and equipment, if applicable, the "operational procedure", "references" and "revisions". A Job Aid was also created to list the SOPs required for manufacturing complete kits. The personnel responsible for manufacturing the media reviewed each SOP prior to performing the tasks. A Document Control system was established to oversee the utilization and review of procedures.

Establishing sterile and endotoxin-free components

Each component and material ordered for use in the MCCT was shipped directly to the site and opened under the established SOP for reviewing and recording shipments received. Components that met high sterility and high purity standards were preferred. The Certificate of Analysis (C of A) and Certificate of Sterility (C of S) documents for each component used to make the media were examined. If these documents did not state that the product met sterility standards (GMP, USP, Pharma) and endotoxin levels were not confirmed to be less than 1 EU/ml, we proceeded with the sterilization protocol within the GMP facility. If sterility standards were met, then the product could be used as is for the media kit.

Components that did not meet this standard were sterilized with a 0.2 □m polyethersulfone filter system with attached sterile reservoir. The components purchased for AA2P storage were sterilized with ethylene oxide treatment in the NMH facility, which undergoes regular calibration and testing. AA2P was tested for sterility by dissolving the

lyophilized powder in a sterile diluent at the same concentration that will be used in the kit. Stock solutions of media components were created when necessary. In this case a 20% PVP-25 solution was made with sterile water and filter sterilized before taking samples for endotoxin and sterility testing. Sterility testing of these solutions included 14 day anaerobic, 14 day aerobic and 28 day fungal testing as performed by the MCCT SOPs. Endotoxin testing was performed with Endosafe according to the MCCT SOPs. Passive air testing was also performed using open settle plates in close proximity within the biological safety cabinets. Aseptic technique was used throughout all processes.

Manufacturing batches

Production took place in a Level II vertical laminar flow biosafety cabinet in an ISO Class 7 work suite by two trained personnel who had reviewed the approved SOPs for manufacturing each medium. Media were made in large quantities then aliquotted into 14 containers (28 containers for the CM since it is contained in both kits). Appropriate mixing of the media was done with a serological pipet in between each aliquot. The bottles aliquoted from one batch preparation were considered of the same lot and therefore, sterility and endotoxin testing results from media collected from the first, middle and last bottles were considered the results for that lot. After labeling each bottle appropriately (see below) each bottle was sealed with shrink bands and stored at 4°C.

Labeling

Each bottle was labeled with the specific media label prepared for that lot. An example of a media label with the required information is included in Fig. 2. According to the Code of Federal Regulations, the label on the "drug or drug product" must contain the name and address of the manufacturer, packer and distributor [13]. Additionally, the label must clearly display the unique reference and lot number and expiration date. The labels created for each product also contained the Oncofertility Consortium logo, product name, and symbols for recommended storage temperature. Additionally, each label identified the contents as a single-use product for "research use only," and that instructions should be read prior to using the product.

The product information insert that is part of the packaging listed the contents for each kit, and a legend with descriptions for the symbols used on the product labels (Fig. 2). The package inserts also stated, "These products are intended for the ultra-rapid vitrification of human ovarian tissue. All media preparations and procedures must be carried out in a biosafety cabinet." A list of precautions and warnings are also declared on the packaging insert.

Caution: The user should read and understand all directions for use, precautions and warnings before using Vitrification Kit.

Caution: Handle all human source material using universal precautions. Wear safety goggles and face mask.

Single Use: Kit should be used for one patient. Discard any excess product that remains after procedure is complete.

Each set of instructions describes the protocols as listed here in the Methods section. Additionally, a C of A for each product that contains our release criteria (Table 2) with validation of sterility and results specific to each product is included with each kit.

Production and distribution of records

SOPs were developed for each step to ensure appropriate planning, execution and documentation of each task toward manufacturing and testing of the kits, and follow cGLP guidelines. During the manufacturing process, hard copies of the SOPs, wrapped in plastic lining for adequate sterilization, were marked with permanent ink as each task was completed, and initialed by the 2 trained investigators at critical points of documentation, such as addition of large volumes to a media. These records were then scanned to create digital copies and stored on a secure server. The originals were kept in a binder with the Quality Assurance Officer. The endotoxin and sterility testing results were also scanned and uploaded as digital copies on the secure server.

Quality assurance and quality control

A set of release criteria was established prior to the production of the media (Table 2) and release criteria testing was conducted on aliquots of each manufactured product within the kit and for each batch of that product. These criteria represent the intended outcome of the manufactured product and outline the intended use of the kit as a whole. A separate release criteria form is produced for each product within the kits and is identified by the product name, catalog number, lot number and expiry date. The release criteria form,

which includes Table 2, is reviewed, initialed and dated with the results for each lot of that product. A copy of this document, signed and dated by the Quality Assurance Officer, is included with each kit distribution. The product recipient should inspect the products within the kit and match the visual clarity and color as well as fill volume listed in the report to identify major unforeseen contamination, leakage or pH change (in this case as indicated by the phenol red media color).

A test for identifying morphological endpoints of tissues vitrified with this kit has also been established for the release criteria of the Oncofertility Consortium Human Ovarian Tissue Vitrification and Warming and Recovery Kits. A more stringent functional test can be applied to the release criteria of future kits as needed. We chose to test bovine ovary slices upon completion of each manufactured batch, to ensure that the kit is reliable for down-stream use on human ovarian tissue. The VS+PXZ solution is put through an initial test to ensure that the solution vitrifies without forming crystals, and is part of the initial test for every kit and is listed in the kit instructions. The bovine ovarian cortex tissue is sliced from the whole bovine ovaries and prepared in 5 mm by 5 mm pieces, mimicking what is prepared in the clinic for human tissue. Half of the bovine ovary pieces were saved to represent the initial condition of the tissue received, referred to here as “fresh.” The other half of the tissue pieces are put through the process as described in the kit instructions and vitrified. Upon completion of the protocol, the fresh tissue pieces were fixed. At least 24 hours later, the vitrified tissue is put through the warming and recovery kit instructions and fixed in the same way. Additional sterility and endotoxin testing was performed on the CM used in the first plate of the warming and recovery protocol after the tissue had been washed

in this media. This was to ensure that the whole process was performed with a sterile technique, and that the kit components remained sterile after they were removed from the GMP environment.

At least 5 pieces from each of the fresh and warmed/recovered tissue were analyzed through our Morphological Endpoint SOP. Sections from the ends, and middle of each piece were stained with H&E and observed. Each of the two groups, the fresh and the vitrified/recovered sections were observed in a blind fashion. Notes on the appearance of the tissue, describing presence of follicles, whether or not they appear healthy (healthy oocytes with healthy granulosa cells surrounding them), stroma cell shape and density (whether or not space is visible between cells), and intensity of blue versus pink staining were noted. A "Pass" result is given if these two groups of tissues appear similar in H&E. The characteristic healthy stromal cells appeared elongated, and stained mostly pink with a small granulated nuclear, or blue, stain (Fig.3 a-d). Healthy oocytes are ~20-30 times larger than stromal cells, are round and mostly pink (Fig. 3 a,c).

Additional testing on tissue health was performed on our bovine ovarian cortex slices to further confirm the morphological endpoint of the kit prepared in this batch. Sections of fresh and vitrified/recovered ovarian tissue was stained to identify cells undergoing apoptotic DNA degradation using a TdT-mediated dUTP Nick-End Labeling, or TUNEL, assay (Fig. 3 e-h, Suppl. Fig. 2). The number of TUNEL-positive cells from 4 fresh and 5 vitrified/recovered tissue pieces were calculated and compared. We found that 1 cell out of 11,344 cells analyzed in 4 tissue samples (0.0081 ± 0.0058 %) were positive for TUNEL in the fresh tissue samples and 2 cells out of 10,566 cells analyzed in 5 tissue

samples (0.0178 ± 0.0246 %) were positive for TUNEL in the vitrified/recovered samples and there was no significant difference among the two groups (mean ± standard error, Student's t-test, $p = 0.668$).

Conclusion

Translational research encompasses two phases of interpretation according to the National Institutes of Health (NIH), the dominant funding source for basic biological, and clinical research and training. The first phase requires translating basic research performed on the bench into clinical trials and studies in humans. The second phase requires translation from the clinical trials and studies to best-practices in the clinic or community [14]. A clear understanding of cGLP and cGMP implementation must exist in order to bridge basic research toward clinical trials in humans. This manuscript describes the first steps toward translating bench research into a product that meets the criteria and provides data required for an IND submission to the FDA. These pathways of investigations are performed with the intended outcome of creating safe products for use on human ovarian tissues that may be transplanted back into the patient. Therefore, cGLP and cGMP guidelines were followed to ensure consistent, sterile product kits and good scientific methodologies of testing. These practices included controlled manufacturing environments, skilled personnel, establishment of SOPs, measures for sterility and functionality evaluation and appropriate documentation of procedures.

We describe work done toward creating a reliable method for preserving ovarian cortical tissue through a vitrification kit and reviving this tissue through a warming and

recovery kit, for eventual use in the clinic. These research protocols are established for rhesus macaque and are not currently intended for clinical use [7-9]. The next steps required developing the research protocols and media formulations into a simplified kit with the intention of future use within a fertility clinic as a standardized, replicable procedure to increase the reliability of predicted outcomes. Additional research on human ovarian tissue, including analysis of functional endpoints in vitro following use of the Vitrification and Warming and Recovery Kits, are ongoing to support our IND application. Furthermore, research into the ability of vitrified and recovered ovarian tissue to support hormone secretion and production of a fertilizable egg after transplantation into humans will also be required to demonstrate that full functionality can be preserved using these kits. While these steps describe development and manufacturing for specific kits, they can be translated to the development of other medias or kits that have the potential for translation and in which the researchers hope to submit an IND. Researchers at the apex of translational research should be encouraged to overcome the hurdle of understanding these specific FDA regulations and following the guidelines as these techniques are not much different from good scientific methodologies and general laboratory practices.

Acknowledgments

This work is supported by the Watkins Chair of Obstetrics and Gynecology (TKW), the UH3TR001207 (NCATS, NICHD, NIEHS, OWHR, NIH Common Fund) and the Eunice Kennedy Shriver National Institute of Child Health and Human Development U54HD076188 grant. The Oncofertility Consortium ® is funded by the National Institutes

of Health through the NIH Roadmap for Medical Research, Grant UL1DE19587 and PL1CA133835. MML acknowledges support from The Burroughs Wellcome Fund Career Award at the Scientific Interface. This work was supported by the Northwestern University Mouse Histology and Phenotyping Laboratory and a Cancer Center Support Grant (NCI CA060553). The authors thank Greg Fahy, from 21st Century Medicine, for gifting the Super Cool polymers used in this study, Clarisa Gracia and Jessica Brown, from the University of Pennsylvania for giving us feedback on the operational procedures as performed in a fertility clinic, and Cheryl Hanson from the Mathews Center for Good Manufacturing Practice training and feedback on procedures and Steven Mullen, from Cook Regentec for his role in developing the initial vitrification media recipes. We also thank Keisha Barreto from the Ovarian Histology Core at Northwestern University for her technical expertise.

This work appeared in its original form in the *Journal of Assisted Reproduction and Genetics* (2017).

VITA

Kelly E. McKinnon

4250 N Marine Dr, #1611, Chicago, IL 60613

(312) 503-2530 / (770) 823-9276

www.kellyemckinnon.com

kellyemckinnon@gmail.com

Education / Training

Northwestern University September 2013-June 2018

Chicago, IL

Feinberg School of Medicine, Department of Obstetrics and Gynecology

Laboratory of Teresa K Woodruff, Ph.D.

Co-advised by Spiro Getsios, Ph.D

Ph.D. in Life Sciences

Emory University May 2012-July 2013

Atlanta, GA

Department of Medicine

Laboratory of George R. Beck, Jr., Ph.D.

Undergraduate Research Fellow

Georgia Gwinnett College May 2010-May 2013

Lawrenceville, GA

School of Science & Technology

B.S. in Biology, Biochemistry Concentration

Honors & Awards

Science Outside the Lab – Science Policy Fellow 2017

Awarded to one NU trainee to attend policy workshop in Washington, D.C.

Selected by the Graduate School at Northwestern

Constance Campbell Memorial Travel Grant 2017

Center for Reproductive Science at Northwestern

Conference Travel Grant 2017

The Graduate School at Northwestern

National Institute of Health/National Cancer Institute training grant NRSA T32 CA009560

Carcinogenesis Training Program 2016-2018

Mentor of the Year 2016

Driskill Graduate Program at NU

National Science Foundation – Honorable Mention

Graduate Research Fellowship Program 2015

Constance Campbell Memorial Research Award – Poster Presentation 2015

34th Annual Mini-symposium on Reproductive Biology

Science and Society Class Distinction Award 2014

Northwestern University

HHMI Summer Undergraduate Research Fellowship - Emory University 2012

Teaching & Related Work Experience

Guest Lecturer – "Communicating science to a doubtful world" Winter 2017

Invited speaker for ProSeminar Lecture Series

Northwestern University MS Health Communications Program

Course Director: Kimberley Cornwell, MS

Course Instructor – "Bioengineering the Ovary" Fall 2016

2016 International Oncofertility Consortium Conference – Trainee Education Lab

Program Founder/Director: Teresa Woodruff, Ph.D., Northwestern University

Teacher's Assistant – Cell Biology Spring 2016

Feinberg School of Medicine, Northwestern University

Course Directors: Steven Kosak, Ph.D. and Brian Mitchell, Ph.D.

Course Instructor – "Decellularizing a bovine ovary" 2015-2017

Women's Health Science Program for high school girls

Program Founder/Director: Teresa Woodruff, Ph.D.

Educational Activities and Skills / Career Advancements

Science Writing & Careers – Medill School of Journalism, NU 2015

Skillset includes: Narrative structure, social media, blogging, data visualization

Good Tissue Practice and Good Manufacturing Practice Standard Operating Procedure Training 2014

Under the direction of: Ann LeFever, PhD, Director of MCCT

Skillset includes: environmental monitoring, gowning, sterility testing, supply management, document control

Service, Civic Engagement and Public Outreach

Northwestern University Leadership Council Live Webinar – "Women in Science"

Invited panelist 2018

Women's Health Research Day 2018

Developed, organized and managed pop-up science event at Illinois State Building

Center for Reproductive Science Advisory Board 2017-present

Trainee Representative

Duties include: Evaluate CRS mission, programming, and training endeavors; provide recommendations to improve and strengthen CRS

Reproductive Science and Medicine Summit Planning Committee 2017

March for Science Chicago Expo 2017

Organized, developed materials for, and managed Woodruff Lab science booth at public expo event

Driskill Graduate Program Student Council – Class representative 2016

Northwestern University – The Graduate School

Publications

Kelly E. McKinnon, Rhitwika Sensharma, Chloe Williams, Jovanka Ravix, Spiro Getsios, Teresa K. Woodruff. Microphysiologic modeling of human ectocervical mucosa reveals distinct cellular, biological and molecular profiles for follicular and luteal phases of the menstrual cycle. *(In review)*.

Kelly E. McKinnon**, Shuo Xiao**, Jonathon R. Coppeta**, Jie Zhu**, Hunter Rogers**, Susan A. Olalekan**, Brett C. Isenberg, Danijela Dokic, Alexandra S. Rashedi, Daniel J. Haisenleder, Saurabh S. Malpani, Chanel Arnold-Murray, Kuanwei Chen, Mingyang Jiang, Monica M. Laronda, Thomas Hope, Mary Ellen Pavone, Michael J. Avram, Elizabeth C. Sefton, Spiro Getsios, Joanna Burdette, J. Julie Kim, Jeffrey T. Borenstein, Teresa K. Woodruff. (2017). 28-day Menstrual Cycle Hormone Control of Human Reproductive Tract Function in a Microfluidic Culture System. *Nature Communications.*

***denotes equal first author contribution.*

Monica M. Laronda, Kelly E. McKinnon, Ann LeFever, Teres K. Woodruff. (2016). Good manufacturing practice requirements for the production of tissue vitrification and warming and recovery media for clinical research. *Journal of Assisted Reproduction and Genetics.*

Yiming Lin, Kelly E. McKinnon, Shin W. Ha., George R. Beck Jr. (2014). Inorganic phosphate induces cancer cell mediated angiogenesis dependent on forkhead box protein C2 (FOXC2) regulated osteopontin expression. *Molecular Carcinogenesis*.

Abstract Presentations

Kelly E. McKinnon, Rhitwika Sensharma, Chloe Williams, Hunter Rogers, Shuo Xiao, Spiro Getsios, Teresa Woodruff. Development of novel 3D microphysiologic and microfluidic human ectocervical model systems for studying hormonal effects on differentiation, barrier properties, and infection. Gordon Research Conference (and Seminar) on Epithelial Differentiation and Keratinization. 2017. Lucca, Italy.

Monica Laronda, Kelly E. McKinnon, Allison Ting, Mary Zelinski, Teresa Woodruff. Good manufacturing practice requirements for the production of tissue vitrification and warming and recovery media for clinical research. Annual International Oncofertility Consortium Conference. November 14, 2016. Chicago, IL.

Kelly E. McKinnon, Rhitwika Sensharma, Teresa Woodruff, Spiro Getsios. Ovarian hormone regulation of proliferation, differentiation, and barrier properties of the human ectocervix. Annual Lurie Cancer Center Symposium & Scientific Poster Session. Northwestern University. June 23, 2016. Chicago, IL.

FemKUBE Technology Team: Jonathan Coppeta, Brett Isenberg, Jeffrey T. Borenstein; **FemKUBE Biology Teams**: *EstroKUBE:* Shuo Xiao, Alexandra Rashedi; *TubeKUBE:* Joanna Burdette, Jie Zhu; *UteroKUBE/EndocerixKUBE:* J.Julie Kim*, Susan Olalekan, Sevim Yildiz Arslan, Thomas Hope; *EctocervixKUBE:* Spiro Getsios, Kelly McKinnon; *iPSC Development:* Monica M. Laronda, Hanna Valli; *Gynecology Tissue Core:* Mary Ellen Pavone, Saurabh Malpani, Chanel Arnold-Murray; *Bioengineering:* Peter Chen, Mingyang Jiang , Hunter Rogers; *Pharmacokinetics:* Michael Avram; *Project Management*: Elizabeth C. Sefton; PI: Teresa K. Woodruff. Female Reproductive Tract Integration in a 3D Microphysiologic System. Organ-on-a-chip World Congress, July 7, 2016, Boston, MA.

Kelly E. McKinnon, Paul Hoover, Teresa K. Woodruff, Spiro Getsios. Engineering a three-dimensional human ectocervical tissue model to study hormonal regulation and immune response of female reproductive tract. Lewis Landsberg Research Day. Feinberg School of Medicine, Northwestern University. April 2, 2015. Chicago, IL. *Poster presentation.*

Kelly E. McKinnon, Paul Hoover, Teresa K. Woodruff, Spiro Getsios. Engineering a three-dimensional human ectocervical tissue model to study hormonal regulation and immune response of female reproductive tract. Center for Reproductive Science Minisymposium, Northwestern University, January 26, 2015, Chicago, IL. *Poster presentation.* ***Received the Constance Campbell Memorial Research Award.***